Glutamic Acid 358 is Important for the Normal Allosteric Function and Heterotetramer Formation of Potato ADP-Glucose Pyrophosphorylase

by

KAAN KOPER

A Thesis Submitted to the

Graduate School of Sciences and Engineering

in Partial Fulfillment of the Requirements for

the Degree of

Master of Science

in

Chemical and Biological Engineering

KOÇ UNIVERSITY

JULY 2013

Koç University

Graduate School of Sciences and Engineering

This is to certify that I have examined this copy of a master's thesis by

Kaan Koper

and have found that it is complete and satisfactory in all respects,

and that any and all revisions required by the final

examining committee have been made.

Committee Members:

_____

İ. Halil Havaklı, Ph. D. (Advisor)

_____

Özlem Keskin, Ph. D.

_____

Funda Şar, Ph. D.

Date: _____

ABSTRACT

ADP-glucose pyrophosphorylase (AGPase) is a key enzyme in plant starch biosynthesis. It contains large (LS) and small (SS) subunits encoded by two different genes. Experimental and computational studies indicated that interfacial amino acids in potato AGPase are important for the subunit-subunit interactions and allosterism. Among identified amino acid residues; A91, F101, F311 and E358 on LS (identified through error prone PCR) was found to be potent for influencing the allosteric and the catalytic properties potato AGPase. In this study, effect of these mutations on heterotetramer assembly and allosteric and catalytic properties of potato AGPase were investigated. All mutations were applied on to wild type (WT) potato AGPase large subunit cDNA using site directed mutagenesis PCR. Mutants LS, together with WT-LS, was transformed to *E.coli* glgC$^-$ containing the potato SS cDNA plasmid, that are deficient in glycogen production. All the LS mutants except LS-E358G were able complement glgC- in *E.coli*. LS-E358G mutant subjected to the detailed biochemical characterization to investigate its catalytic allosteric and structural properties. Compared to WT AGPase, AGPase with mutant LS-E358G was found to have a different assembly profile, having more heterotetramers and less monomers and dimers. Its regulatory properties were noticeably altered, its affinity towards its activator reduced and inhibitor increased. Interestingly, although large subunit of potato AGPase is mostly regulatory, this mutation considerably reduced the affinity of the AGPase towards its reverse and forward direction substrates ATP and ADP-glucose, showing potato tuber AGPase large subunit affects the catalytic performance of enzyme.

ÖZET

ADP-glükoz pirofosforilaz (AGPaz) bitki nişasta biyosentezinde rol alan anahtar bir enzimdir. Enzimin iki farklı gen tarafından kodlanan büyük (LS) ve küçük (SS) alt birimleri vardır. Deneysel ve hesaplamalı çalışmalar patates AGPase alt birimleri arası yüzey amino asitlerinin etkileşimlerinin, allosterizm için önemli olduğunu göstermiştir. Belirlenen amino asitler arasından; LS A91, F101, F311 ve E358'in (hataya yatkın PCR vasıtasıyla tanımlanmıştır) patates AGPazının allosterik ve katalitik özellikleri etkilediği bulunmuştur. Bu çalışmada, bu mutasyonların patates AGPazının heterotetramer oluşumu ve allosterik ve katalitik özelliklerine etkisi incelenmiştir. Tüm mutasyonlar, vahşi tip (WT) patates AGPase büyük alt birimi cDNA'sına noktasal mutasyon PCR'ı ile uygulanmıştır. WT-LS ile mutant LS'ler, glikojen üretiminde yetersiz olan E.coli glgC (patates SS cDNA'sını içeren) hücrelerine transform edilmiştir. LS-E358G dışındaki tüm LS mutantları E.coli glgC-hücrelerini tamamlamıştır. LS-E358G mutasyonunu, katalitik, allosterik ve yapısal özelliklere etkisini anlamak amacıyla, ayrıntılı biyokimyasal karakterizasyonu tabi tutulmuştur. Mutant AGPaz LS-E358G'nin daha fazla heterotetramere ve daha az monomere ve dimere sahip olduğu gözlenmiştir. WT AGPase ile karşılaştırıldığında, mutantın allosteric ve katalitik özellikleri belirgin biçimde değişmiştir. Mutantın aktivatörüne afinitesine azalmış ve inhibitör yönelik afinitesi artmıştır. İlginç bir şekilde, patates AGPase LS daha çok düzenleyici olarak rol almasına rağmen, bu mutasyonun patates AGPase enziminin katalitik performansını etkilediği bulunmuştur. Ters ve ileri yön aktivite deneyleri ATP ve ADP-glükoz olan afinitenin azaldığını belirlemiştir.

NOMENCLATURE

AGPase	ADP-glucose pyrophosphorylase
CFE	Cell free extract
CFE_{HS}	Cell free extract after heat shock step
DTT	Dithiothreitol
FT	Flow through
G1P	Glucose-1-phosphate
G6PDH	Glucose-6-Phosphate dehydrogenase
HRP	Horseradish peroxidase
LB	Luria Bertani
LS	Large subunit
Native-PAGE	Native (non-denaturing) polyacrylamide gel electrophoresis
NAD	Nicotinamide adenine dinucleotide
PCR	Polymerase chain reaction
PGM	Phosphoglucomutase
PMSF	Phenylmethanesulfonylfluoride
P_i	Inorganic phosphate
PP_i	Pyrophosphate
SDS-PAGE	Sodium dodecyl sulfate polyacrylamide gel electrophoresis
SS	Small subunit
TC	Total Cell
UGPase	UDP-glucose pyrophosphorylase
WT	Wild type
3PGA	3-Phosphoglyceric acid

ACKNOWLEDGEMENTS

I would like to sincerely thank my advisor İ. Halil Kavaklı for his guidance encouragements, continuous support, advices and patience. His experience, extensive knowledge and creative thinking did not only reshaped my way of thinking but also motivated me to continue my academic career. It has been a great pleasure and privilege to work with him and I will always be proud of being a part of his research group.

I acknowledge the financial support of the Scientific and Technological Research Council of Turkey (TÜBİTAK) and the Koc University during my whole graduate study.

I would like to sincerely thank İbrahim Barış, Ph.D. for his guidance and encouragements. Without his organization of the lab, it would be considerably harder making research.

I deeply thank Ayşe Bengisu Seferoğlu for teaching me the lab techniques and the know-how and more so for her endless support, guidance and patience.

I would sincerely like to thank my dear friends Bengisu Seferoğlu, Elif Muku, Hande Asımgil, Mehmet Tardu for great two years, all the fun and intellectual dialogs. I would also like to thank our new lab members Derya Yarparvar and Ehsan Sarayloo and old lab members Hüseyin Tayran and Oytun Aygün and especially Bilal Çakır.

I gladly thank all of the undergraduate students for their help and eagerness to learn. I especially like to thank Fatma Betül Can who dedicated a great amount time to work, help and learn at our lab. I hope I have been at least as helpful to all of you, as you all have been to me.

I would like to thank all of my professors for shearing their knowledge with me and for their eagerness to help without hesitation.

I would like to give special thanks to my old friends Mert Yumak, Faruk Yasa, Sadettin Esenlik, Noyan Kaya, Gökhan Özoğur and Can Poyrazoğlu for their support and whole lot of good and fun memories.

Last but not the least, I would like to thank all of my family, especially my mother and father for their, endless encouragement, support and love at every step of my life.

Table of Contents

LIST OF TABLES

LIST OF FIGURES

CHAPTER 1

INTRODUCTION

Starch is the primary long term storage polysaccharide of certain azeotropic cyanobacteria and plastid containing eukaryotes, including plants. In addition to its fundamental biological role, starch also act as a major food source and raw material for many industrial applications and processes [1] [2].

Biosynthesis of starch is accomplished in a series of enzyme catalyzed reaction. Key, rate limiting step of this pathway is the conversion of glucose-1-Phosphate (G1P) and ATP to ADP-glucose and pyrophosphorylase (PPi). This step is catalyzed in the plastids and in some plants (grasses) both in cytosol and plastids, by the allosteric enzyme ADP-glucose pyrophosphorylase (AGPase). AGPase catalyzes the rate limiting step in starch biosynthesis, it ultimately decides flux of free sugar molecules to starch. As AGPase is responsible for such a critical role, it activity is tightly regulated according to the metabolic state of the cell. Most plant AGPases are activated by the presence of allosteric activator 3-phosphphoglyceric acid (3PGA) and inhibited by the presence of allosteric inhibitor inorganic phosphate (Pi). As a result, inside plant cells, 3PGA/Pi ratio determines the activity of AGPase [3].

AGPases of plants are heterotetrameric enzymes of two identical small subunits (SS) and two identical large subunits (LS). Through the course of evolution, these two subunits evolved to fulfill different function. Among the two, SS acts as the catalytic subunit; it provides much of the catalytic activity of enzyme and yet it also has some minor regulatory functions. Other subunit, LS, is mostly regulatory, providing much of the sensitivity of the enzyme towards regulators. Even so, LS of certain plants, such as *Arabidopsis,* has some minor catalytic activity [4, 5].

Although AGPase is a considerably well studied enzyme, to date no group successfully managed to obtain the crystal structure of a plant AGPase in heterotetrameric form. As a result most of the data regarding to the structure function relationship of plant AGPases are obtained either by modifying specific amino acid residues or motifs found on AGPase and

than monitoring the change in the properties of enzymes and relating this information to the structure or from computational studies.

Previously our group generated several second-site revertants through error prone PCR to alter the heterotetrameric assembly of AGPase [6]. In this study, investigated amino acid residues were found to alter properties of AGPase when Ala 91 was mutated to Thr, Phe 101 was mutated to Leu, 311 was mutated to Leu and Glu 358 was mutated to Gly. Mutations were introduced to the potato tuber LS AGPase by site directed mutagenesis PCR. The effect of the amino acid changes on the AGPase was assessed by computational and experimental analysis [7-10].

Results indicated among the four mutants, AGPase containing mutant LS -E358G has unusual properties compared to wild type AGPase. Analysis of mutant LS-E358G AGPase by native gel revealed that mutant has enhanced heterotetrameric assembly compared with wild type AGPase. Furthermore, E358G mutation strikingly altered both catalytic and allosteric properties of the enzyme, compared to wild type; mutant enzyme had lowered affinity towards forward direction substrate ATP and reverse direction substrate ADP-glucose. It had lower affinity towards activator 3PGA but had higher affinity towards inhibitor Pi.

CHAPTER 2

LITERATURE REVIEW

2.1. Properties Storage Polysaccharides

The storage of carbohydrates as polysaccharide molecules is an essential adaptation allowing cells to accumulate and stock sugar molecules when resources are abundant and mobilize these stocks when resources are scarce. Two such storage polysaccharides are glycogen and starch.

Glycogen is the major storage polysaccharide of the animal, fungal and bacterial kingdoms. Its biogenesis is initiated when glucose-1-phosphate and either UTP or ATP are converted to corresponding nucleotide sugar, UDP-glucose or ADP-glucose, and pyrophosphate by the action of either enzymes UDP-glucose pyrophosphorylase (UGPase) in eukaryotes without plastids or ADP-glucose pyrophosphorylase (AGPase) in bacteria. In the next step, UDP-glucose in eukaryotes without plastids or ADP-glucose in bacteria are converted into glycogen by the action of the glycogen synthase and branching enzyme, releasing corresponding nucleoside diphosphate UDP or ADP **(Figure 2.1)** [11, 12]. Even though, genomes of bacteria, green algae and plants also encode for UGPases, they are not involved in glycogen synthesis[4]. In these organisms, storage polysaccharide biosynthesis is initiated by AGPase.

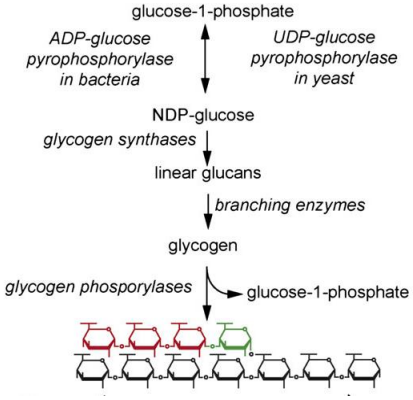

Figure 2.1: Diagram showing the components of glycogen synthesis in prokaryotic bacteria and eukaryotic yeast. Adopted from [5]

Starch acts as the storage polysaccharide of diazotrophic (nitrogen fixing) cyanobacteria and plastid-containing eukaryotes, which include *Archaeplastida*, e.g., green plants, green algae, red algae, and glaucophytes, and *Chromalveolata*, e.g., brown algae, diatoms, dinoflagellates, cryptophytes, and haptophytes. [5, 7, 13-15]. Although a great majority of these organisms are photosynthetic, some non-photosynthetic members are also present, such as apicomplexa parasites or non-photosynthetic dinoflagellates[11].

Starch biogenesis is initiated by conversion of glucose-1-phosphate and ATP into ADP-glucose and pyrophosphate. The Resulting ADP-glucose molecules are connected to each other via a 1, 4-alpha glycosidic bond forming long chains of amylose and releasing ADP. Finally, a starch- debranching enzyme connects these amylose chains by forming 1, 6-alpha glycosidic bonds, thus forming branched amylopectin [11, 16, 17]. The genomes of land plants and green algae contain at least two genes for AGPase subunits, four or more starch synthase genes, three genes for branching enzymes and two classes of debranching enzymes, indicating that at least the regions bearing these genes on these organisms experienced several duplication events and over time both duplicates evolved to gain separate, more specialized functions. [18, 19].

Although the storage polysaccharide of red algae is floridean starch, which is thought to be a type of starch composed of pure amylopectin, genetic analysis has so far not revealed a gene encoding for an AGPase but only a single isoform of UGPase. These observations suggest a starch biogenesis pathway initiated by UGPase is present in red algae. These findings are further supported by the fact that red algal starch synthase has a higher affinity towards the nucleotide sugar end product of UGPase, UDP-glucose, or than to the nucleotide sugar end product of AGPase, ADP-glucose[4, 18]. Accumulation of red algal starch within cytosol where UGPase is also found provides additional evidence that the reaction is catalyzed by UGPase, since with the exception of endosperm of grasses (Poaceae), AGPase is found exclusively in plastids in *Viridiplantae* and therefore starch also accumulates in plastids.[4, 20].

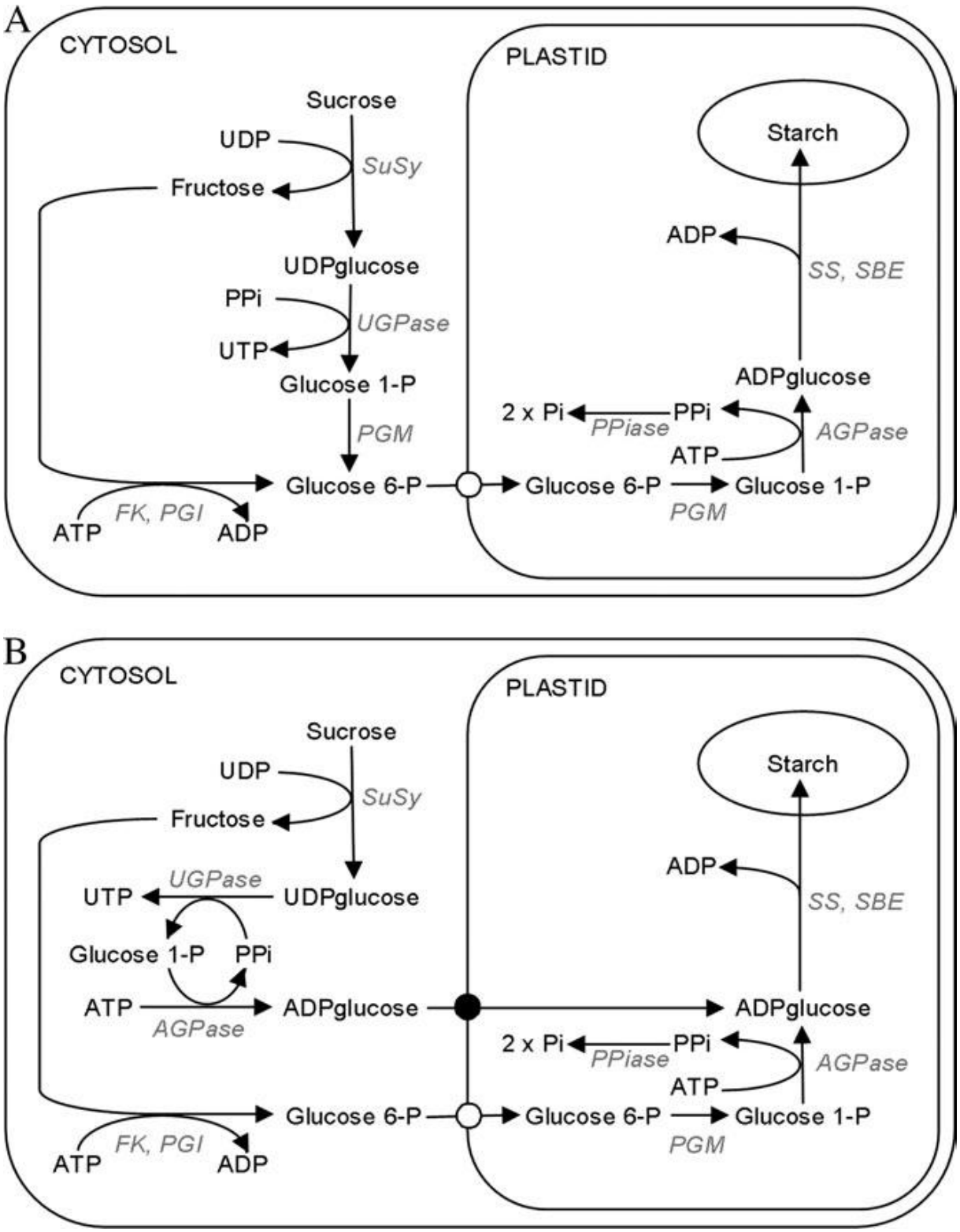

Figure 2.2: Diagram showing the starch synthesis pathways of plants. A) Starch synthesis in non-Grass (non-Poaceae) species showing starch is produced inside plastid by the action of the plastidal AGPase. B) Starch synthesis in Grass (Poaceae) species showing starch is produced inside plastid but both cytosolic and plastidal isoforms of AGPase contributes to its production. Retrieved from [18]

2.2. Endosymbiosis and Evolution of Starch in Eukaryotes

Like other eukaryotes, such as modern day animals and fungus, before the acquisition of plastids, the ancestral eukaryotic cells that would give rise to *Archaeplastida* and *Chromalveolata* were heterotrophic organisms whose storage polysaccharide was glycogen[5, 21]. However, approximately 0.7–1.5 billion years ago, one such eukaryotic cell engulfed an ancestral diazotrophic cyanobacterium, but, for some reason, failed to digests it. This event can be traced back to a single ancestral pair of organisms that endosymbiotic relationship first started which ultimately yielded phototrophic eukaryotes [5, 14, 22-24].

In the following many millions years after the initial endosymbiosis this event, majority of cyanobiont (cyanobacterial-symbiont) genes that were nonessential for photosynthesis, maintenance or division were either lost or moved from cyanobacterial genome to host eukaryotic genome. One such group of genes included those responsible for starch generation in ancestral cyanobacteria. As these genes moved from the cyanobiont genome to the ancestral archaeplastidal genome, the host cells gained the ability to generate starch in cytosol, which ultimately replaced glycogen as a storage polysaccharide. On the other hand the cyanobiont lost its ability to produce starch [5]. This cytosolic starch accumulation phenotype is still present in certain modern day archaeplastidals such as red algae (*Rhodophyceae*). *Rhodophyceae* still accumulate floridean starch inside the cytosol rather than inside rhodoplasts [5]. As the cyanobiont evolved into a true organelle or plastid, a complex protein targeting machinery between cytosol and plastid also evolved. In *chloroplastida* (plants and green algae) this protein movement between cytosol and plastid allowed the re-introduction of starch biogenesis within the plastid. Consequently, modern plants and green algae generate and stores starch inside plastids (amyloplast) **(Figure 2.3)** [4, 5, 21].

Interestingly, ADP-glucose which is required for the synthesis of starch is exclusively produced in plastid in the majority of plants since AGPase of these organisms also localizes to plastids. However, Grasses evolved two different AGPase isoforms, one plastidal, the other cytosolic, which allows them to produce ADP-glucose at both plastid and cytosol [25].

In the cytosol of non-photosynthetic tissues of non-grass plants, imported sucrose and UDP are converted fructose and UDP-glucose by the enzyme sucrose synthase (SuSy). Fructose is converted to glucose-6-phosphate by the enzymes fructose kinase (FK) and phosphoglucose isomerase (PGI). Mean while UDP-glucose is converted glucose-1-phosphate by UGPase and this glucose-1-phospate is converted to glucose-6-phosphate by phosphogluco mutase (PGM). Cytosolic glucose-6-phosphate is then transported to amyloplast and converted back to glucose-1-phosphate by PGM. In the next step AGPase catalyses the conversion of glucose-1-phosphate and ATP to pyrophosphate (PPi) and ADP-glucose. In the final step starch synthase adds these ADP-glucoses to a growing amylose chain **(Figure 2.2-A)**.

In the endosperm of grasses where both cytosolic and plastidal isoforms of AGPase are expressed, the glucose-1-phosphate produced within the cytosol is not converted to glucose-6-phosphate but directly converted to ADP-glucose by cytosolic AGPase. This cytosolic ADP-glucose is exported into the plastid as no metabolic function has been associated with ADP-glucose inside cytosol **(Figure 2.2-B)**. This additional feeding of ADP-glucose to plastid from cytosol in grass endosperm tissue accounts for the high starch content of grass seeds. For instance, as much as 70-80% of the dry weight of mature maize kernels comes from starch [18, 26].

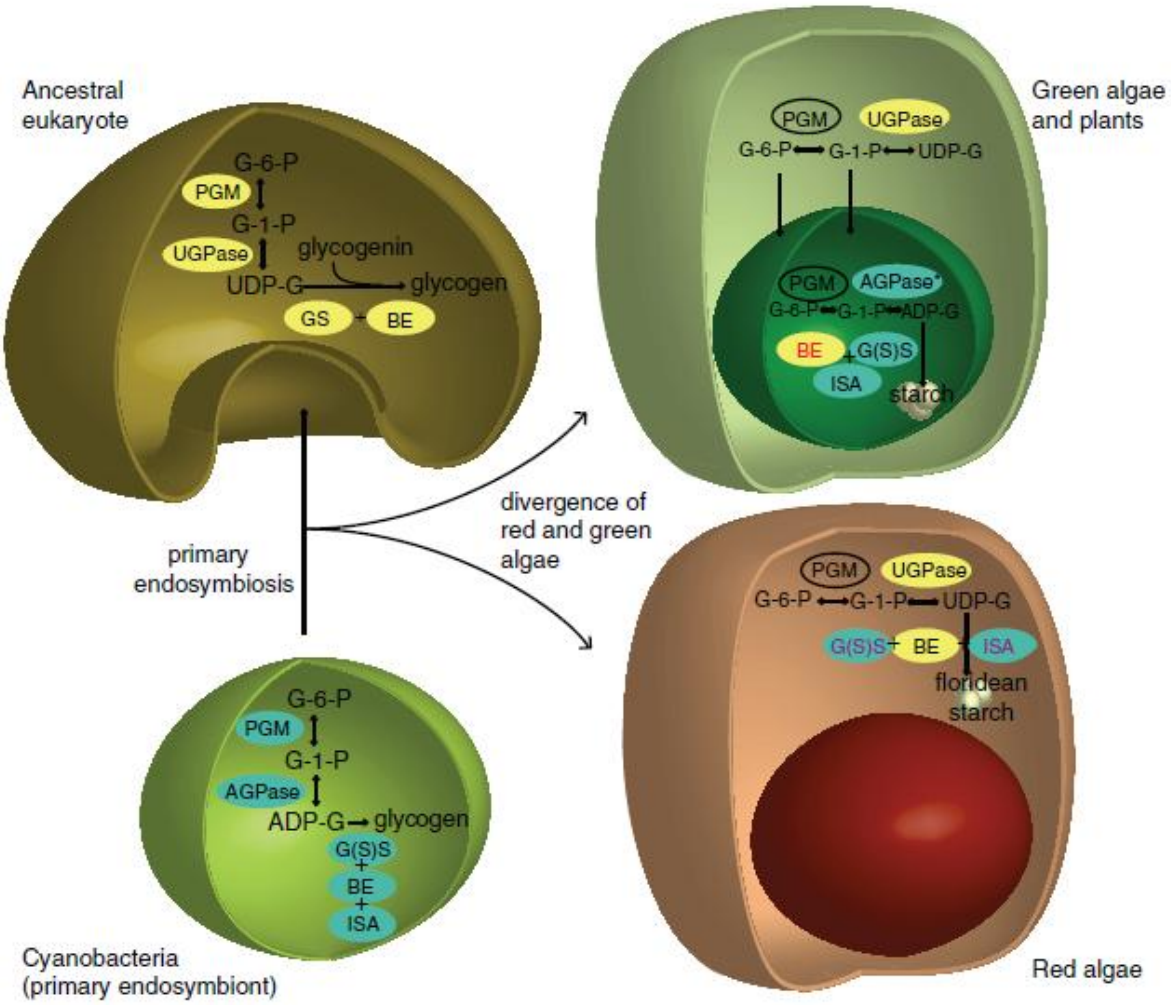

Figure 2.3: Proposed endosymbiosis event between ancestral eukaryote and primary endosymbiont and which resulted of Archaeplastida (green and red algae).Retrieved from [4]

Similar to the primary endosymbiosis in which the ancestral cyanobacteria became internalized by ancestral *archaeplastida*, which ultimately gave rise to the evolution plastids in these organisms, archaeplastidals themselves were also subjected to endosymbiosis by other non-photosynthetic eukaryotes. This secondary endosymbiosis gave rise to a second group of photosynthetic eukaryotes known as *chromalveolata*, which includes brown algae, diatoms, dinoflagellates, cryptophytes, and haptophytes[5]. Although all these lineages contain a secondary plastid that resulted from a secondary endosymbiosis event involving a photosynthetic alga and a non-photosynthetic eukaryote, it is not clear exactly how many times this endosymbiosis event had happened [27]. Plastids of most *chromalveolata* contain at least four membranes; inner two of these membranes are theorized to originate from the primary endosymbiont cyanobacteria, whereas the third and fourth membranes originates from the plasma membrane of the alga subjected to endosymbiosis and the phagosomal membrane of the host cell [5, 27, 28]. Interestingly, like primary endosymbiosis, which allowed the eukaryotic host cell to replace its glycogen metabolism with a starch metabolism, this secondary endosymbiosis also allowed the host eukaryote to replace glycogen metabolism with starch metabolism. In fact, the majority of *chromalveolata* produce starch either in their cytosol or between the second and third membranes of the plastid, an area called the periplastidial space, which corresponds to the ancient cytosol of the internalized alga. It can be assumed that the original archaeplastidal endosymbiont was a cytosolic starch accumulator much like modern day red algae and, after the secondary endosymbiosis event, certain *archaeplastida* genes involved in starch metabolism moved to the host genome, whereas in other organisms they either stayed in the plastid or moved to the host genome and were then re-wired to the periplastidial space [5, 27, 28].

2.3. Properties and Biosynthesis of Plant Starch

Starch is a large, insoluble polysaccharide made up of two glucose polymers in the form of amylopectin and amylose. In photosynthetic and non-photosynthetic tissues of higher plants, starch is synthesized and stored plastids [2, 5].

During photosynthesis certain amount of fixed carbon is converted to starch and stored at the chloroplast rather than being converted to sucrose and exported to other tissue. This type of starch is known as the transitory starch **(Figure 2.4, left)**. Transitory starch is degraded during the night (or when photosynthesis is not available) to assure the continuity of cellular respiration and production of sucrose that would be sent to other tissue[2].

In non-photosynthetic tissue (such as those found at roots, tubers, stems and seeds) that rely on sucrose influx originating from photosynthetic tissue (such as leafs), some fraction of sucrose can be converted to starch and accumulated at amyloplast for long term storage **(Figure 2.4, right)**. This type of starch is known as storage starch and it is mobilized once again when there is an intense need for energy which cannot be provided by photosynthesis (either unavailable or insufficient), such as seed germination, awaking from dormant state after winter and nectar production [2].

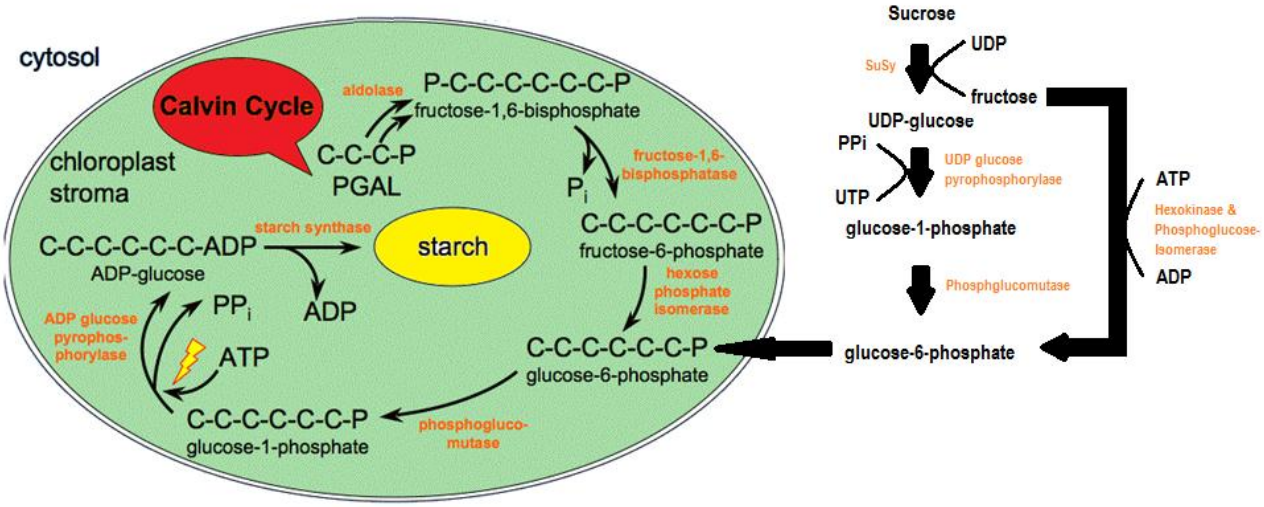

Figure 2.4: Starch synthesis fueled by photosynthesis (right) or by conversion of sucrose glucose-6-phosphate which is transported to plastid (left).Adopted from[29]

Within plant cells, starch accumulates as semi-crystalline granules of two different polysaccharides of glucose; amylose and amylopectin. Among these two, amylopectin accounts for more than 75% of starch granule where as amylose makes up less than 25%. Although both molecules are structurally similar, their sizes and branching levels are considerably different. Molecular weight of a large branched amylopectin molecule is approximately 10^7 to 10^9 Daltons [2, 5, 30]. The glucose residues of amylopectin are linked to each other by α-1, 4- glycosidic bonds which results in chains containing between a 10^5 to 10^6 glucose residues. Those individual chains are connected to each other by α-1, 6-bonds forming the branched structure [2, 30]. Amylose on the other hand is also formed through α-1, 4- glycosidic bonding of glucose residues but overall structure is much smaller ranging between 10^5-10^6 Daltons , it is much less branched and its synthesis requires a pre-existing amylopectin [2, 5]. In fact, only less than 1% of amylose is composed of branches whereas between 4-6% of amylopectin is composed of branches **(Figure 2.5)** [5].

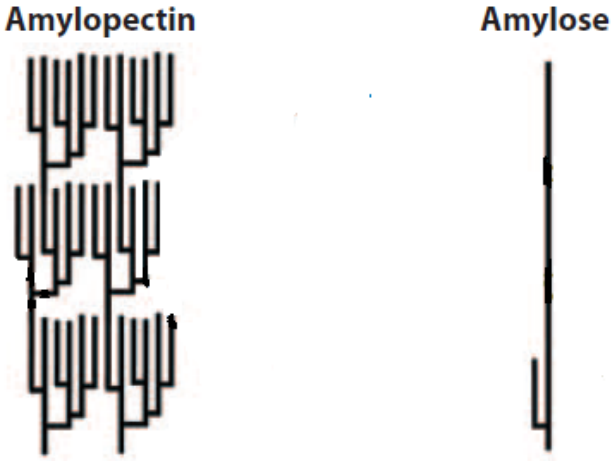

Figure 2.5: Schematic Representations of highly branched amylopectin and amylose. adjacent chains of amylopectin form helices with each other and collapse. Adopted from[30]

Main purpose of storage polysaccharide is to give a cell the ability store carbohydrates, in a form that is osmotically less active than its monomers. By achieving this, a cell can store excess glucose within the cytoplasm without disturbing the osmotic balance or using high amounts of energy [2, 5, 18]. One such major storage polysaccharide is glycogen, compared to glucose it is considerably less active and therefore allow accumulation larger amounts of carbohydrates. Yet glycogen is amorphous **(Figure 2.6-a)** and water-soluble and even though it is osmotically more tolerable compared to glucose, there is an osmotic limit for its storage. Starch on the other hand is and water-insoluble crystal. During starch synthesis **(Figure 2.7)**, as the large amylopectin chains form; they pack together as helices, become insoluble and collapse into crystals forming the granulated structure of starch **(Figure 2.6-b)**. This property of starch makes it osmotically inert and therefore allows accumulation of virtually unlimited amounts of glucose. One such drawback of his property is; as starch is insoluble, an enzyme working on this molecule should be able work on solid state which makes catabolism of starch more complex compared to glycogen[5].

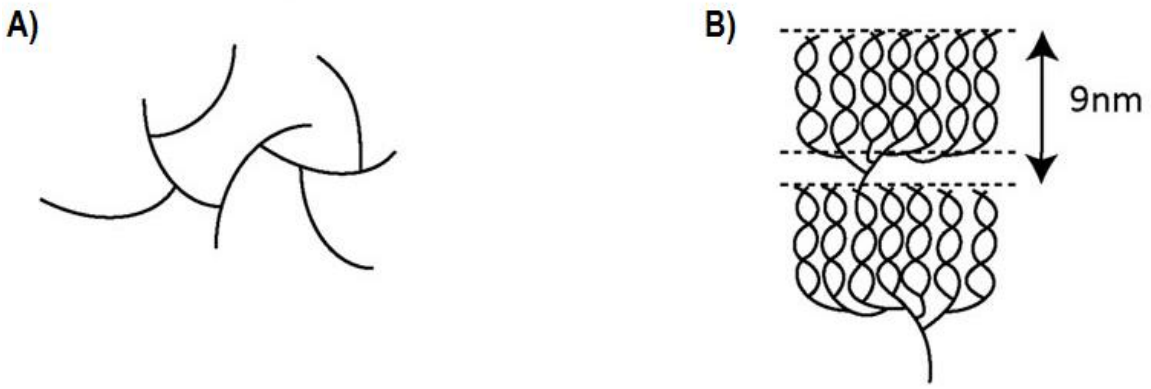

Figure 2.6: Schematic diagram showing the structure of a section A) amorphous glycogen and B) section of starch crystal composed of two clusters of amylopectin. Adopted from [5]

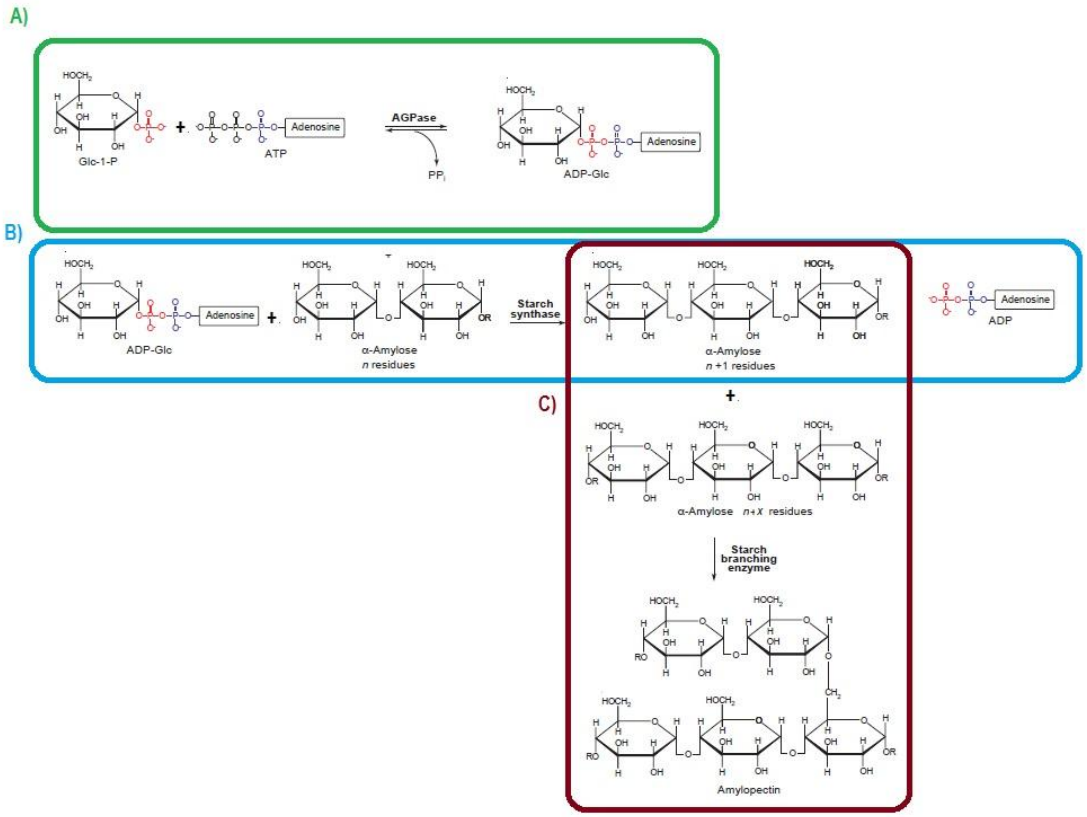

Figure 2.7: Diagram showing the molecular basis of starch synthesis. A) First committed step of starch synthesis where G1P and ATP are converted to ADP-Glucose and PPi through the action of AGPase. B) Second step of starch synthesis where ADP-Glucose is added to a growing α-amylose chain through the action of starch synthase enzyme. C) Final step of starch synthesis where two α-amylose chains are connected to each other by starch branching enzyme.[1]

2.4. Properties and Evolution of AGPase and Its relation Starch Biosynthesis within Eukaryotes

ADP-glucose pyrophosphorylase (AGPase) is an enzyme belonging to the nucleotidyltransferase superfamily. It catalyzes the first committed step of storage polysaccharide biosynthesis in a variety of organisms. AGPase reversibly catalyzes a reaction in which glucose-1-phosphate (G1P) and ATP are converted to ADP-glucose and pyrophosphate in the presence of Mg^{+2} cation **(Figure 2.8)** [3, 12, 17, 19, 31]. In the majority of bacteria, the resulting ADP-glucose is converted to the storage polysaccharide glycogen in a series of enzyme-catalyzed reactions. On the other hand, in certain cyanobacteria, photosynthetic eukaryotes and their non-photosynthetic descendants it is converted into starch [7, 11]. AGPase and starch can be found in certain cyanobacteria, but their presence does not necessarily imply that AGPase is strictly used for starch biosynthesis, as resulting ADP-glucose may also be employed for other purposes[5, 7, 11, 15, 25].Red algae (*Rhodophyceae*) store their polysaccharides as starch granules (floridean starch) yet, biosynthesis of floridean starch is initiated by UDP-glucose pyrophosphorylase (UGPase)[32]. Whereas in *Viridiplanta*e, e.g., green algae and plants, starch biosynthesis is initiated by ADP-glucose pyrophosphorylase (AGPase)

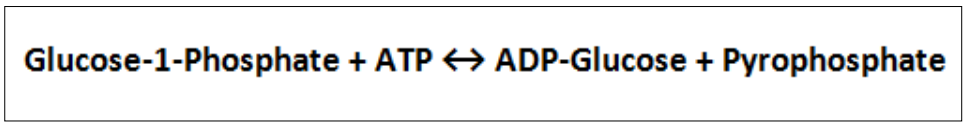

Figure 2.8: Diagram showing the reaction catalyzed by AGPase. AGPase can freely catalyze the reaction in both forward and reverse directions in vitro, yet in cellular conditions it is mainly in forward direction [3, 31].

2.4.1. Evolution of AGPase and Its relation Starch Biosynthesis

Bacterial AGPases are homotetrameric enzymes composed of four identical subunits. Plant and green algae AGPases on the other hand, are heterotetrameric enzyme composed of two identical small subunits (SS) and two identical large subunits (LS). There can also be multiple isoforms of LS and SS, for example large subunit of AGPase has three isoforms in potato, four in *Arabidopsis*, and four in rice whereas grass species has cytoplasmic and plastid isoforms of both large and small subunits[4, 18]. Both subunits of plant AGPase are related to bacterial AGPase, particularly those of cyanobacteria. In fact, cyanobacterial

AGPase is more closely related to small subunit of plant AGPase than to those of other heterotrophic bacteria. Due to this similarity between cyanobacterial AGPase and small subunit of plant AGPase and the fact that, genome of no eukaryote except those containing plastids encode for an AGPase, it is toughed that plants gained the ability to synthesize AGPase after the endosymbiosis of cyanobacteria and the subsequent gene transfer from endosymbiont genome to the host genome[4, 19, 33, 34].

As cyanobacterial AGPase is a homotetramer of identical subunits, ancestral AGPase plants obtained from the cyanobiont was also a homotetramer. However AGPases of modern day *chloroplastida* (plants and green algae) are heterotetramers. Presence of heterotetrameric AGPases in all *chloroplastida* (whose members are only distantly related) indicates that, in a very early stage of chloroplastida evolution, a gene duplication event created two paralogs of AGPase encoding gene and both of those paralogs got functionalized[19, 35]. As a result of this, every chloroplastida evolved later had two paralogs of AGPase gene which through the course of evolution became small and large subunits of heterotetrameric AGPase. Additional duplication events in angiosperm created additional paralogs and some of these paralogs got specialized according to the needs of the tissue they are expressed in, creating other AGPase isoforms found in higher plants[34].

Even though AGPase subunits are named as small (50–54 kDa) and large (51–60 kDa), difference between these subunits in some organisms (ex: potato) can be less than 1 kDa [3, 33]. Among different *chloroplastida*, large subunits show low degree of conservation across species, whereas small subunits of AGPase are highly conserved [36]. Furthermore, compared to large subunit, small subunit shows higher degree of identity to cyanobacterial AGPase. These observations indicate that after the initial gene duplication event, one of the AGPase paralogs had more evolutionary constrains compared to other since, at least one of the paralogs should be able to effectively perform original AGPase activity and as a result of this, it is more conserved [36]. In contrast, other paralog got independent of same constrains since, those functions were already being complimented by the other paralog. Therefore LS had more evolutionary flexibility and evolved to carry out other functions[4, 36, 37]

2.4.2. Regulation of AGPase

As AGPase is an enzyme that catalyzes the rate limiting step of storage polysaccharides production, it needs to be tightly regulated. Usually production of storage polysaccharide happens under "high energy conditions" where both carbon sources and energy are abundant; therefore AGPase is allosterically activated by the presence of molecules that indicate a "high energy status", such as 3-PGA, fructose-1, 6- bisphosphate (FBP), fructose-6-phosphate (Fru6P), and pyruvate. Alternatively cells tend to use their polysaccharide stocks under "low energy conditions" where carbon and energy sources are in short supply .Therefore activity of AGPase is allosterically inhibited under those conditions where, metabolites that represent "low energy status", such as inorganic orthophosphate (Pi), AMP, and ADP are present, to prevent polysaccharide production. In addition to allosteric regulations, AGPase of higher plants are found to be subjected to transcriptional regulation and certain post-translational modifications such as redox regulation and protein phosphorylation **(Figure 2.9)**.

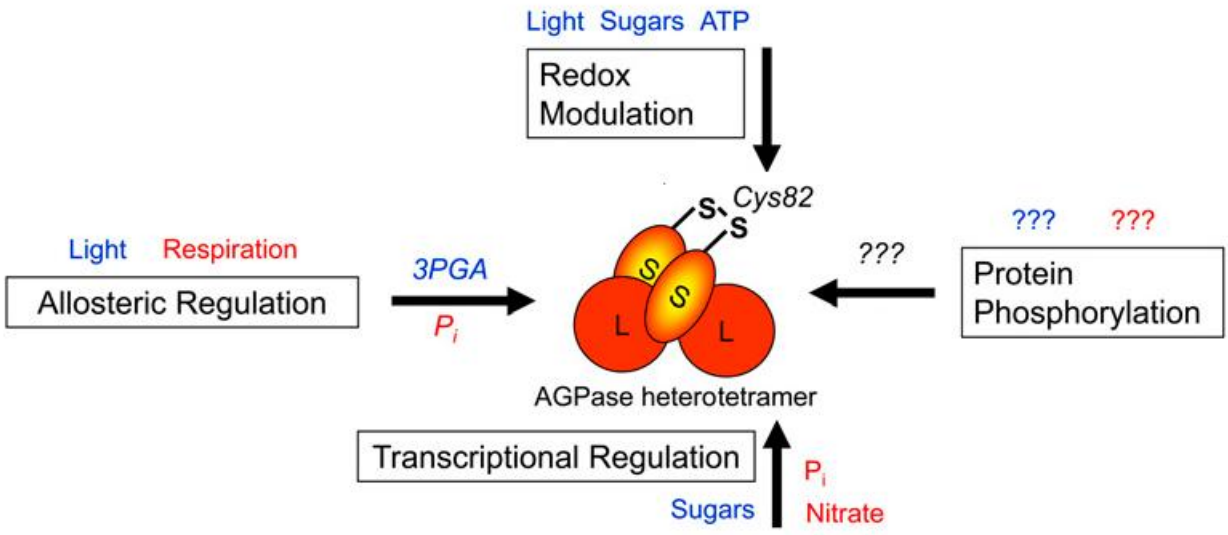

Figure 2.9: Different regulatory mechanisms acting on higher plant AGPase. Adopted from [38]

2.4.2.1. Allosteric Regulation of AGPase

Among bacteria, allosteric activators and inhibitors of AGPase show great diversity. This great diversity arise from the fact that, bacterial species inhabit different environments and therefore have evolved different metabolic pathways, specific for their particular habitat. Consequently, main metabolic pathways operating in the respective organism are different, as so the substrates, metabolic intermediates and end products of these pathways. Since AGPase activity is regulated according to the metabolic state of the organism, different main metabolic pathways resulted in different allosteric regulators among different bacteria species (**Table 2.1)** [19, 31].

Regulation of AGPase was tightly coupled to the Calvin cycle and photosynthesis within cyanobacteria even before the endosymbiosis event and after the endosymbiosis, major regulatory mechanisms of AGPase were conserved and passed to the archaeplastida [5, 31]. Even so, cyanobacterial AGPase is made up of four identical subunits meaning both catalytic and regulatory properties are gathered on a single protein. On the other hand, AGPases of higher plants and algae are made up of two different subunits [31]. Presence of two different subunits allowed each subunit to specialize in a different function and so, small AGPase subunit become the major catalytic compartment and large AGPase subunit become the regulatory compartment. However, function separation between large and small AGPase subunits is not absolute meaning; even if small subunit is mainly catalytic it has certain regulatory functions and large subunit, at least in certain organisms such as *Arabidopsis thaliana*, have low catalytic activity [19, 39, 40]. Therefore, it can be said that both subunits have a certain degree of catalytic and regulatory functions [37].

Organism	Main carbon utilization	ADP-Glc PPase	
		Allosteric regulators	
		Activator(s)	Inhibitor(s)
Prokaryotes			
Escherichia coli *Salmonella enterica* serovar Typhimurium *Enterobacter aerogenes*	Embden-Meyerhof pathway (glycolysis)	Fru 1,6-bisP	AMP
Aeromonas formicans *Micrococcus luteus* *Mycobacterium smegmatis*	Glycolysis	Fru 1,6-bisP, Fru 6-P	AMP, ADP
Serratia marcescens *Enterobacter hafniae* *Clostridium pasteurianum*	Glycolysis	None	AMP
Agrobacterium tumefaciens *Arthrobacter viscosus* *Chromatium vinosum* *Rhodobacter capsulata* *Rhodomicrobium vannielii*	Entner-Doudoroff pathway	Pyruvate, Fru 6-P	AMP, ADP
Rhodobacter gelatinosa *Rhodobacter globiformis* *Rhodobacter sphaeroides* *Rhodocyclus purpureus*	Glycolysis and Entner-Doudoroff pathways	Pyruvate, Fru 6-P, Fru 1,6-bisP	AMP, Pi
Rhodospipillum rubrum	Tricarboxylic acid cycle	Pyruvate	None
Rhodospirillum tenue	Reductive carboxylic acid cycle		
Bacillus subtilis *Bacillus stearothermophillus*	Tricarboxylic acid cycle during sporulation	None	None
Cyanobacteria			
Synechococcus sp. strain PCC 6301 *Synechocystis* sp. strain PCC 6803	Oxygen evolving photosynthesis	3-PGA	Pi
Anabaena sp. strain PCC 7120	Calvin cycle		

Fru, fructose; P, phosphate; bisP, bisphosphate; Pi, inorganic phosphate.

Table 2.1: Different main carbon utilization pathways among different bacteria and resulting change in AGPase allosteric regulators. Adopted from [31]

Much like cyanobacteria, main allosteric activator of plant AGPase is also 3PGA (3-Phosphoglyceric acid) and allosteric inhibitor is also Pi (inorganic phosphate) (**Table 2.2**). Photosynthetic organisms follow Calvin Cycle or reductive pentose phosphate pathway to photoassimilate atmospheric carbon dioxide where 3PGA forms as the first a metabolic intermediate. Consequently 3PGA levels increase when Calvin cycle is active and drops when Calvin cycle slows down or stops .Furthermore, during light-dependent photosynthesis, Pi levels reduce since Pi acts as a substrate for the regeneration of ATP from ADP. Vice versa, when rates of light dependent photosynthesis drops, Pi levels once again increase due dark-cycle of photosynthesis and other metabolic activities where ATP got hydrolyzed to ADP and Pi. Overall, increase in 3PGA levels and decrease Pi levels indicate increased rate of photosynthesis and therefore a "high-energy state" whereas decreased levels of 3PGA and increased levels of Pi indicate low levels or no photosynthesis and thus a "low energy state". Since AGPases need to operate effectively under "high-energy state" and stop working under "low energy state", they are typical regulated according to the 3PGA/Pi ratio [3, 31, 37].

	ADPGlc PPase	
	Allosteric regulators	
	Activator	Inhibitor
Eukaryotes		
Green algae		
Chlamydomonas reinhardtii, *Chlorella fusca*, *Chlorella vulgaris*	3-PGA	Pi
Higher plants		
Photosynthetic tissues: leaves of spinach, wheat *Arabidopsis*, maize, rice	3-PGA	Pi
Non-photosynthetic tissues		
Potato tubers	3-PGA	Pi
Endosperm of maize, barley and wheat	None directly, 3-PGA and Fru 6-P reverse inhibitors	Pi, ADP, Fru 1,6-bisP

Table 2.2: Allosteric regulators of AGPases found at Green Algae and Photosynthetic and non-photosynthetic tissue of higher plants. Adopted from [3]

Although 3PGA act as an activator and Pi act as the inhibitor of AGPase at the photosynthetic tissues of majority of plants, the relative sensitivity of AGPase to these allosteric effectors depend on the species, tissue and subcellular localization. At endosperm of wheat and certain other cereals for instance, AGPase is allosterically inhibited by Pi, ADP and fructose 1,6-bisP. This inhibition is reversed by the presence of 3PGA and fructose 6-P which individually (in the absence of the inhibitors) have no effect on the enzyme activity. Oppositely, in endosperm of maize and plants that follow Crassulacean acid metabolism (also known as CAM photosynthesis which is water conserving, carbon fixation mechanisms evolved certain plants such as cacti as an adaptation to arid conditions), AGPase is allosterically activated by the presence of 3PGA. This activation can be reversed by Pi which individually has no effect on enzyme activity. Alternatively, at endosperm of barley, AGPase is only slightly activated or inhibited by 3PGA or Pi; however these regulators greatly alter the affinity of AGPase to its substrate ATP (**Table 2.3**) [3, 38].

Even if within plant cells AGPase works as a heterotetramer of two large and two small subunits, experimental evidence indicate that in the absence of large subunits, small AGPase subunits of at least certain higher plants can form functional homotetramer of four small subunits, although it requires elevated levels of 3PGA to get activated and is more sensitive to Pi inhibition. These observations were made on isolated small subunits of potato AGPase small subunits which formed functional homotetramer in vitro and on *Arabidopsis thaliana* mutant TL-46 which is large subunit deficient but can still retain 40% as much as starch in vivo as the wild-type plant[41, 42].

Principal effector	Secondary effector	Main effect on	Regulatory effect	ADPGlc PPase from
3PGA and Pi	Pi and 3-PGA	V_{max}	Ultrasensitive interaction between effectors	Cyanobacteria, green algae, spinach leaf, potato tuber
Pi	3-PGA	V_{max}	3-PGA reverses inhibition caused by Pi	Wheat endosperm
3PGA	Pi	V_{max}	Pi only inhibits the enzyme activated by 3-PGA	Leaf of CAM plants, maize endosperm
3-PGA	Pi	K_m	3-PGA increases affinity for the substrate, ATP, and Pi reverses the effect	Barley endosperm

Table 2.3: Different types of regulatory patterns found at AGPase from different species or tissues. Adapted from [3]

2.4.2.2. Transcriptional Regulation

AGPase regulates the first committed step of starch synthesis and therefore its expression is regulated according to carbon and nutritional status of the cell as well as according to the environmental factors. AGPases of green algae and higher plants are a heterotetramer of two small and two large subunits and in order to have a functional enzyme with adequate activity, both subunits need to be expressed in sufficient amounts. In many higher plants, multiple isoforms of both subunits are present, particularly isoforms of large subunit. Abundant evidence indicate that, multiple genes coding for these large subunit isoforms show strong specificity in their expression according to the tissue type or environmental or internal factors. Some of these isoforms might only be restricted to certain tissue whereas other isoforms might be expressed in response to certain environmental or internal factors [38, 43]. Since large subunit of AGPase is mainly regulatory, differential expression of these multiple large subunit isoforms in different tissue or in accordance to different internal/external factors allow production of AGPases with different sensitivity allosteric regulators. This allows the synthesized AGPase to be specific to the needs of the tissue or to the new internal/external factor, since different allosteric properties means different enzymatic activity in a given situation. In general, expression of AGPase subunits increases in response to sugars and decrease in response to nitrate and phosphate [38, 44, 45].

2.4.2.3. Regulation trough Post-Translational Redox Modulation

It is known that certain chloroplast enzymes are regulated through reversible thiol/disulfide interchange. During light dependent phase of photosynthesis, electron transport leads to the reduction of ferredoxin. Following this event, ferredoxin:thioredoxin reductase transfers these reducing groups on ferredoxin to thioredoxins , these thioredoxins than further reacts with their targets [46, 47]. It is known that Enzymes of the Calvin cycle, ATP synthesis and NADPH export from chloroplasts are activated by reduction of their cysteine residues by activated thioredoxins (Trx). It has also been found that Cys-82 residues of AGPase small subunit is also subjected reduction by thioredoxins. Once reduced by thioredoxins, AGPase experiences dramatic alteration on its kinetic properties which results in an increase in its activity. Its affinity towards both of its substrates increase, its sensitivity

towards allosteric activator 3PGA increase whereas sensitivity towards allosteric inhibitor Pi decrease. Such tight coupling of AGPase activity with photosynthesis ensures that, AGPase responds to changes in photosynthesis level much before other effectors such as changes in 3PGA or Pi concentrations reach to a sufficient degree to affect AGPase activity[38, 48-51].

2.4.2.4. Regulation trough Post-Translational Protein Phosphorylation

Recent studies suggest protein phosphorylation may play a role in AGPase activity. In Arabidopsis, certain in vitro experiments determined large and small subunits of AGPase as reversible phosphorylation targets. Furthermore, certain protein kinases and phosphatases have been identified to be potentially located in the plastid. While the underlying mechanism is largely unknown, in vivo experiments proving the relevance of this mechanism are needed since in vitro phosphorylation assays are known to be prone to yield false positives[38, 52, 53].

2.5. Structure of AGPase

Crystal Structure of plant AGPases were not solved in heterotetrameric form so far. However, crystal structure of homotetrameric potato tuber AGPase, composed of four small subunits was obtained [54]. Although this crystal structure reflects an inactive conformation due to the presence of high concentrations of ammonium sulfate resulting from the crystallization procedure, valuable information regarding to the potential binding sites were obtained using modeling approaches based on other known nucleotidyltransferase [54].

According to these results, small subunit monomer of potato AGPase is composed of a N-terminal catalytic domain and a C-terminal domain that makes strong hydrophobic interactions with catalytic domain. The N-terminal catalytic domain is made out of mostly parallel but mixed seven stranded β-sheets covered by α-helices, a type of fold that resembles dinucleotide binding site [55]. An α-helix found at the N-terminal catalytic domain makes strong hydrophobic interactions with the C-terminal β-helix domain. The catalytic domain is also connected to the N-terminal via a 20 amino acid long loop. This loop

also interacts with the equivalent region of another subunit and each monomer makes a disulfide bond with its equivalent subunit (A and A' with B and B', shown in **Figure 2.10**).

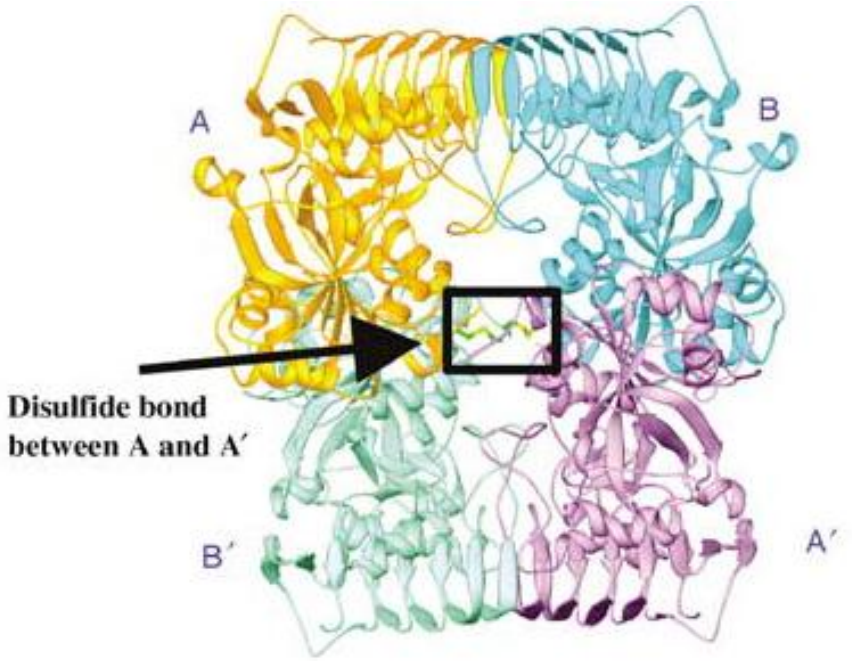

Figure 2.10: Structure showing the positions of A, A', B, and B' subunits of potato AGPase small subunit homotetramer and the disulfide bond between A and A'. Retrieved from [54]

Crystal structure results also show two sulfate ions bind to a cavity that is found between N and C terminus whereas a third one bind to a region that is found between subunits. All known plant allosteric regulators of plant AGPases (Pi, F-6-P, G-6-P, and 3PGA) contains phosphate components and due to structural similarity it is thought that the regions that bind to sulfate ions found in AGPase crystal structures ,normally occupied by Pi or other phosphorylated ligands such as 3PGA. Experimental studies also suggest that different allosteric regulators compete for same or adjacent regions in plant AGPases and the ability of Pi or sulfate to reverse the activation mediated by 3PGA may results from this competition **(Figure 2.11-A)** [56].

When AGPase is crystallized in the presence of ATP, it is found that ATP binds to a sugar/adenine binding region that is conserved in other related nucleotidyltransferase. Furthermore, even if all subunits of the tetramer are identical, ATP binds to only two of the subunits indicated as A and A'. Binding of ATP to these two subunits causes an identical

conformational change on these subunits, however, binding even induces a conformational change on the two unbound subunits indicated as B and B', (**Figure 2.11-B)**. When AGPase is crystallized in the presence of ADP-glucose, it is found that ADP-glucose binds to three subunits (A, A' and B). Binding of ADP-glucose induces an identical conformational change that binding of ATP causes, on subunits A and A'. Furthermore, on subunits A and A', adenine and ribose of ADP-glucose is positioned identically to those of ATP. On B' subunit, adenine and ribose of ADP-glucose is positioned very similar to that of subunits A and A'. However, both B, which binds to ADP-glucose, and B', which is unbound, experience very large subdomain movements in response to ADP-glucose binding,(**Figure 2.11-C)**. These results suggests, even if the potato AGPase homotetramer subunits are identical in terms of sequence, they show different affinities towards substrates and acquire different conformations [54].

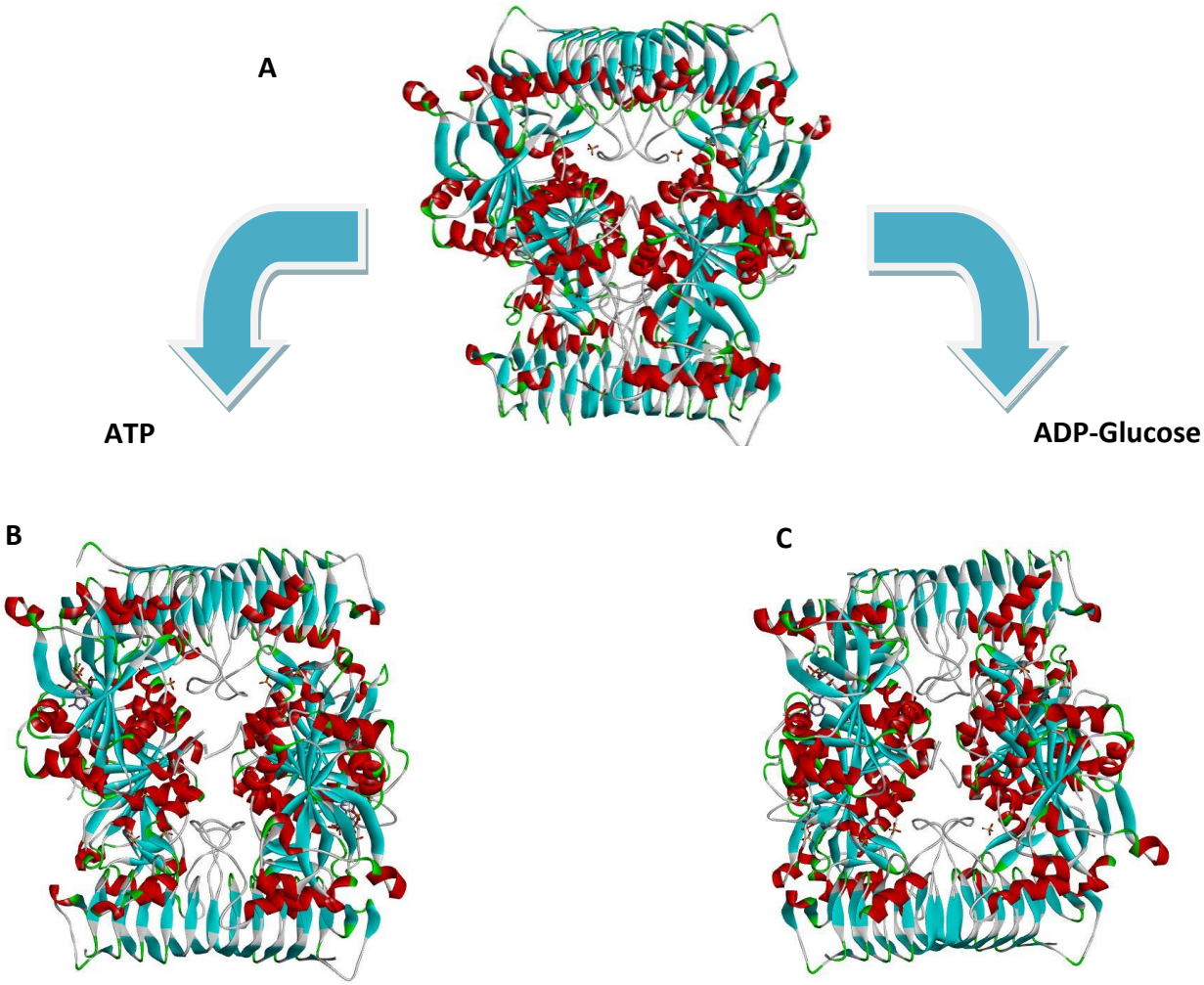

Figure 2.11: Structure of potato tuber AGPase small subunit homotetramer in sulfate bounded form. A) Unbound state, B) ATP bound state, C) ADP-glucose bound state [54].

A and A' subunits of homotetramer has high affinity towards adenine and adenine sugar moiety and therefore A and A' can bind to both ATP and ADP-glucose. On the other hand, B subunit has high affinity towards glucose moiety, and therefore it binds to ADP-glucose. Overall, this results in binding of two ATP and three ADP-glucose molecules to the homotetramer [54]. In fact, these results cohere with the experimental results obtained from studying *E.coli* AGPases which also suggests binding of two ATP and three ADP-glucose molecules [57].

Conclusion to be made from these results is, even when the enzyme is a homotetramer of identical subunits, formation of tetramer imposes non-identical conformations for subunits. Conformations of A and A' can change with binding of substrates or regulators to the protein however A and A' are always identical to each other, B and B' on the other hand must adopt different conformations according to the changes A and A' experience in order to maintain the tetramer. While this asymmetry of subunits is clearly visible in homotetramer, it is thought to be even more oblivious in heterotetrameric enzyme where subunits are not identical. Under such conditions catalytic small subunits are thought to behave very similar to A and A' changing conformation according to the binding of other molecules but maintaining identity to one another. In contrast, regulatory large subunits are thought to behave much like B and B', shifting to different conformations enforced by inter-subunit interactions and binding of other molecules, while maintaining tetramer structure [54].

Determination of crystal structure of heterotetrameric plant AGPase in its active form will reveal its structure-function relationship and how exactly it catalyzes and get regulated. However, until that time structure function relationship of AGPase and its catalytic and regulatory mechanisms will be determined using experimental approaches and computational work.

2.6. Structure-Function Relationship of Plant AGPase

Although many groups tried to obtain the crystal structure of AGPases, only a very limited amount of information regarding to the structure of AGPases were obtained from these approaches. Crystal structure of AGPase from bacterium *Agrobacterium tumefaciens* is obtained in 2008. However, as this enzyme belongs to bacteria it is homotetrameric and regulated by different set molecules compared to many plant AGPases [58]. Only crystal structure data for plant AGPase comes from a study that managed to obtain crystal structure of potato AGPase in small subunit homotetramer form [54]. This research provided valuable information about plant AGPases, however structure obtained in this research is a small subunit homotetramer and represents a "low-activity" form of AGPase that is naturally found only in residual amounts in plant cells. In addition to this, crystal structure of both *A. tumefaciens* and potato AGPases were obtained in inactive conformations due to the presence of ammonium sulfate salt used in crystallization process [54, 58]. Never the less both studies yielded invaluable information about the substrate and regulator binding sites of the AGPase and gave overall insight about its structure. Data obtained from these crystal structure studies are used for the generation of homology models of many other plant AGPases and allowed researchers to design more precise experimental approaches to determine structure-function relationship of plant AGPases.

2.6.1. Experimental Approaches to Determine Structure-Function Relationship

Even before any of crystal structure data was available, researchers determined certain regions and residues that play important roles in determining AGPase functionality. Much of these data relating AGPase structure to its function was obtained using random and site directed mutagenesis approaches and yeast two hybrid screenings.

Basic approach followed in these studies is to clone the genes encoding AGPase subunits to separate bacterial expression vectors and then to express these genes in an *E.coli* strain ($glgC^-$) lacking intrinsic AGPase activity. As untransformed $glgC^-$ cells lack AGPase activity, they are unable to produce glycogen. However, when plasmids encoding large and small subunits of AGPase are expressed in *E.coli* $glgC^-$ cells, AGPase activity is restored and therefore glycogen is produced. Presence of AGPase within *E.coli* glgC cells than can be screened with certain methods such as iodine staining. However, when either one of the

AGPase genes on bacterial expression vectors are subjected to random mutagenesis and then transformed to glgC$^-$ cells together with the wild-type of the other subunit, some cells fail to gain the ability to produce glycogen or produce it in low levels even if they are transformed with both AGPase subunits. This inability of transformed cells to produce glycogen, or produce to produce glycogen in low amounts, can be resulting from several factors such as defects in catalytic or/and allosteric function, loss of subunit interaction or protein stability. After such dead or low activity mutants of AGPase are obtained, genes encoding them are isolated and sequenced to indentify the mutations. Through investigation of these mutation that caused loss of enzyme function, residues and regions that plays roles in catalytic or/and allosteric functions, subunit interaction or protein stability are determined [59, 60]. Furthermore, genes encoding dead or low activity mutants of AGPase can further be subjected to mutagenesis and then can be screened for gain of function. Cells that gained back AGPase activity indicate the newly introduced mutations may have complimented the original mutation that caused loss of function [60]. Investigation of these secondary mutations would provide further insight about structure-function relationship. In addition to this yeast two hybrid screenings can be used to determine if any of these mutations effect subunit subunit-subunit interactions. All these approaches together revealed many hot spots on AGPase that alter enzyme function.

2.6.2 Binding Sites of Allosteric Effectors and Substrates

Previously, it was determined that mutation of a proline, on potato AGPase large subunit at position 52, to Leu cause significant changes in the affinity of enzyme towards 3PGA. This mutant required 45-fold more of it to reach maximum activation [59]. In another study, specific arginine residues on both small and large subunits of maize AGPase are found to play critical role on enzyme function. Those arginine residues were determined according to the sulfate binding residues on AGPase small subunit crystal structure and corresponding residues on both small and large subunits of maize AGPase were determined accordingly. When those arginine residues were mutated to Ala, it is found that the enzymes allosteric properties were drastically altered [61]. In a separate study, researchers indentified most of the mutations on potato large subunit that restore AGPase activity concentrates around the C- and N- terminals of the large subunit. Characterization of these mutants revealed they either show increased sensitivity to 3PGA or increased resistance to Pi inhibition. In addition

to this, Lys-197, Pro-261, and Lys-420 residues were found to be conserved among all known plant AGPases and when these residues are changed with site-directed mutagenesis, enzymes affinity towards 3PGA and Pi gets dramatically altered. These results suggest, these residues are in close proximity to the binding site of effectors [62, 63] .

Similar studies on other residues revealed that, mutating certain residues alters the affinity of the enzyme towards is substrates. For example, in the study conducted by Laughlin et al in 1997 [64], mutating aspartic acid 252 to asparagine lowered the enzymes laffinity towards glucose-l-phosphate and replacement of aspartic acid 121 to asparagine resulted in an enzyme with lower affinity to both glucose-1-phosphate and ATP, while the Ala 106 to Thr substituted enzyme contains altered sensitivity primarily to ATP

2.6.3. Regions on AGPase that Modulate Subunit-Subunit Interactions and Stability

Although both monomers of both AGPase subunits are shown to have activity [39], their activities as monomers are very low and proper enzymatic activity requires the formation of a stable tetramer. In addition to this, it was also determined that proper allosteric regulation of AGPase is not be provided by large subunit alone (although Large subunit plays a larger role), but requires presence and synergy of both large and small subunits together in heterotetramer form [65]. Crystallization studies of AGPases from both *Agrobacterium tumefaciens* and potato suggest that the enzyme is a dimer of dimers [54, 58]. This means that monomers first form dimmers and than those two dimers come together to form the tetramer. Key factor than exclusively determines this subunit-subunit interaction is the interface residues that is found between the two subunits. Specific regions and residues that play important roles in subunit interactions were previously determined. In 1998, Laugin et al determined that when a 19 amino acid long segment is deleted from the C-terminal of either subunit, it causes the abolishment of the heterotetramer formation. These 19 amino acids are thought to play important roles in the assembly of heterotetramer. In a separate study, researcher expressed maize small subunit with the potato large subunit and developed a chimeric AGPase protein. This chimeric AGPase is shown to have low enzymatic activity, much less then either potato or maize AGPases. Further research revealed this loss of activity resulted due to a 55- amino acid long motif found on small subunit (amino acids 322-376). This motif differs only five amino acids between potato and maize AGPase small

subunit yet it is found to play a critical role in small-large subunit interaction and tetramer stability [66].

2.6.4. Computational Approaches to Determine Structure-Function Relationship

One drawback of experimental approaches to determine structure-function relationship of AGPase is; it is very time consuming. As exact structure of heterotetrameric plant AGPase is not known researchers had a very limited initial predictions about structure-function relationship of AGPase and each experiment is required to start from scratch. Consequently, a large number of potential residues and regions that play a role in AGPase function are initially determined and these potential candidates are narrowed to a smaller set of residues or regions in a step by step fashion until the exact residues and regions are determined. In order to shorten this method, many research groups made use of computational approaches to give a preliminary direction to their experiments. These computational methods ranged from providing certain predictions about the structure and giving potential candidates, to the generation of homology models of heterotetrameric plant AGPases. In each case, this allowed experiments to start from a smaller set of candidates, reducing the time and increasing the efficiency of experimental methods.

In the study conducted by Tuncel et al, in 2012 researchers used the crystal structure of homotetramer potato AGPase to generate the homology model of heterotetrameric potato AGPase (**Figure 2.12 and Figure 2.13**). Trough the usage of experimental and computational approaches based on this model, they predicted the assembly order of AGPase heterotetramer and residues that take part in subunit interaction. According to their study, AGPase is formed by the longitudinal and lateral interactions of large and small subunits. Their results suggest, as AGPase heterotetramer forms, large and small subunits first form a dimer vertically and such two dimers come together and the interaction between reciprocal large and small subunits cause two dimers to join and form the tetramer. They also suggested that arginine 88 of large subunit plays a role in both longitudinal and lateral interactions [10]. In another study based on this one, R88 of large subunit is mutated to Ala and as a result heterotetramer formation is abolished [60]. Other researchers used computational methods to generate homology models of other plant AGPases in heterotetrameric form such as , rice [67] and wheat[10].

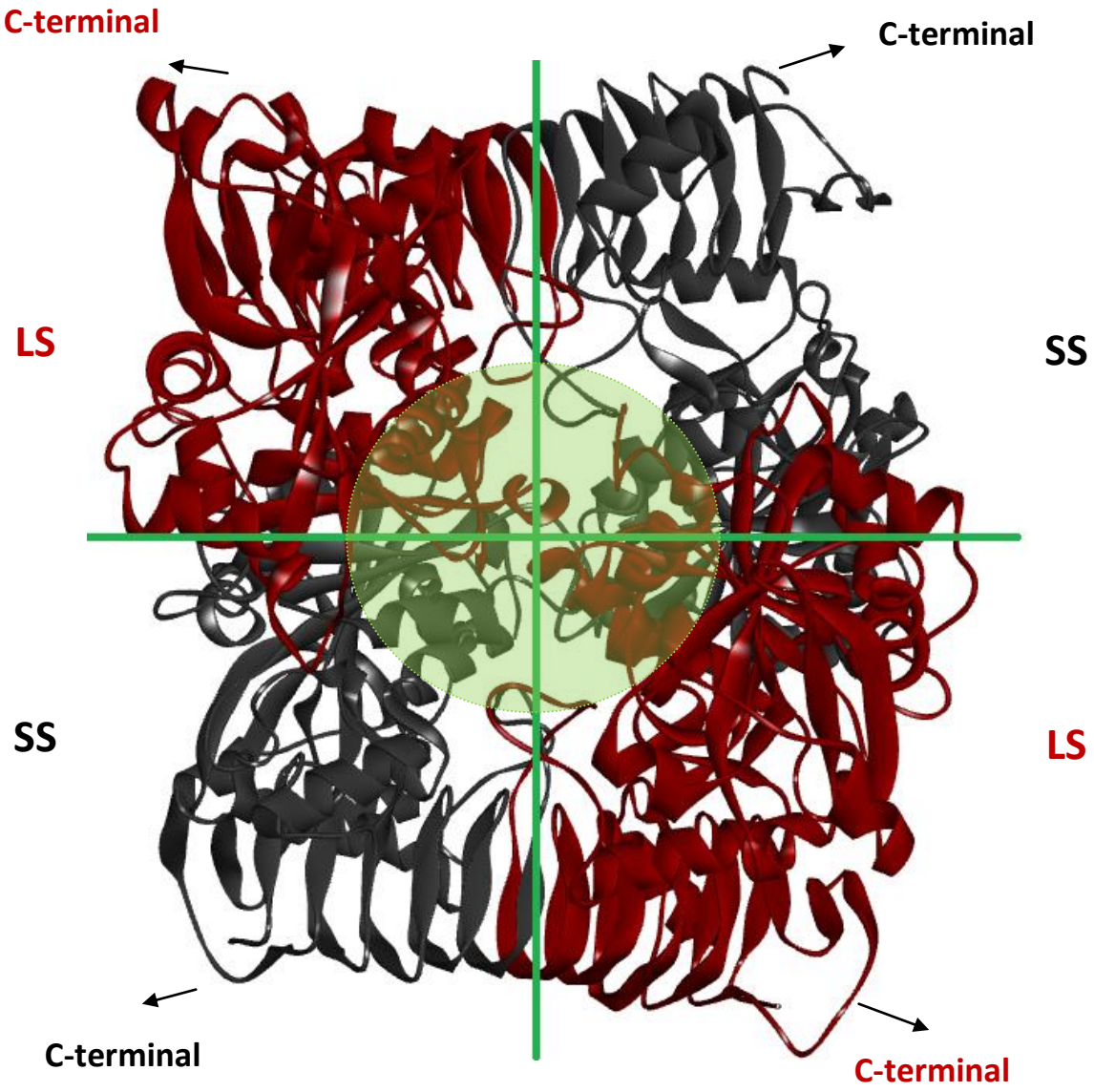

Figure 2.12: Homology model of Heterotetrameric potato AGPase. Large subunits are represented by red and small subunits are represented by black. Green circle in the middle shows the N-terminals of all subunits. [10]

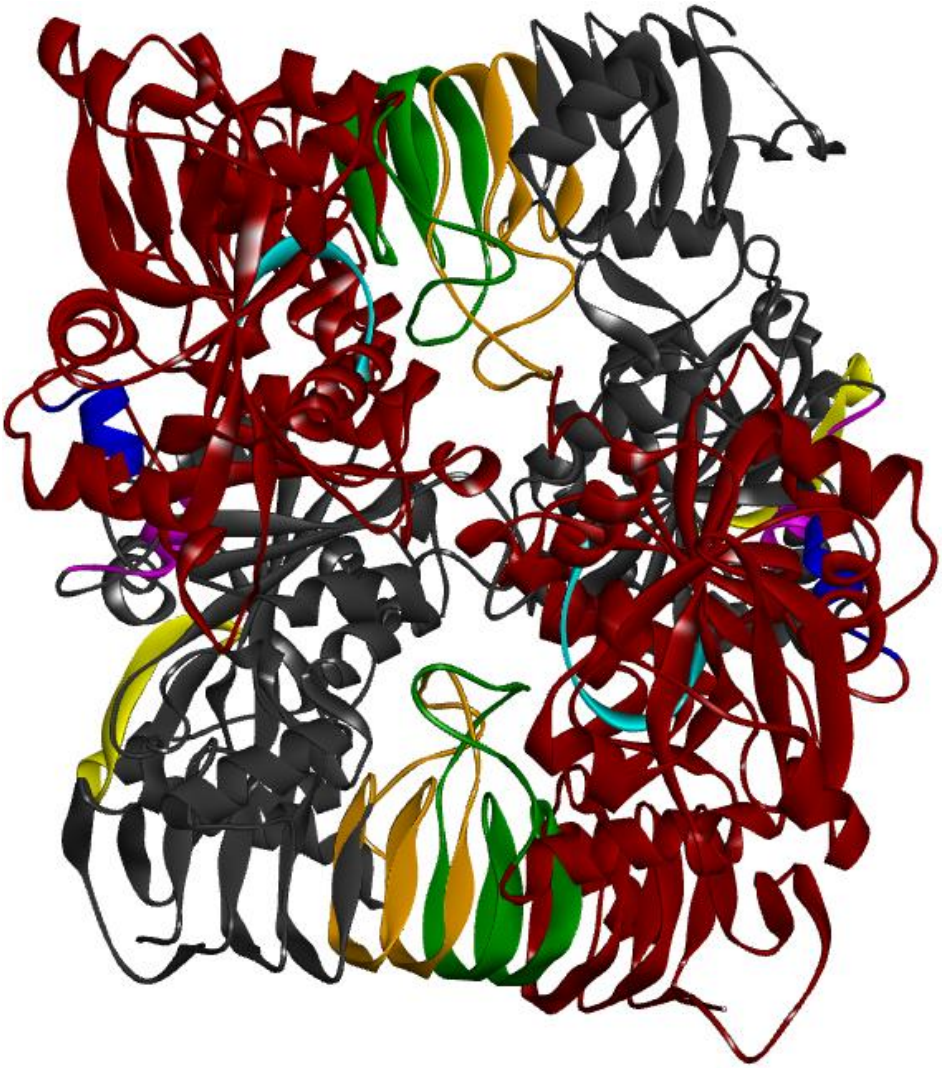

Figure 2.13: Potato AGPase model (adapted from [10]) showing the functional motifs (adapted from [68]). Green; G1P binding motif on LS. Blue; ATP binding motif on LS. Cyan; catalytic motif on LS. Orange; G1P binding motif on SS. Purple; ATP binding motif on LS. Yellow; catalytic motif on L

CHAPTER 3

MATERIALS AND METHODS

3.1. Determination of Mutants to be investigated

AGPase single mutants to be investigated were selected from the research of Bengisu [6]. Originally, selected mutations were one of several mutations found in clones RM16 and RM27. These two clones were observed to have restored synthesis of glycogen in glycogen deficient AC70R1-504 glgC$^-$ *E.coli* cells. In order to define the contribution of selected single mutations on AGPase function, WT-AGPase genes on expression plasmids (pML7) were subjected to site directed mutagenesis to obtain the single mutants.

3.2. Used Cell Lines and Their Preparation

3.2.1 Preparation of Chemically Competent DH5α *E.coli* Cells

DH5α cells from the stock were streaked on a LB agar plate and a single colony is selected and grown in 50ml liquid LB medium overnight. Following day the 50 ml grown cell culture was inoculated into 500 ml liquid LB medium. Cell density of the medium was measured at OD_{600} using a spectrophotometer until the OD_{600} value reached to 0.3-0.4 When desired OD value is reached, culture is cooled using ice until it gets cold. After this, culture was transferred into sterile, pre-chilled centrifuge tubes. Inside a centrifuge that is cooled down to 4°C, cell culture is centrifuged at 4053 rcf (6000 rpm) for 10 minutes. Supernatant is discarded and obtained cell pellet is kept on ice. Pellet is then resuspended in 100ml ice-cold $MgCl_2$ -$CaCl_2$ solution (80mM $MgCl_2$, 20mM $CaCl_2$), centrifuged at 4°C, 4053 rcf for 10 minutes and supernatant is discarded. This washing step was repeated two to three times where pellet was resuspended in 50ml, 25ml and 10 ml of $MgCl_2$ -$CaCl_2$ buffer respectively in each step. Finally, pellet was dissolved in 1ml, ice-cold 100mM $CaCl_2$, 25% glycerol solution and 100µl aliquots were transferred into pre-chilled eppendorfs. Those eppendorfs were subjected to shock-freezing using liquid nitrogen and stored at -80°C for future use.

3.2.2. Preparation of Electrocompetent AC70R1-504 (glgC$^-$) *E.coli* Cells

GlgC$^-$ cells from the stock were streaked on a LB agar plate and a single colony is selected and grown in 50ml liquid LB medium overnight. Following day the 50 ml grown cell culture was inoculated into 500 ml liquid LB medium. Cell density of the medium was measured at OD_{600} using a spectrophotometer until the OD_{600} value reached to 0.6 When desired OD value is reached, culture is cooled using ice until it gets cold. After this, culture was transferred into sterile, pre-chilled centrifuge tubes. Inside a centrifuge that is cooled down to 4°C, cell culture is centrifuged at 4053 rcf (6000 rpm) for 10 minutes. Supernatant is discarded and obtained cell pellet is kept on ice. Pellet is then resuspended in pure and sterile 100ml ice-cold dH_2O, centrifuged at 4°C, 4053 rcf for 10 minutes and supernatant is discarded. This washing step was repeated one more time with pure, sterile dH_2O and two times with %10 glycerol solution in dH_2O. Finally, pellet was dissolved in 1ml, ice-cold %10 glycerol solution in dH_2O and 40µl aliquots were transferred into pre-chilled eppendorfs. Those eppendorfs were subjected to shock-freezing using liquid nitrogen and stored at -80°C for future use.

3.3. Transformation Protocols

3.3.1. Transformation of Chemical Competent DH5α *E.coli* Cells

Transformation of DH5α cells was achieved using heat shock. First appropriate amount of plasmid (<50ng) was added to 100ml of competent cell and the cell-plasmid mixture was incubated on ice for 15 minutes. In the next step, cell-plasmid mixture was transferred to a water bath at 42°C, incubated there for 90 seconds and immediately put back on ice for 2 minutes. After this, 900ml of LB medium with no selection was added to the cells and incubated at 37°C shaker for 45-60 minutes. Finally, cells were plated on an agar medium plate with appropriate selection.

3.3.2. Transformation of Electrocompetent glgC$^-$ *E.coli* Cells

Transformation of glgC$^-$ cells was achieved using Bio-Rad Micropulser. First, 50-100 ng of plasmid was added to 40µl of electrocompetent glgC$^-$ cell. Cell/plasmid mixture was mixed gently and incubated on ice for 1-2 minutes. Next cell/plasmid mixture is transferred to a appropriate, pre-chilled Bio-Rad electroporation cuvette. Filled electroporation cuvette was quickly placed inside the micropulser and pulsed. Transformation of plasmid is successful, if the obtained ms value is around 5.00 or higher. Immediately after the pulse is given, electroporation cuvette was taken out and 900ml of non-selective SOC medium was added. Content inside the electroporation cuvette is transferred to a sterile eppendorf and incubated inside a 37°C shaker for 45-60 minutes. Finally the cells were plated on an agar medium plate with appropriate selection.

3.4. Site Directed Mutagenesis

Wild-type potato AGPase large subunit gene that was previously cloned on an expression vector (pML7) ,with spectinomycin selection, was subjected to site directed mutagenesis using a PCR machine and an appropriate set of site directed mutagenesis primers. Reaction was carried out in a 50µl mixture containing 50-100ng template DNA, 10pmol of each primer, 0.2mM dNTPs, 1X Pfu reaction buffer and one unit of Agilent technologies Pfu-turbo as the DNA-polymerase. PCR conditions for denaturing, annealing and extension were set to 94°C for 10 seconds, 55°C for 30 seconds and 69 for 12 minutes respectively and repeated for 25 cycles. After PCR is over, content was digested with DpnI restriction enzyme to clear former DNA templates. Template free sample then transformed into chemically competent DH5α *E.coli* cells, which are than plated on LB agar with spectinomycin (50µg/ml) selection and incubated overnight at 37°C. Positive colonies are isolated and grew overnight in 10 ml liquid media with spectinomycin (50µg/ml) selection. Finally plasmids were obtained with miniprep, sequenced and mutations were confirmed with BLAST analysis.

3.5. Screening and Selection

Wild-type potato tuber AGPase large subunit was transformed to glgC$^-$-SS cell that were already carrying an expression plasmid (pML10) for potato tuber AGPase small subunit with kanamycin selectivity (**Appendix B)**. As presence of both large and small subunits in glgC-SS/LS$_{WT}$ restored the AGPase activity in glgC$^-$ cell regained the ability to generate glycogen.

After the plasmids carrying the genes for desired potato tuber AGPase large subunit mutants are obtained with site directed mutagenesis and confirmed with sequencing, these plasmids were sequentially transformed to glgC$^-$-SS cells, generating glgC$^-$-SS/LS$_{mutant}$. In order to determine the effect of each mutation on AGPase function glgC-SS/LS$_{WT}$ and each glgC-SS/LS$_{mutant}$ were plated on Kornberg medium containing 2% glucose and 50µg/ml spectinomycin and kanamycin. Glycogen accumulation of cell WT and mutants was detected using iodine staining by exposing the plates to Sigmas iodine beads for 1 minute. Staining profile of mutants was compared with the staining profile of WT and mutants with unusual (either high or low staining) phenotypes were selected for further investigation.

3.6. AGPase Characterization

3.6.1. Protein Expression

GlgC$^-$-SS/LS$_{WT}$ and glgC$^-$-SS/LS$_{mutant}$ cells were plated on LB agar media with 50µg/ml spectinomycin and kanamycin. Single colonies were selected and inoculated overnight inside 10ml liquid LB medium with 50µg/ml spectinomycin and kanamycin. Next day, 500µl of overnight cell culture was transferred to 50ml fresh LB medium with 50µg/ml spectinomycin and kanamycin. When the OD$_{600}$ of the fresh media reached to 1, 10mg/L nalidixic acid and 200mM Isopropyl β-D-1-thiogalactopyranoside (IPTG) were used to induce potato tuber AGPase large subunit encoding pML7 and potato tuber AGPase small subunit encoding pML10 expression vectors respectively. Cells were induced for 20 h at room temperature.

3.6.2. Crude Extract Preparation

Induced cells were cooled on ice and then harvested by centrifugation at 4053 rcf (6000 rpm) for 10 minutes at 4°C.Supernetant is discarded and obtained pellet was washed once with 20 ml Tris-buffered saline (TBS, 50 mM Tris, 150 mM NaCl) and centrifuged at 4053 rcf for 10 minutes at 4°C. Supernatant is discarded and obtained pellet is placed on ice. Cell pellet is resuspended in 1ml cell lysis buffer containing 10% glycerol, 50mM Tris-HCl at ph:8.0, 5mM $MgCl_2$, 400mg/ml Lysozyme, 1mM phenylmethanesulfonyl fluoride (PMSF), 5mM protease inhibitor cocktail (Sigma)and 1.7mM Ethylenediaminetetraacetic acid (EDTA) and incubated on ice for 10 minutes and then sonicated. 100 µL sample representing total cell (TC) extract was taken from the sonicated cell solution and stored in an eppendorf. Remaining cell solution was centrifuged at 16.000 g for 10 minutes. Resulting supernatant, known as cell free extract (CFE), was taken to a clean eppendorf. Protein levels within the CFE was measured using Bradford Assay [69] by using Bio-Rad Laboratories Bradford Assay reagent according to the manufacturer specifications.

3.6.3. Reverse Direction Specific Activity Assay of Crude Extract

A nonradioactive, reverse direction AGPase activity assay developed by Sowokinos[70] was used to determine amount of Glucose-1-Phosphate produced. Production of Glucose-1-Phosphate was coupled with the production of NADPH by utilizing phosphoglucomutase (PGM) and glucose-6-phosphate dehydrogenase (G6PDH). During the assay, Glucose-1-Phosphate produced by AGPase was converted to glucose-6-phosphate by the action of PGM. This glucose-6-phosphate, together with the $NADP^+$ found in assay mixture, acted as a substrate for G6PDH which catalyzes their conversion to NADPH, 6-phospho-glucono-1,5-lactone and H^+. Change in NADPH concentration was measured at OD_{340}, which NADPH gives a peak absorbance, using a spectrophotometer.

Standard, 100µL, primary reaction mixture contained 100mM HEPES (ph 7.4), 1mM NaPPi, 5mM 3PGA, 3mM ADP-Glucose, 5mM $MgCl_2$, 4mM DTT and 0.4mg/ml BSA. Reaction were initiated by the addition of 2-5 µL crude extract containing AGPase (appropriate dilutions must be made to avoid saturation) and incubation of the mixture at 37°C for 10 minutes. After 10 minutes, reaction was terminated via denaturing AGPase by boiling the

mixture for 2 minutes. In the next step, amount of Glucose-1-Phosphate produced was detected by adding a second, 250µL, reaction mixture containing 100mM HEPES (ph 7.4), 0.6mM NADP, 7mM $MgCl_2$, 0.1mg/ml BSA, 0.5 U PGM and 0.5 U G6PDH on top of the first mixture that was terminated by boiling and incubated at room temperature for 5 minutes. Finally, the mixture was centrifuged at 16.000 g for 5 minutes and the absorbance of the clear supernatant was determined at OD_{340}. Amount of glucose-1-Phosphate produced is determined by using a glucose-1-Phosphate standard curve. This standard was produced by adding defined concentrations of glucose-1-Phosphate to the primary reaction mixture and omitting crude extract containing AGPase. Absorbance readings from these mixtures with known glucose-1-Phosphate concentrations were used to generate a standard curve which was used to determine the amount of glucose-1-Phosphate produced by AGPase.

3.7. Partial AGPase Purification

Proteins were expressed and induced in 1L LB medium containing 50µg/ml spectinomycin and kanamycin as described in 3.6.1. After the induction cells were harvested by centrifugation at 4053 rcf (6000 rpm) for 10 minutes at 4°C.Supernetant is discarded and obtained pellet was washed once TBS and centrifuged at 4053 rcf for 10 minutes at 4°C. Pellet is resuspended in 10ml buffer A (10% glycerol, 50mM Tris-HCl at ph:8.0, 5mM $MgCl_2$) containing 400mg/ml Lysozyme, 1mM PMSF, 5mM protease inhibitor cocktail (Sigma) and 1.7mM EDTA and incubated on ice for 20 minutes and cells were disturbed with sonication. Content was centrifuged at 21.000 rcf (14000 rpm) for 1 hour at 4°C. Pellet containing cell debris was discarded and CFE got subjected to further purification steps.

CFE was first subjected to sequential ammonium sulfate precipitation by increasing the final ammonium sulfate concentration within the CFE solution to 30% and 55% by addition of ammonium sulfate salt. At first step, slowly increasing ammonium sulfate concentration to 30% results in salting out of certain proteins but the majority of AGPase did not precipitate. 30% Salt-CFE solution was centrifuged at 21.000 rcf (14000 rpm) for 1 hour at 4°C in order to remove the precipitated proteins. Supernatant was transferred to a clean beaker and its ammonium sulfate concentration was slowly increased to 55% which cause AGPase to precipitate. Precipitated AGPase was harvested by centrifugation at 21.000 rcf

(14000 rpm) for 1 hour at 4°C. Resulting supernatant is discarded and pellet containing AGPase was resuspended in 5ml buffer A. In the next step, resuspended protein extract was subjected to heat shock at 55°C for 5 minutes with gentle mixing and then incubated in ice for 5 minutes. Heat unstable proteins are removed through centrifuged at 21.000 rcf (14000 rpm) for 1 hour at 4°C. Resulting supernatant (CFE_{HS}) that is rich in AGPase is transferred into a dialysis bag for desalting overnight in buffer A. In the next day, desalted sample was flowed through column packed with Macro-Prep High Q Support strong anion exchange support that was previously equilibrated with buffer A. Sample was eluted by using buffer A with gradient NaCl concentration (0-0.5M). Obtained fractions were analyzed with SDS-PAGE (described in 3.9.1.) and reverse direction activity assays (described in 3.8.1) to determine fractions with highest concentration of AGPase.

3.8 Kinetic Characterization

3.8.1. Reverse Direction Kinetic Characterization

Reverse direction kinetic characterization was conducted as described in 3.6.3. with following alterations. While keeping all other substrates and effectors at saturating concentrations (saturating concentration of 3PGA and ADP-Glucose are 5mM and 3mM respectively) varying concentrations of either 3PGA (10mM, 7.5mM, 5mM, 1mM, 0.5mM, 0.25mM and 0mM), Pi (0mM, 0.2mM, 0.5mM, 1mM) and ADP-glucose (0mM, 0.5mM, 2mM, 3mM, 6mM, 10.4mM) were added to the reaction mixture together with 2-5µL of partially purified AGPase with appropriate dilution. Obtained absorbance values at OD_{340} was plotted with Graph Pad (Graph Pad Prism 5), fitted to a Michaelis-Menten equation and Km and Vmax values are calculated for 3PGA and ADP-glucose. Ki value for Pi was determined according to the concentration at which half of AGPase is inhibited.

3.8.2. Forward Direction Kinetic Characterization

Forward Direction Kinetic assay was conducted as described by Hannah et. al. in 2005 [71]. Forward assay was used to determine the increase in pyrophosphate concentration by coupling it to the decrease NADH concentration trough the usage of Pyrophosphate reagent (P7275 Sigma). 100µL Primary reaction mixture contained 50mM HEPES (ph 7.4), 15mM $MgCl_2$, 5mM DTT, 5mM ATP, 5mM glucose-1-Phosphate and 5mM 3PGA. Reaction were initiated by the addition of 2-5 µL partially purified AGPase with pre-calculated appropriate dilutions and incubation at 37°C for 10 minutes. After 10 minutes reaction was terminated by boiling for 2 minutes. After AGPase reaction was terminated, 1 bottle of PPi reagent was dissolved in 22.5ml dH_2O and 150 µL of this dissolved Ppi reagent was added to the terminated primary mixture. Decrease in NADH concentration was monitored at OD_{340} and PPi production was determined according to a Ppi standard curve produced by adding PPi to AGPase free complex reaction mixtures and measuring absorbance at 340nm.

Kinetic characterization was done by keeping all other substrates and effectors at saturating concentrations (saturating concentration of 3PGA,ATP and G1P are 5mM for each) varying concentrations of either 3PGA (2.5mM, 1.25mM, 0.75mM, 0.5mM, 0.25mM, 0.1 mM 0.05mM and 0mM), ATP (2.5mM, 1.25mM, 0.75mM, 0.5mM, 0.25mM, 0.1mM 0.05mM and 0mM), G1P (2.5mM, 1.25mM, 0.75mM, 0.5mM, 0.25mM, 0.1mM 0.05mM and 0mM) and Pi (2.5mM, 1.25mM, 0.75mM, 0.5mM, 0.25mM, 0.1mM 0.05mM and 0mM) were added to the reaction mixture together with 2-5µL of partially purified AGPase with appropriate, pre-calculated dilution. Obtained absorbance values at OD_{340} was plotted with Graph Pad (Graph Pad Prism 5), fitted to a Michaelis-Menten equation and Km and Vmax values are calculated for 3PGA, ATP and G1P. Ki value for Pi was determined according to the concentration at which half of AGPase is inhibited.

3.9. Biochemical Characterization

3.9.1 SDS-PAGE

SDS-PAGE analysis was performed on protein samples to validate the expression of AGPase inside the cells and to determine the quality of fractions obtained during the partial purification (section 3.7.). Analysis was done based on the protocol described by Shapiro et. al. in 1967 and Laemmli in 1970[72, 73]. A 5% stacking SDS-PAGE was added on top of a 10% separating SDS-PAGE gel. Appropriate amounts of proteins were mixed with loading dye (50mM Tri-HCl ph:6.8, 12.5mM EDTA, 1% β-mercaptoethanol, 2% SDS and 0.02% bromophenol blue and 10% glycerol), boiled for 5 minutes and then loaded to wells. Until the samples leave stacking gel, gels were subjected to 90 V and after they enter to the separating gel they were subjected to 140 V for 1.5-2 hours inside SDS-tank buffer. After gel electrophoresis was completed, gels were either stained with coomassie brilliant blue staining or further processed for western blot analysis (described in section 3.9.3.).

3.9.2 Gradient Native-PAGE

Gradient, non-denaturing (native) polyacrylamide gels that preserve the native 3D structure of proteins were prepared in order to distinguish monomers dimers and tetramers of AGPase. Gels were produced in a similar fission to the gels described in section 3.9.1., omitting denaturing agent SDS in the mixture. Gradient structure of gel was provided by a gradient maker by mixing 13% and 3% native gels. On top of this separating gel, a 3% stacking native polyacrylamide gel was added. Samples were mixed with native loading dye and loaded to the wells. Gels were subjected to 90 V for 30 minutes with blue cathode buffer and then gels were subjected 160V for 2 hours with native-tank buffer. After gel electrophoresis was completed, gels were further processed for western blot analysis (described in section 3.9.3.).

3.9.3 Western Blotting

Western immunoblottings were done according to the method developed by Burnette in 1981[74].Either SDS or native Gels that were ran with proteins described in sections 3.9.1. and 3.9.2. transferred to a polyvinyl difluoride membranes (Biotrace PVDF, Pall Corporation, FL, USA) using a semi-dry blotter. After the transfer to the PVDF membrane is complete, it was incubated with 5% BSA in 0.1% Tween20/TBS for 1 hour for blocking. After blocking membrane as incubated with primary anti-LS or anti-SS antibodies (1:7500 dilution in 0.1% Tween20/TBS). After 1 hour membranes were washed with 0.1% Tween20/TBS for clearing unbound primary antibodies and then were incubated with anti-rabbit-HRP conjugated secondary antibody (1:15000 dilution in 0.1% Tween20/TBS) for 1 hour. Membrane was washed with 0.1% Tween20/TBS for clearing unbound secondary antibodies and proteins were visualized using electrochemical luminescence.

3.10. Computational Methods

3.10.1. Visualization of Protein PDB

PDB visualization was made using Accelrys **Discovery Studio 3.1 (**Accelrys Corporation, San Diego, CA, USA).

3.10.2. Conservation Analysis Using ConSurf

Conservation of amino acids of AGPase among a wide range of organisms was calculated using ConSurf Server. ConSurf calculates conservation based on phylogenetic relations between homologous sequences and according to the known 3D structures. ConSurf can automatically search different databases to find homologues sequences and it can use different multiple sequence alignment tools.

Extent which an amino acid position is evolutionary conserved is strongly associated with the functional or structural roles is has. Based on this, ConSurf applies multiple sequence alignment to sequences of AGPase homologues from a wide range of organisms and determines homologous proteins with known 3D structures. If given, ConSurf would use both uploaded sequence and structure data. However, if structure is not available, it would start in ConSeq mode and would only use sequence data but later it would look for known structures that share high similarity with given sequence. Based on these two factors, conservation scores of each amino acid position and the possible structural and functional roles are associated to each position [8] [75].

ConSurf was applied to the Potato AGPase large subunit sequence with accession number Q00081. As no structure was given ConSurf started in ConSeq mode. Multiple sequence alignment was built using MAFFT, the homologues were collected from UNİREF90 and homolog search algorithm was CS-BLAST. CS-BLAST E-value was set to 0.001 and number of iterations was set to 3. Maximum and minimum %ID between homologues was set to 95% and 35% respectively. No limit was given about the maximum number of homologues to be used homologues and therefore this was set to all homologues. Phylogenic Tree was built based on neighbor joining with ML distance. Conservation scores were calculated using Bayesian method.

3.10.3. Effectors Binding Energy and Conformation Calculations Using AUTODOCK

AUTODOCK is a automated docking tool that is designed for predicting how small molecules (ligands) bind to large 3D structure such as a proteins. Autodock calculates the optimum conformation of a small molecule when it binds to a protein and the associated binding energy. Autodock assumes a rigid protein molecules, although side chains can be assumed to be flexible if user desires, and a flexible ligands. Although, generally known as the AUTODOCK, AUTODOCK itself is composed of two main programs known as autogrid4 and autodock4. Autogrid4 calculates grids on a protein for each type of atom find on the ligand molecule. These grids, also known as grid maps, describe the 3D structure of a protein in terms of interaction potential and electrostatic potential. After grids map are calculated, autodock4 calculates the conformation and binding energy based on the information stored on these grid maps and according to the its built-in scoring function [9].

Running AUTODOCK requires four input files; PDBQT files of ligand and the protein, grid parameter file (GPF) and docking parameter file (DPF). All four of these can be created with the program Autodock Tools. PDBQT files were prepared with autodock tools, mostly in an automated fashion, by adding non-polar hydrogen's and Kollman charges. GPF stores the parameters about the number of grid maps to be produced, size and coordinates of the grid box and the spacing between two grid points. GPF that was used in this research is given in appendix (**Appendix C**) DPF stores the parameters about the docking setup such as which docking algorithm is going to be used, number of generations, number of runs and evaluations. DPF that was used in this research is given in appendix (**Appendix C**).

CHAPTER 4

RESULTS

4.1. Location of Mutations

Positions of original (non-mutated) amino acids of selected mutations A91T, F101L, F311L, and E358G are shown on protein sequence potato tuber AGPase large subunit with accession number Q00081 (**Figure 4.1**, **Appendix A**). These mutations are number according to the original amino acid positions given in potato tuber AGPase large subunit homology model generated in the study of Tuncel et. al. in 2008 [10]. As this model lacked the first 12 amino acids shown in potato tuber AGPase large subunit sequence (Q00081), mutation numbers do not match with this sequence. On this sequence they correspond to A103T, F113L, F323L, and E370G.

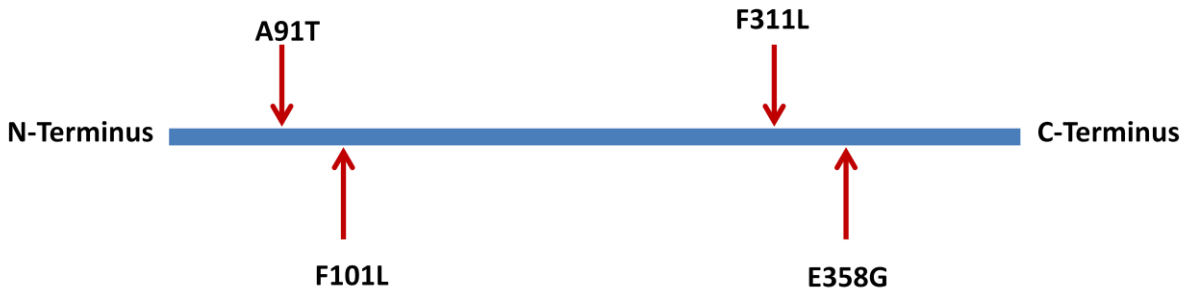

Figure 4.1: Positions of selected mutations on potato AGPase large subunits with accession number Q00081

According to the 3D model generated by Tuncel et.al. in 2008 [10] all mutations with the exception of F311L are found in regions that have functional and/or structurel importence. Mutations A91T, F101L and E358G are found in close proximity with LS-SS interface whereas F311L is moderetly close to the interface (**Figure 4.2**). In addtion to this, mutations A91T, F101L are at the N-terminal of large subunit (**Figure 4.2-A, B**). This region is at a critical position of the heterotetramer where all four subunits make an interface with one another. Especially F101L seems to be at LS-LS interface that is created by the two identical regions of two large subunits. Mutation E358G on the other hand, is on a critical region where both allosteric effectors 3PGA and Pi and the substrate glucose-1-phospahate bind **(Figure 4.2-D)**.

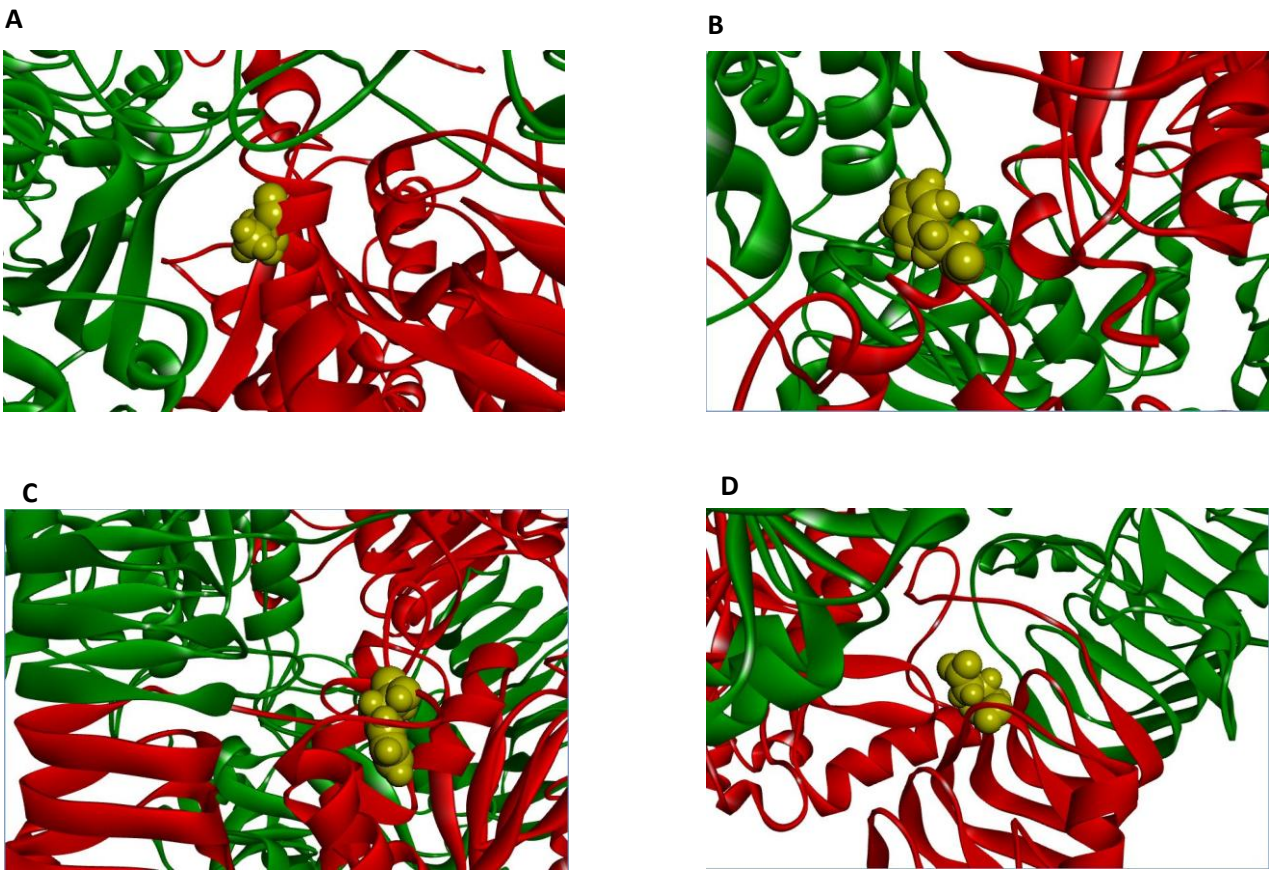

Figure 4.2: Locations of mutation on 3D structure of potato tuber AGPase large subunit. Small and Large subunits are represented by green and red colors respectively, mutations A91t on a), F101L on b), F311L on c), and E358G on d) are represented by yellow color.

4.2. Conservation of Mutated Amino Acids and Regions

Analysis of the locations of the selected mutations indicated that, at least three mutations (A91T, F101L and E358G) correspond to structurally and/or functionally important regions as shown in section 4.1. If this is the case, it is expected that these amino acids and the regions they are found on would be conserved, since mutations happening on the amino acids found on these regions would have evolutionary constrains and therefore such mutations would be under negative selection. In order to check this, conservation of the selected amino acids and the regions they are found on is investigated with ConSurf with the conditions explained in section 3.10.2.

During the analysis, ConSurf homolog search algorithm CSI-BLAST revealed 230 AGPase homolog sequences, where 218 of them were unique. These sequences were originating from a wide range of organisms including many plants, algae and bacteria. ConSeq calculated the conservation scores of every amino acid within the uploaded potato tuber AGPase large subunit sequence according to the variance observed in homologs and specified the most commonly found amino acids at that position (**Appendix D**). Conservation scores are then normalized in such a way that amino acids with average conservation received scores around zero whereas highly conserved amino acids received negative and weakly conserved amino acids received positive scores.

Among the amino acids that correspond to selected mutations, A91 received a normalized conservation score of 0.042 which indicates that Ala at this position has an average conservation. ConSeq indicated that among AGPase homologs most commonly found amino acids at position 91 from highest appearance to lowest is F, S, A, T, N, K, Y, V, H, Q, R, G, L. This result indicates that at least among 218 known AGPase there are certain AGPases that naturally bear Thr at position 91. Furthermore, even if A91 has average conservation score, it is found in a highly conserved region shown in **Figure 4.3** where position 91 corresponds to 103 in given sequence. This highly conserved regions starts from 38th amino acids and spans to 145th amino acid where only few weak conserved amino acids are found.

Amino acid F101 received a conservation score -0.625 indicating that it is highly conserved amino acid. In addition to this, as predicted in section 4.1, ConSeq proposed F101 to be a functional residue (**Figure 4.3)**. Amino acids found at position 101 from highest appearance to lowest are S, A, F, T, N, P, K, Y, C, I, R, L indicating Leu is found at position 101 only in few organisms. Like 91, 101 is also found at the same highly conserved region.

Amino acid F311 received a conservation score -0.564 indicating that it is a highly conserved amino acid. Amino acids found at position 101 from highest appearance to lowest are F, M, C, I, L indicating Leu can be found at position 101 but not commonly.

Amino acid E358 received a conservation score 0.032 indicating that it is an averagely conserved amino acid. Amino acids found at position 358 from highest appearance to lowest are F, N, P, E, V, Q, D, I, L indicating among AGPase homologs Glu at position 358 does not known naturally to evolve to Gly (E358G). This points out that even if E358 has average conservation; its evolution to Gly is under strong negative selection. Furthermore, ConSeq did not assigned a functional or structural property to position 358, yet it is found to be in between two extremely conserved amino acids at positions 357 and 359 with conservation scores of -1.063 and -0.970 respectively. ConSeq assigned 357 to be a structural and 359 to be a functional amino acid (**Figure 4.3)**. Interestingly, as position 358 does not naturally known to bear a Gly among AGPase homologs, position 357 is not known to have any amino acid besides Gly (zero variance). Moreover, this phenotype is not just limited position 358, in fact Gly is found extremely rarely around position 357(**Appendix D**)

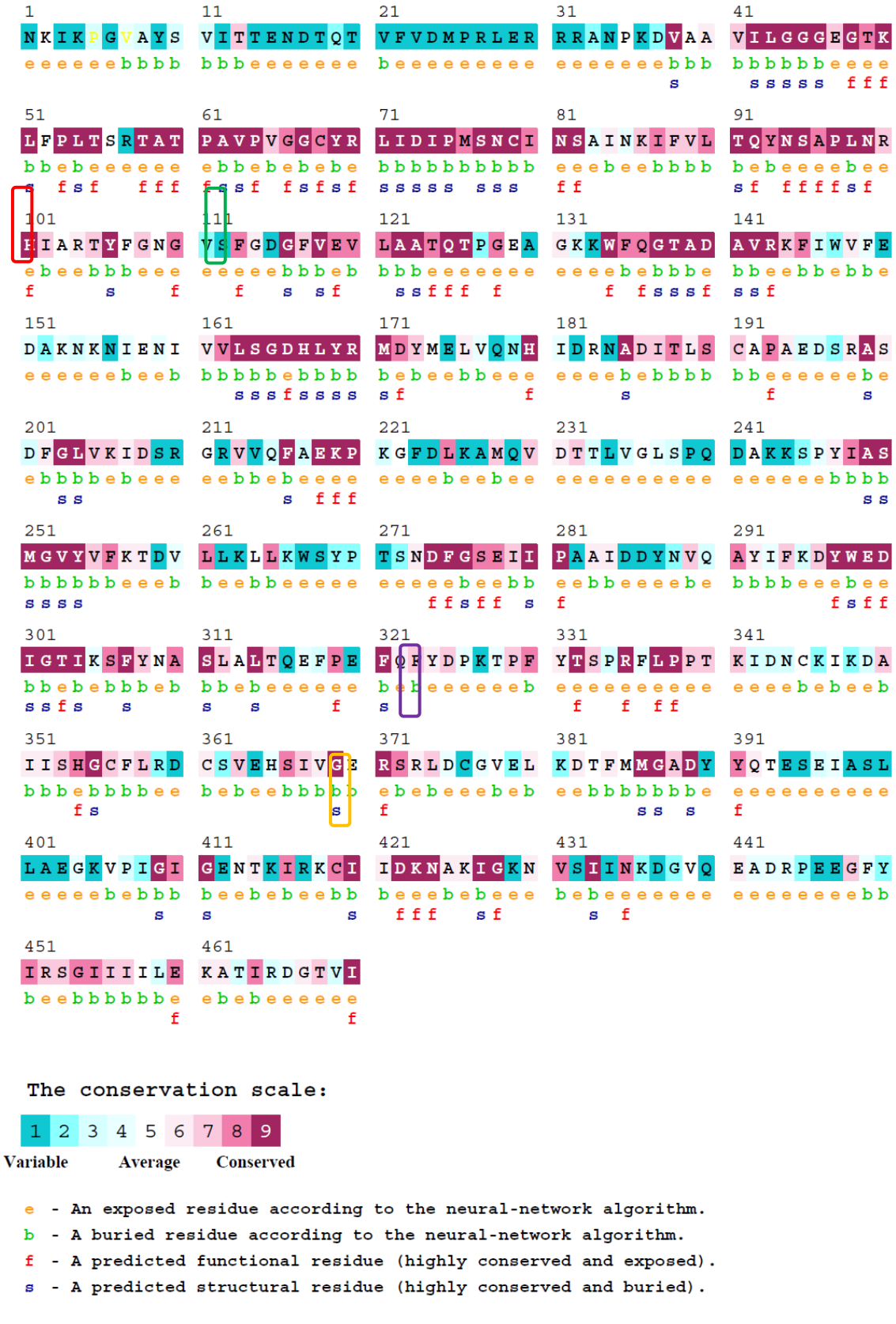

Figure 4.3: ConSeq output of amino acid conservation analysis of potato tuber AGPase large subunit. Amino acids corresponding to mutated A91T, F101L, F311L and E358G are marked with red, green, purple and orange boxes.

4.3. Site Directed Mutagenesis

4.3.1. Mismatch Primer Design

Mismatch site directed mutagenesis primers, which introduce single nucleotide mutations, were designed. Forward and reverse primer pairs ware exactly complimentary to each other but they had a single nucleotide mismatch with wild-type potato AGPase large subunit sequence (accession number: X61187.1). When a PCR was conducted, these mismatch primers introduced a mutation on wild type sequence and caused a predefined nonsynonymous codon substation of wild type amino acid to desired amino acid. **Figure 4.4** shows the forward pairs of 4 different site directed mutagenesis primers, where they correspond on wild type AGPase gene and the nonsynonymous codon substation they cause.

4.3.2. Site Directed Mutagenesis Results

Site directed mutagenesis PCR was performed as described in section 3.4. After the PCR was completed, reaction content was loaded to a 0.8% agarose gel. If the PCR worked it should yield a 6kb PCR product. **Figure 4.5** shows successful site directed mutagenesis PCR and a negative control lacking DNA polymerase.

4.3.3. Transformation to DH5α *E.coli* Cells and Miniprep Extraction Results

PCR products were digested with Dpn-I restriction enzyme. Dpn-I recognizes and digest methylated plasmid DNA and therefore remove former parental plasmid DNA, leaving in vitro amplified plasmids during the site directed mutagenesis PCR. After digestion with Dpn I, plasmids were transformed to *E.coli* DH5α cells described in section 3.3.3. Cell were grown on LB agar plates under spectinomycin selection and grown colonies were inoculated overnight in 10ml liquid LB with spectinomycin selection. Next day plasmids are purified and the quality of plasmid are controlled by spectrophotometer and DNA gel electrophoresis (**Figure 4.6-A**).

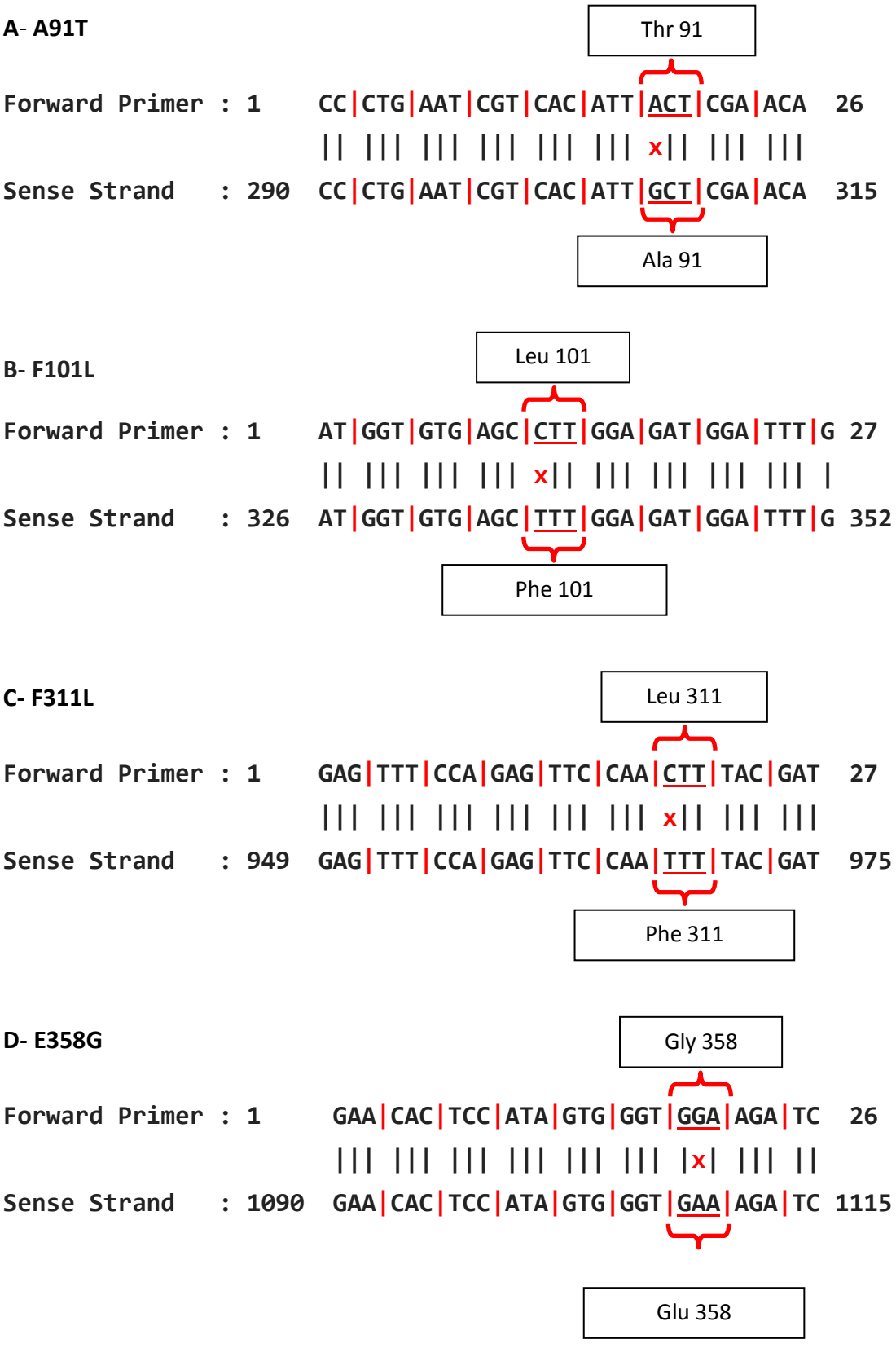

Figure 4.4: Mismatch site directed mutagenesis primers. Sense strand shows wild-type nucleotide sequence and the corresponding amino acid at the highlighted site of potato AGPase large subunits. Primer sequence shows the introduced mutation (red cross) and the corresponding amino acid at the highlighted site.

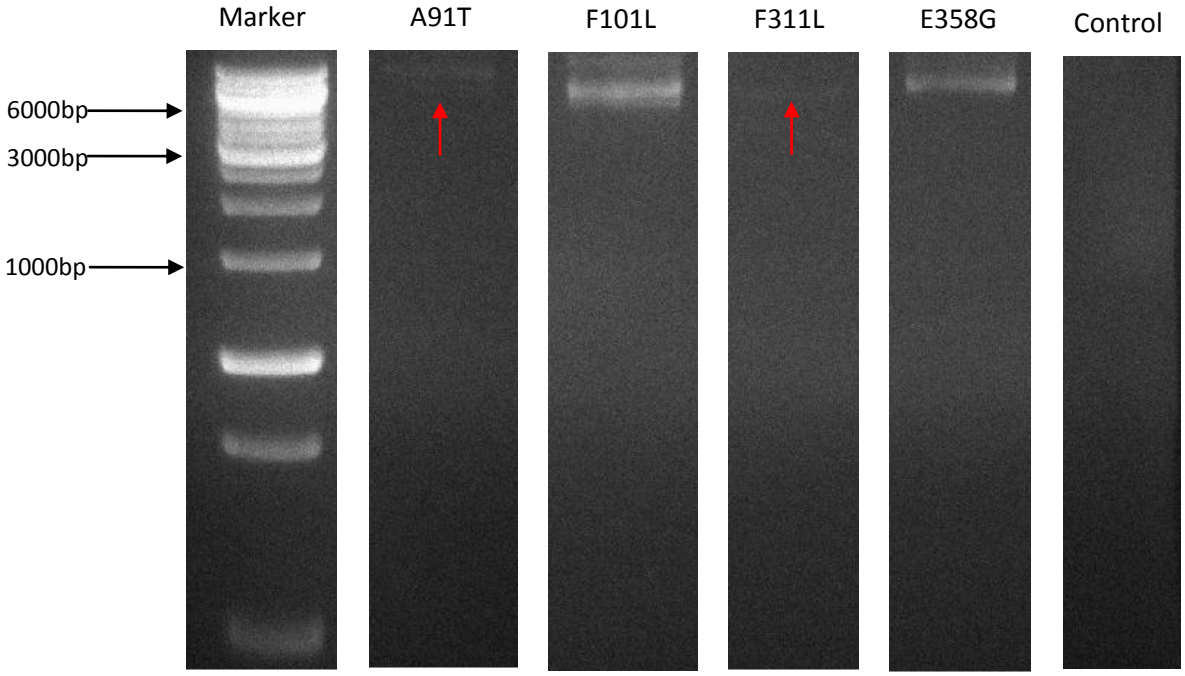

Figure 4.5: SDM PCR results of A91T, F101L, F311L and E359G. PCR products around 6000 basepairs indicate successfully amplification. Red arrows indicate pale SDM products. Representative Control PCR lacked DNA polymerase and therefore no amplification happened.

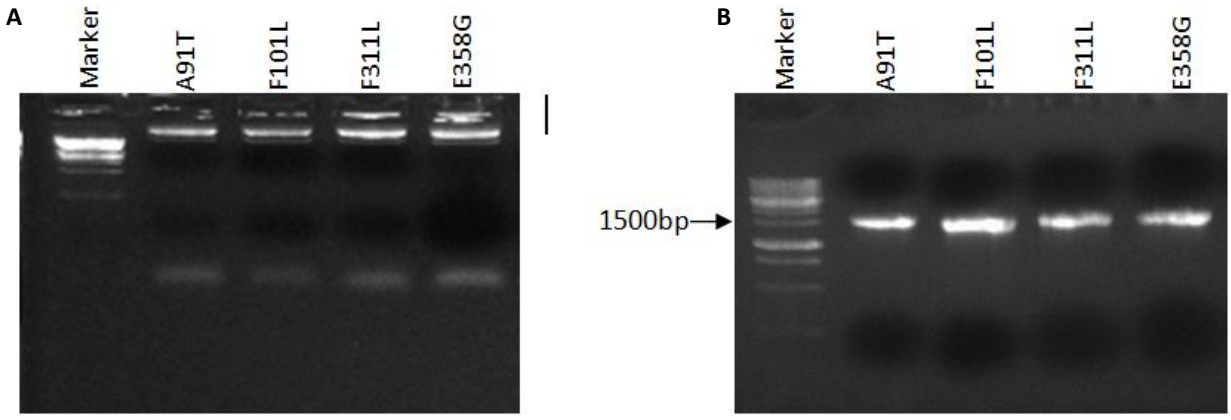

Figure 4.6: (A) Miniprep plasmid extractions of mutant plasmids A91T, F101L, F311L and E358G, as the marker is a linear DNA marker, obtained plasmids are appearing above it. (B) PCR conducted on plasmids obtained through miniprep to verify the existence of AGPase gene inside plasmids and to amplify the gene for sequencing.

4.3.4. Conformation of the Mutations through DNA Sequencing

Plasmids were subjected to PCR with appropriate primers. Then amplification of the plasmids was verified by DNA gel electrophoresis PCR product (**Figure 4.6-B**). Then PCR products were transferred to the *E.coli* and plasmids were isolated. The presences of the mutations were verified by sequencing with appropriate set of sequencing primers and mutations were verified on both nucleotide and amino acid level (**Figure 4.7**).

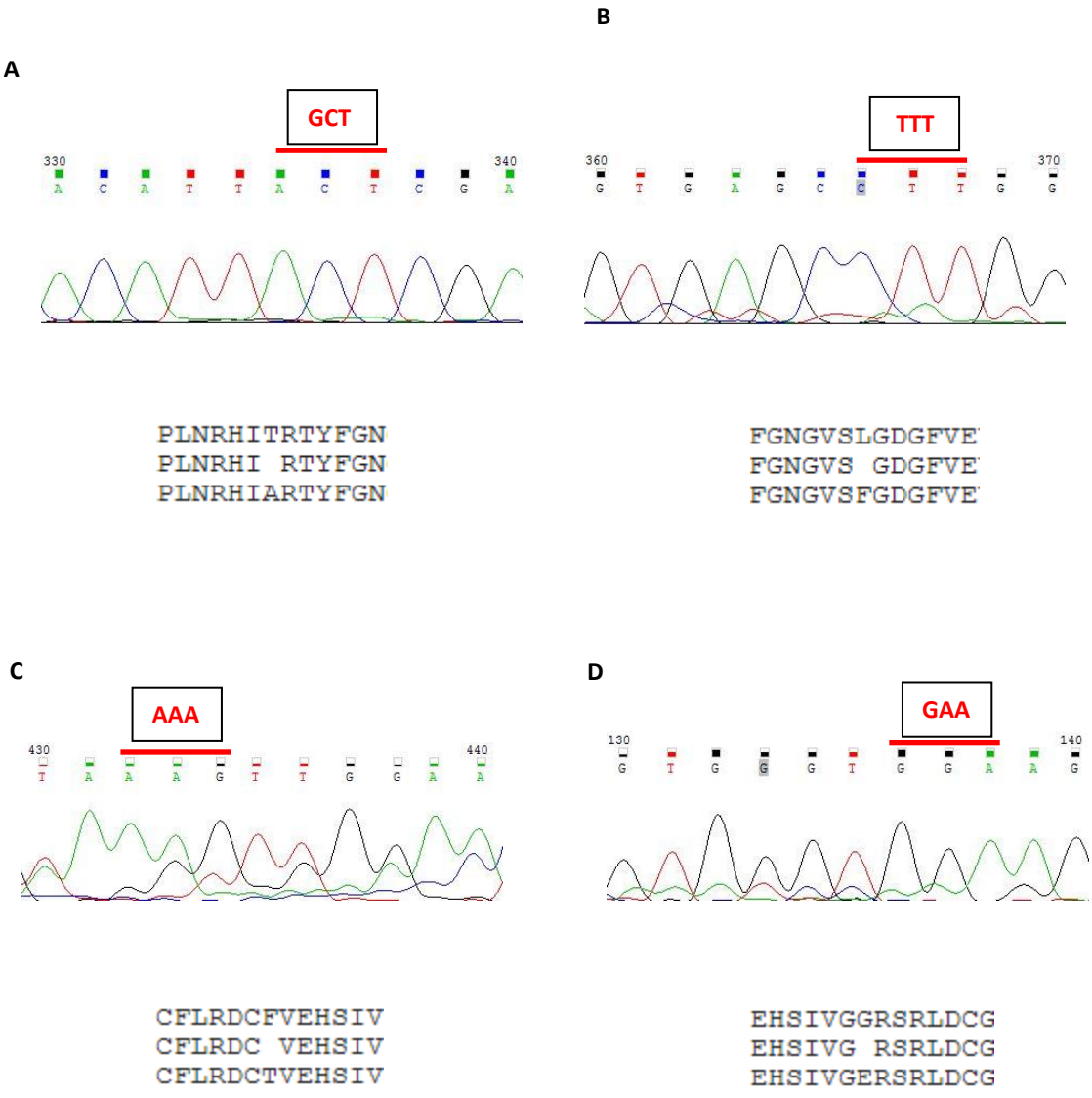

Figure 4.7: Sequencing results and the BLASTX verification of the resulted amino acid change. Red lines show the mutated codon and the boxes above show the wild type codon before mutation. (A) A91T, (B) F101L, (C) F311L, (D) E358G.

4.4 Characterization of Mutants by Iodine Staining

Effect of mutations on AGPase activity was first assessed with iodine staining. Both wild type and mutant potato tuber AGPases large subunit (LS) genes were transformed to *E.coli* glgC$^-$ that contains small subunit (SS) AGPase cDNA as described in section 3.3.2. Transformants were streaked on KB medium containing glucose and grown overnight. Next day cells were subjected to iodine vapor to see the level of the glycogen accumulation in bacterial cells. Stained mutants reflected restoration glycogen production by an active AGPase whereas unstained mutants reflected an inactive AGPase mutant incapable of restoring glycogen synthesis in viable amounts (**Figure 4.8**). Among the selected mutations, glgC$^-$SS transformed with mutant LS-A91T were being stained less compared to the wild type. This indicated that A91T mutation reduced the activity of potato tuber AGPase in *E.coli* system. GlgC$^-$SS transformed with either mutant LS-F101L or LS-F311L were being stained similar to the wild type, indicating these two mutations did not effected AGPase activity in a significant level that is observable in *E.coli* system. GlgC$^-$SS transformed with mutant LS-E358G were completely unstained. This indicated that, E358G mutation caused the potato tuber AGPase to lose activity in *E.coli* system in such a level that the glycogen production can no longer be detected by iodine staining.

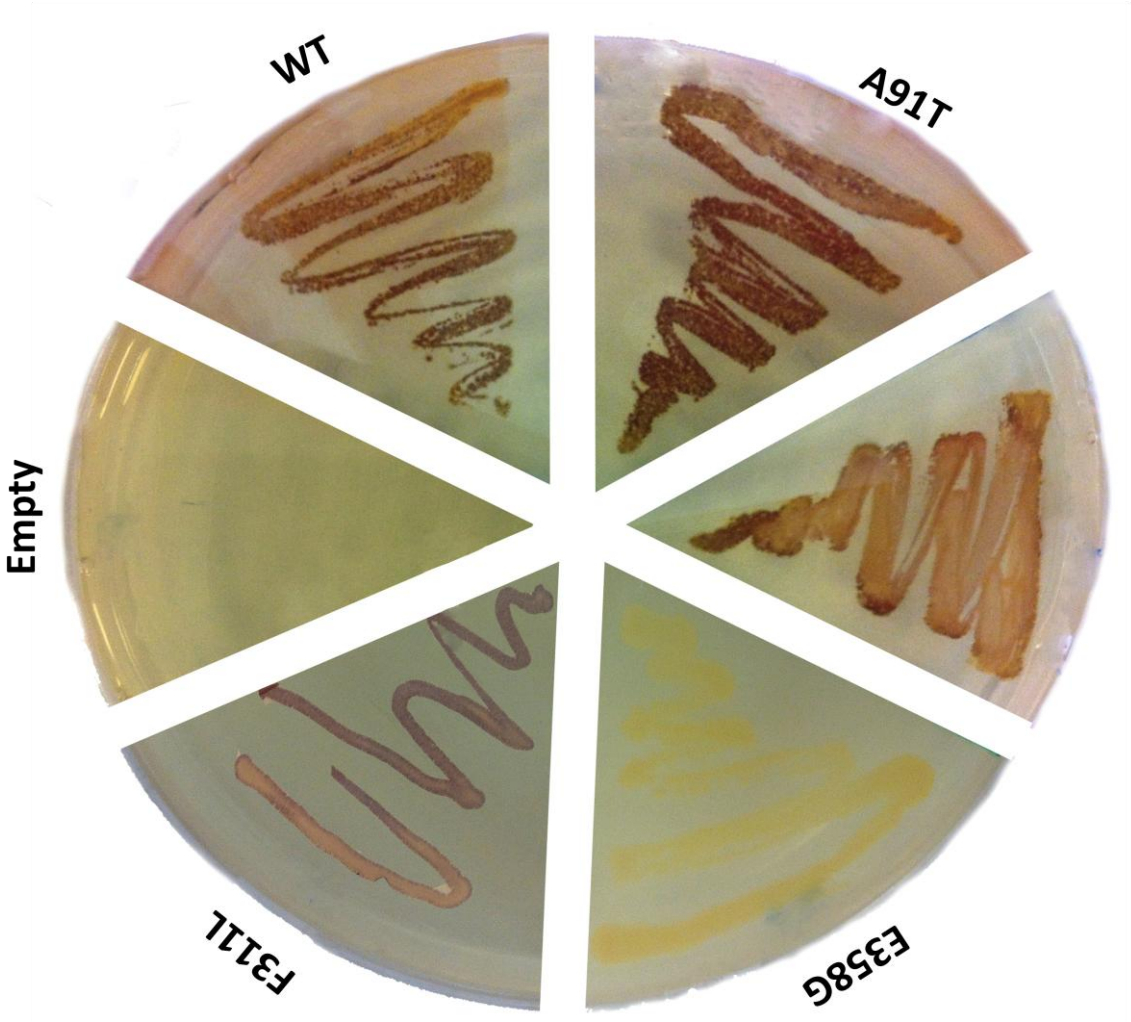

Figure 4.8 Iodine Staining of glgC⁻SS transformed with wild type or mutant (A91T, F101L, F311L and E358G) large subunits. Empty contains no cells.

4.5. Verification of AGPase Protein Expression, Stability and Tetramer Formation

Inability of mutant LS-E358G to restore glycogen synthesis in GlgC$^-$SS raised the question whether this inability was resulting from the loss of enzymatic activity or simply from loss of protein expression, loss of large subunit stability or loss of heterotetramer formation. In order to answer these questions, mutant was biochemically characterized using SDS and Native PAGEs followed by western blots.

4.5.1. Verification of Equal Protein Expression of AGPase Large Subunit-E358G Mutant

Since cells containing LS mutants A91T, F101L and F311L were able to be stained with iodine vapor, there was no doubt about the expression of these mutant LS. However as the GlgC$^-$SS cells transformed with mutant LS-E358G was not staining, expression of the LS-E358G must be verified. This verification was done by preparing the crude extracts of GlgC$^-$SS cells transformed with WT-LS or mutant E358G-LS (section 3.6.1-2) and then making SDS-PAGE followed by western blot of these samples (**Figure 4.9**). Results indicated LS mutant E358G was being expressed inside transformed GlgC$^-$SS cells and since 5µL CFE samples from both WT and mutant E358G showed equal amount of signal their expressions of proteins were similar.

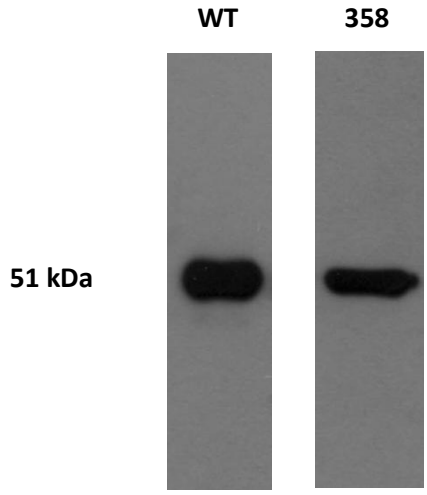

Figure 4.9: Expression of mutant E358G. SDS-PAGE followed by Western blot analysis of GlgC$^-$SS cells transformed with either WT-LS or mutant E358G-LS and. 5µL CFE of each sample is loaded and the presence of large subunit was detected in both samples using anti-LS antibody.

4.5.2. Verification of Assembly and Tetramer Formation of AGPase Large Subunit Mutants

After the expressions of all mutants were ensured, ability and extent of these mutants to form heterotetramers were investigated using native-PAGE. As native-PAGE conserves the 3D structure of proteins, when AGPase mutants were loaded, it was possible to observe the monomer, dimer and tetramer forms of AGPase. AGPase is thought to be a dimer of dimers meaning LS and SS subunits join together and form a heterodimer and two such dimers came together and form the heterotetramer. As a result of this, when wild-type AGPase was expressed in *E.coli* and the collected cell extract was subjected to native-PAGE followed by western blot, all forms (monomer, dimer and tetramer) were detectable using both anti-LS and anti-SS antibodies (**Figure 4.10-A, B**).

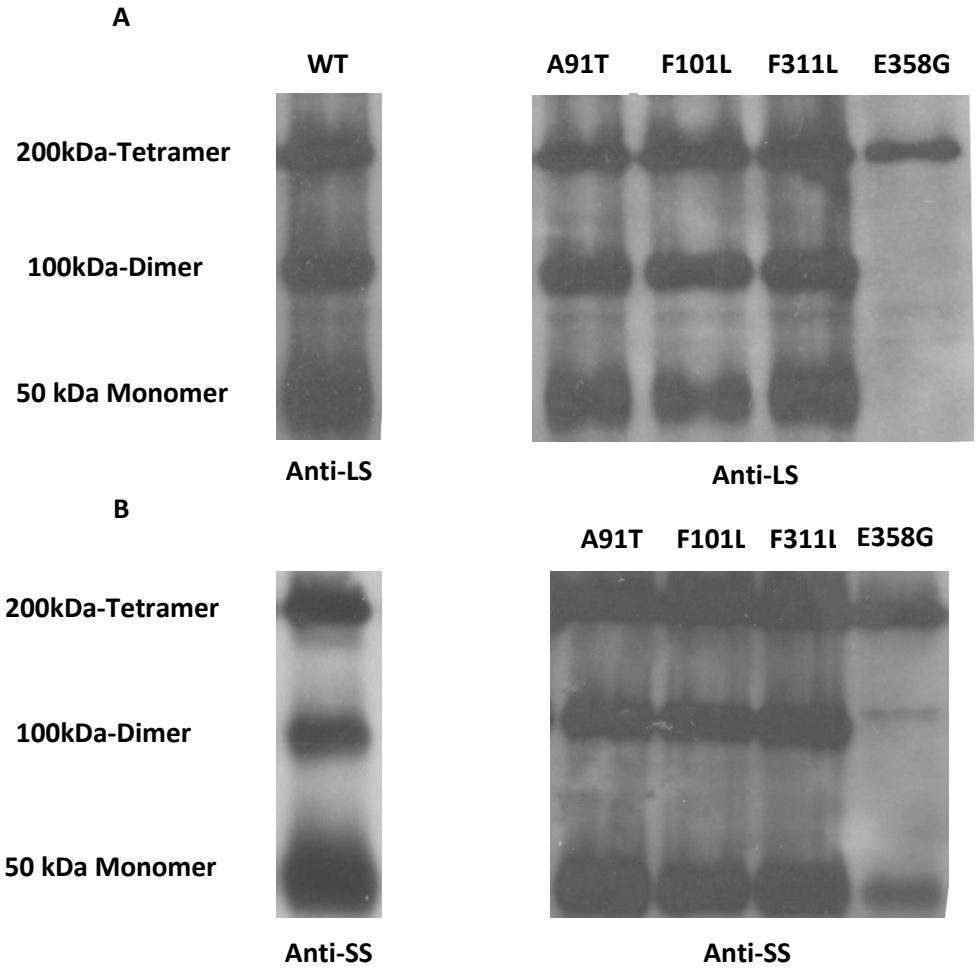

Figure 4.10: Assembly of WT and Mutant AGPases. Native-PAGE followed by western blot analysis of GlgC⁻SS cells transformed with either WT-LS or one of mutant A91T-LS, F101L-LS, F311L-LS E358G-LS. 5µg CFE of each sample is loaded and the presence of large subunit was detected in (A) using anti-LS antibody and small subunit in (B) using anti SS-antibody.

Assembly of AGPases containing large subunit Mutants A91T, F101L and F311L were very similar to assembly of wild type AGPase. These three mutants, along with wild type, showed 3 distinct lanes for monomer dimer and tetramer. However, LS-E358G mutant showed a highly unusual assembly profile, where monomers and dimers were almost completely disappeared and all AGPase was found in heterotetrameric form. Under equilibrium, wild type AGPase is found in all three forms (monomer, dimer and tetramer) within an *E.coli* cell and as presence of tetrameric AGPase is not possible without presence of monomers or dimers, reduction in the amount of monomer and dimer within the cell by found within the cell can be explained by the shifting of equilibrium to the tetramer.

In order to better characterize the assembly of AGPase containing mutant LS-E358G and to ensure that the observations are not just resulting from the amount of protein loaded to the gel, different amounts of WT and mutant LS-E358G was subjected to a native page followed by western blot(**Figure 4.11-A**) . Results showed that, regardless of the amount of protein loaded to the gel, mutant LS-E358G has higher fraction of heterotetramer compared to the wild type according to both anti-LS and anti-SS antibodies (**Figure 4.11-C, E)**. In terms of the total signal obtained from AGPase, it was found that 1µg total protein sample containing WT AGPase gave most similar total signal to the 2µg total protein sample containing mutant AGPase LS-E358G (or 1µg WT to 0.5 µg E358G)for both anti-LS or anti-SS antibodies. This indicated that expression of WT AGPase within *E.coli* GlgC^{-}SS cells is two times higher than expression of AGPase with mutant LS-E358G. However, amount of signal obtained from the tetramer fraction is higher for both cases, with comparable total signals (2µg WT and 1µg E358G, 1µg WT and 0.5µg E358G) and with equal amount of total protein (2µg WT and 2µg E358G, 1µg WT and 1µg E358G, 0.5µg WT and 0.5µg E358G) (**Figure 4.11-B, D)**. Detection of AGPase with anti-SS antibody exhibited a phenotype, which indicated as if mutant AGPase LS-E358G forms no monomers and dimers. However this phenotype did not resulted from absence of monomers and dimers but instead, it results from the fact that SS of AGPase is limiting (since SS can also form SS homotetramers) and therefore enhanced heterotetramer formation means all available SS monomers and dimers form heterotetramers.

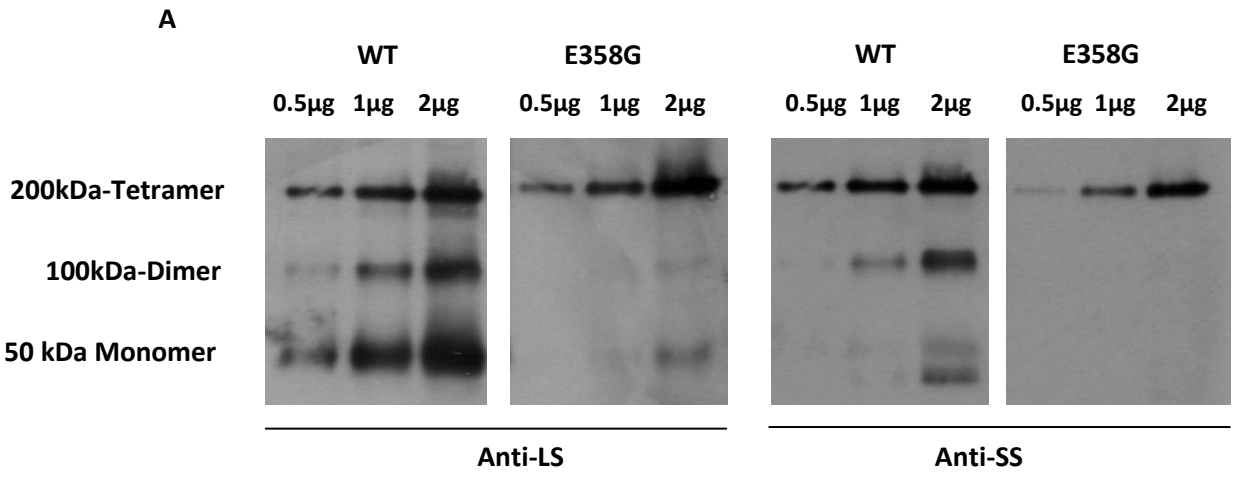
A
WT
E358G
WT
E358G
0.5µg 1µg 2µg
0.5µg 1µg 2µg
0.5µg 1µg 2µg
0.5µg 1µg 2µg
200kDa-Tetramer
100kDa-Dimer
50 kDa Monomer
Anti-LS
Anti-SS

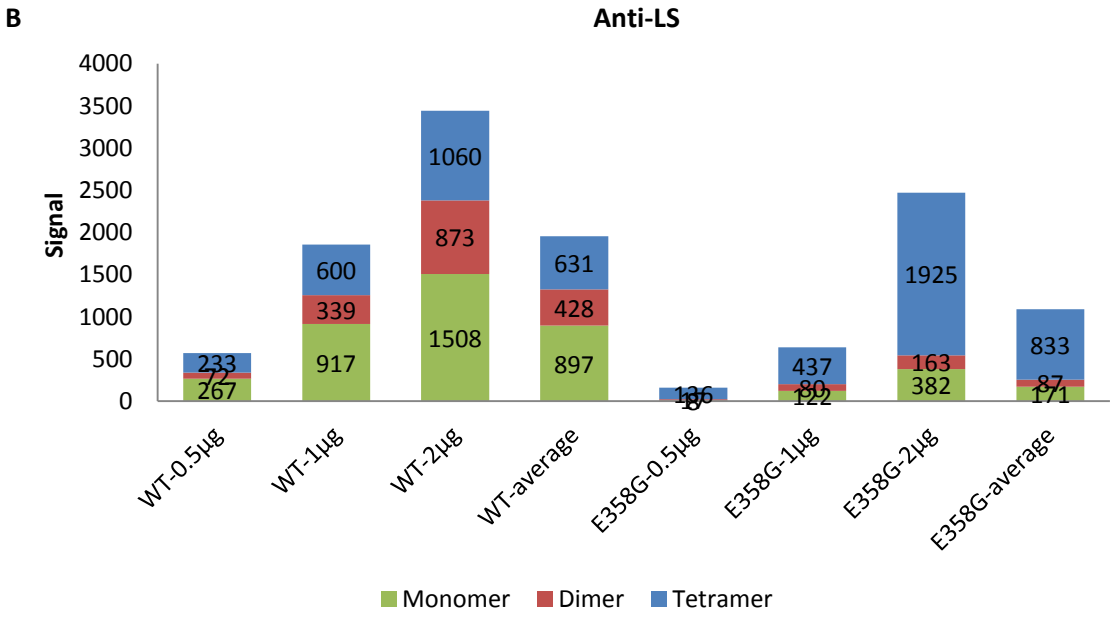
B
Anti-LS
Signal
4000
3500
3000
2500
2000
1500
1000
500
0
233
72
267
600
339
917
1060
873
1508
631
428
897
136
18
437
80
122
1925
163
382
833
87
171
WT-0.5µg
WT-1µg
WT-2µg
WT-average
E358G-0.5µg
E358G-1µg
E358G-2µg
E358G-average
Monomer
Dimer
Tetramer

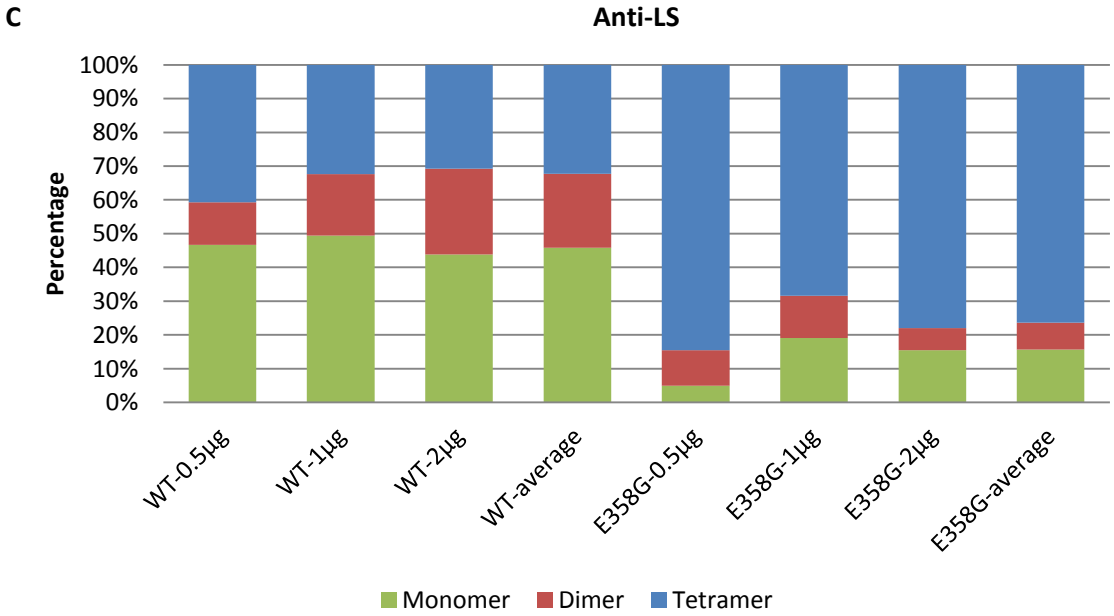
C
Anti-LS
Percentage
100%
90%
80%
70%
60%
50%
40%
30%
20%
10%
0%
WT-0.5µg
WT-1µg
WT-2µg
WT-average
E358G-0.5µg
E358G-1µg
E358G-2µg
E358G-average
Monomer
Dimer
Tetramer

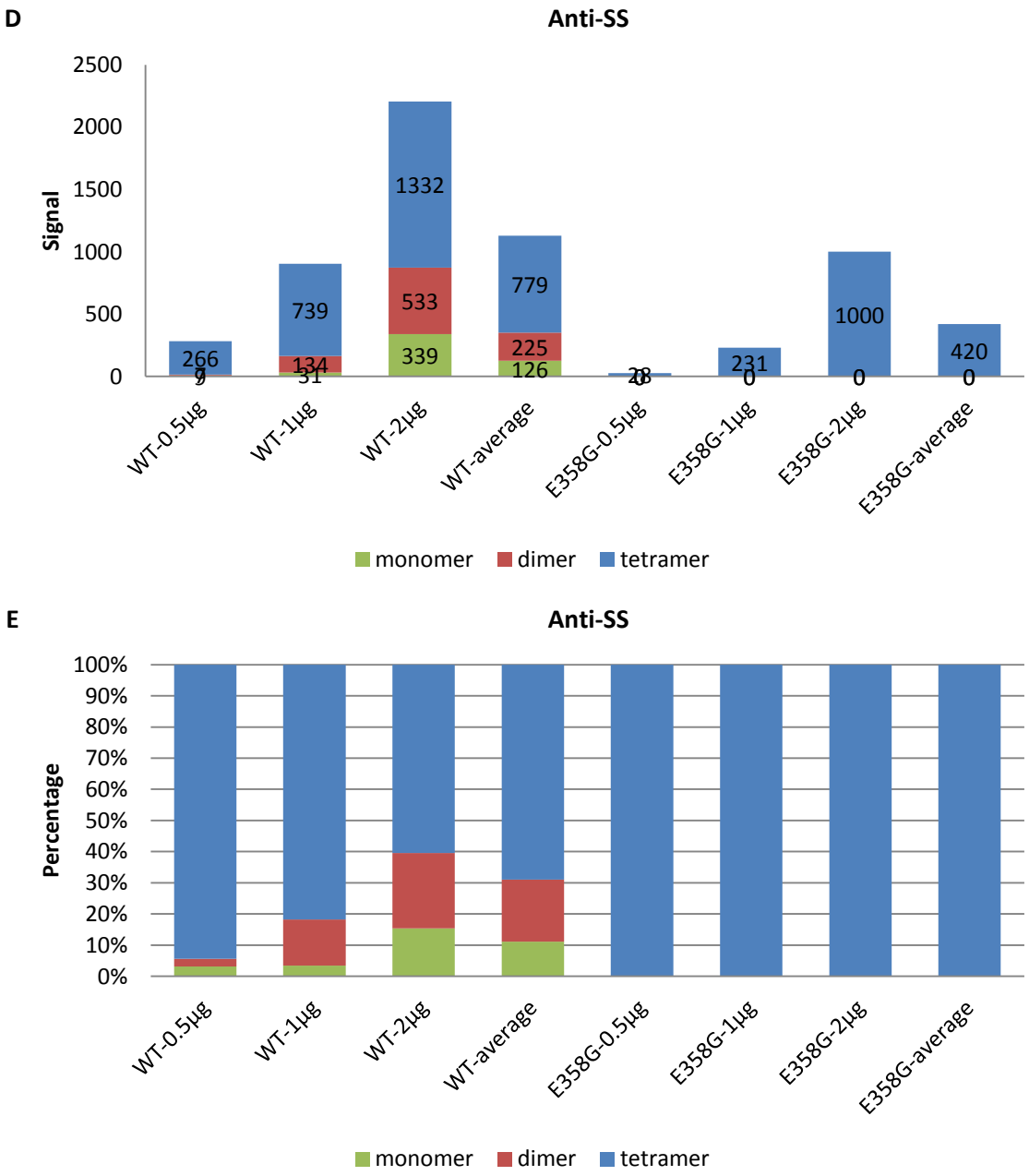

Figure 4.11: Titration Assay of WT and E358G and quantification of western blot bands. (A)Native-PAGE followed by western blot analysis of GlgC^{-}SS cells transformed with either WT-LS or mutant E358G-LS. 0.5, 1, 2µg CFE of each sample is loaded to the gel and the presence of subunits were detected using anti-LS antibody and anti SS-antibodies to ensure that the protein around 200 kDa and 100 kDa was the heterotetramer and heterodimer of AGPase respectively. (B) Quantification of signals, obtained in A, from monomer, dimer and tetramer fractions of WT AGPase and mutant AGPase LS-E358G using anti-LS antibody. (C) Percentage of monomer, dimer and tetramer fractions found in WT and mutant AGPase and according to anti-LS antibody. (D) Quantification of signal, obtained in A, from monomer, dimer and tetramer fractions of WT AGPase and mutant AGPase LS-E358G using anti-SS antibody. (E)Percentage of monomer, dimer and tetramer fractions found in WT and mutant AGPase according to anti-SS antibody.

4.5.3. Stability of AGPase containing Mutant LS-E358G

4.5.3.1. Tetramer Stability

Since mutant AGPase containing LS-E358G increased showed significantly higher heterotetramer composition compared to the wild type AGPase, we hypothesized that this mutation might in fact increase the stability of the tetramer causing the equilibrium to shift towards tetramer. It is know that even the heterotetramer of wild type (WT) AGPase is heat stable protein up until 60°C, although its dimer and monomer loses their stability after 45°C - 50°C. [76] If mutant LS-E358G causes the formation of a more stable AGPase tetramer, it is expected that the heat stability of the heterotetramer also increases protein. To test this, separate cell free extracts obtained from glgC$^-$SS cells transformed with WT-LS or mutant E358G-LS were subjected to heat shock assays at 0°C 50°C 60°C 62°C and 64°C for 5 minutes. Next the samples were centrifuged at 21.000 rcf for 15 minutes to remove the denatured proteins. Finally all samples were subjected to native-PAGE followed by western blot (**Figure 4.12**).

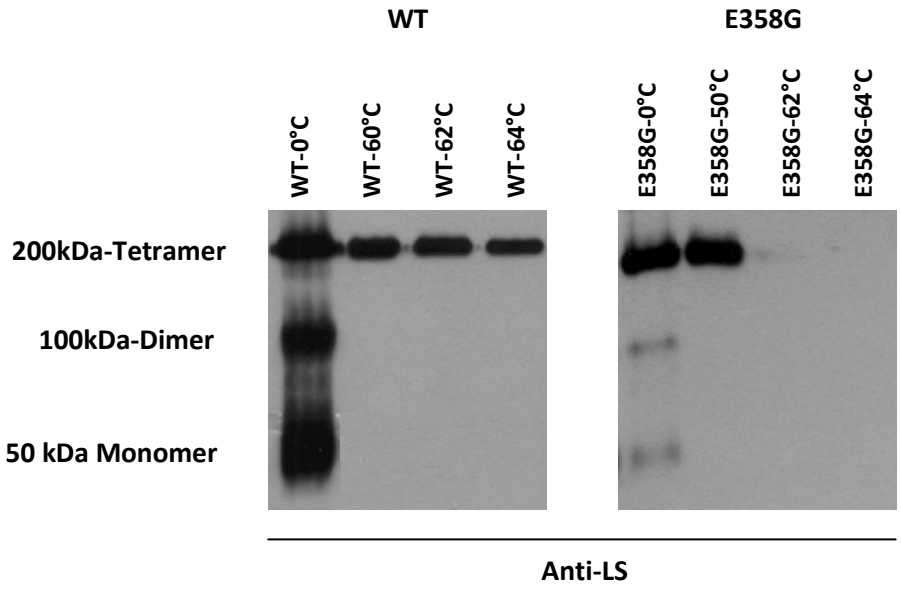

Figure 4.12: Heat stability assay of WT and mutant E358G.Native-PAGE followed by western blot analysis of GlgC$^-$SS cells transformed with either WT-LS or mutant E358G-LS. Samples were subjected to heat shock at denoted temperatures for 5 minutes. 2µL heat shocked CFE of WT and 2.5µL heat shocked CFE of E358G is loaded to the gel and western blot detection was made using anti SS-antibodies

Results of the heat shock assay revealed just the opposite of what was hypothesized. Aside from being more stable than heterotetramer of AGPase with wild type LS, heterotetramer of AGPase with mutant LS-E358G is in fact far more unstable. Although heterotetramer of AGPase with wild type LS did not lost stability until 62 °C, at the same temperature stability of AGPase with mutant LS-E358G is almost completely gone. These results showed increased heterotetramer fraction of AGPase with mutant LS-E358G cannot be explained directly with increased heterotetramer stability (see section 4.7 and Discussion).

4.5.3.2. Monomer Stability

If the increase in heterotetramer and decrease in dimer and monomer fractions of AGPase with mutant LS-E358G is not due to direct increase heterotetramer stability, we hypothesized that it might be resulting from decrease in the stability of LS-monomer and heterodimer. If this is the case, at cellular conditions heterotetramer of AGPase with wild type LS and mutant LS-E358G has similar stabilities but the LS-monomers and heterodimers of mutant LS-E358G is less stable than those of wild type. Therefore AGPase with mutant LS-E358G shows much less heterodimer and LS-monomer compared to AGPase with wild type LS. In order to test this, wild type LS and mutant LS-E358G was expressed inside GlgC cells in the absence of small subunit and total cell and cell free extract samples were subjected to SDS-PAGE followed by western blotting (**Figure 4.13**). Even the large subunit of wild type AGPase is known to be unstable when expressed in the absence of small subunit. When AGPase small subunit is not present, only a small number of AGPase large subunits stay as soluble proteins and the majority of AGPase large subunits form insoluble inclusion bodies. If the LS-monomer of mutant LS-E358G is less stable compared to wild type, it is expected to form more inclusion bodies and less soluble large subunits compared to the wild type.

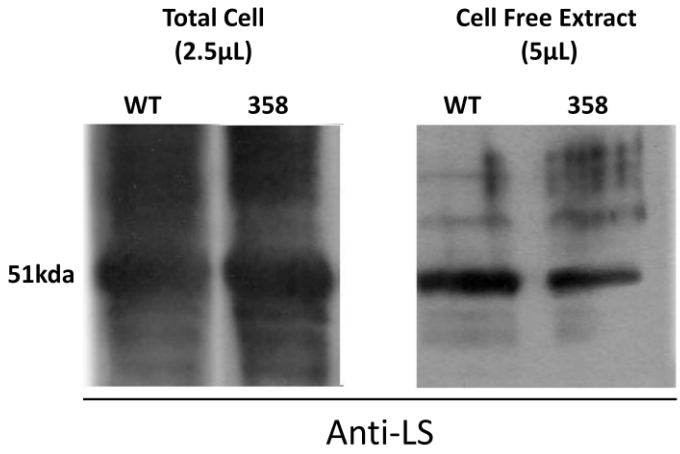

Figure 4.13: LS-E358G monomer stability of WT and E358G. SDS-PAGE followed by western blot analysis of GlgC cells transformed with either WT-LS or mutant E358G-LS. 2.5µ Total cell samples show the whole protein whereas cell free extract show the soluble proteins.

Results of the LS-E358G monomer stability assay revealed that there was no significant stability difference between the WT LS and mutant LS-E358G monomers. This result together with the tetramer stability assay revealed that increased heterotetramer fraction of AGPase with mutant LS-E358G cannot be directly and solely explained by the changes in the stability of monomer or tetramer. Although LS mutation E358G caused the AGPase heterotetramer fraction to increase and the heterodimer and monomer fractions to decrease, this effect seem to happen due to a secondary affect this mutation induces.

4.6. Partial Purification of AGPase containing Wild Type and Mutant LS-E358G

Based on the interesting phenotype of mutant AGPase containing LS-E358G, this mutant was selected for kinetic characterization. As a result of this mutant AGPase containing LS-E358G along with AGPase containing wild type LS was partially purified (**Figure 4.14 and 4.15**) as described in section 3.7. Quality of purification and which fractions to store were made based on SDS-PAGE and reverse direction specific activity assays. Purification results summarized in **table 4.1** .

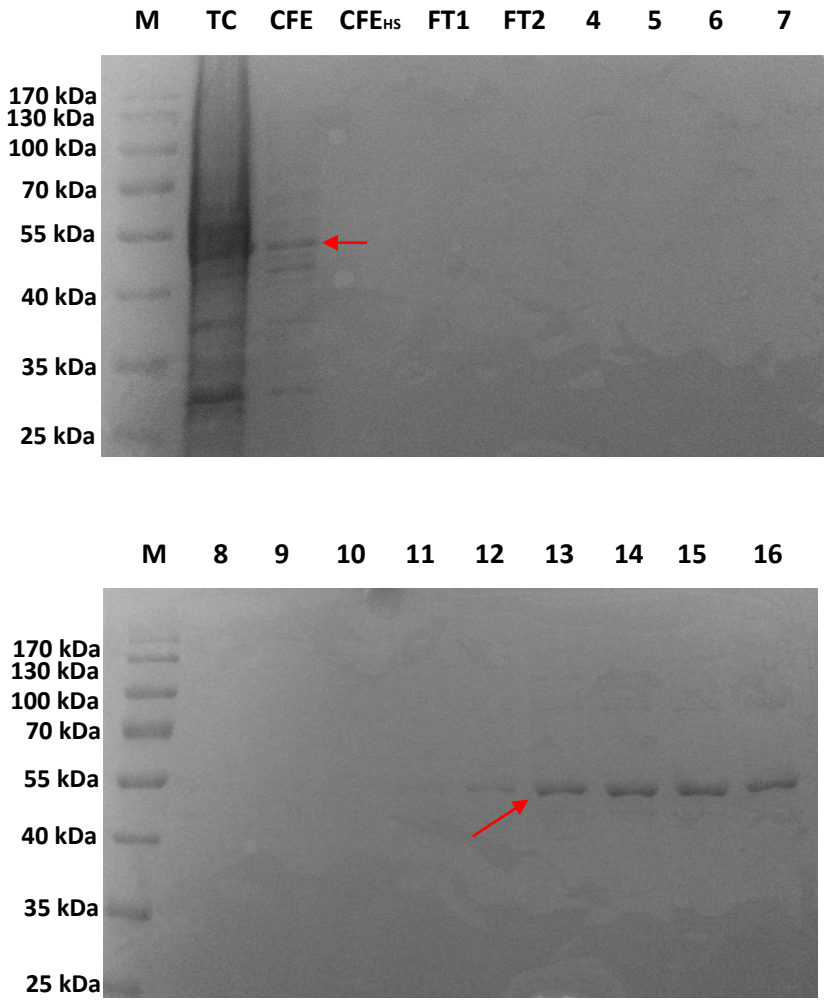

Figure 4.14: SDS-PAGE analysis followed by Coomassie blue staining of partial purification samples of the AGPase with wild type LS. Quality of the purified samples was monitored using SDS-PAGE sample with highest AGPase fraction was chosen (fraction 13). Red arrows indicate the location of AGPase which appears around 51 kDA. TC: total cell, CFE: cell free extract, CFE_{HS}: cell free extract after heat shock, FT1,2: flow through 1 and 2, numbers 4-16: 4^{th} to 16^{th} fractions obtained during the elution of AGPase.

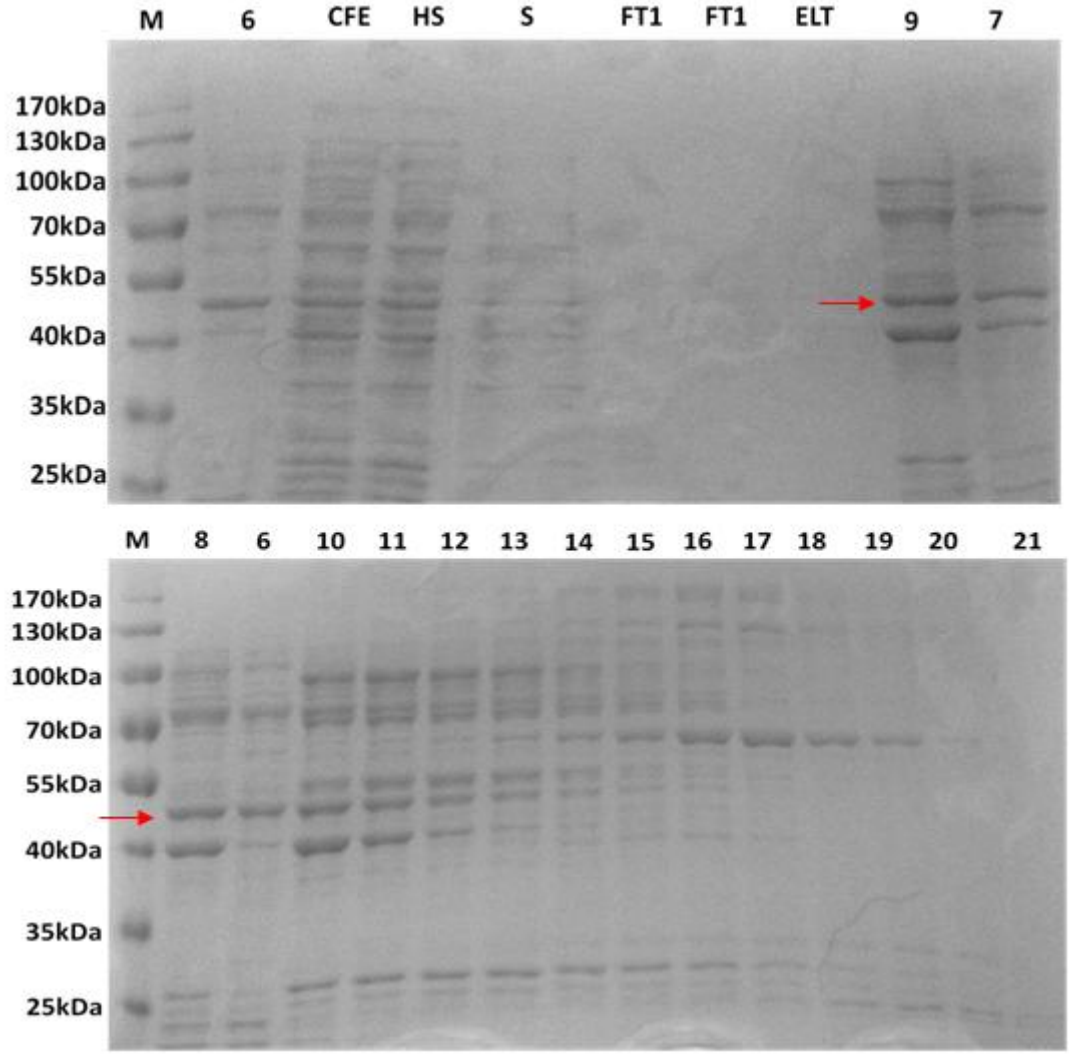

Figure 4.15: SDS-PAGE analysis followed by Coomassie blue staining of partial purification samples of the AGPase with mutant LS-E358G. Quality of the purified samples was monitored using SDS-PAGE sample with highest AGPase fraction was chosen (fraction 8 and 9). Red arrows indicate the location of AGPase which appears around 51 kDa. CFE: cell free extract, HS: cell free extract after heat shock, FT1,2: flow through 1 and 2, ELT: final elute, numbers 6-21: 6^{th} to 21^{th} fractions obtained during the elution of AGPase.

Sample	Volume (µL)	Protein (mg)	Activity (units)	Specific Activity (unit/mg)	Fold Purification
WT LS-CFE_{HS}	3	0.52	55	52.9	1
WT LS-Fraction 13	1.5	0.29	55.8	96.2	1.82
E358G LS-CFE_{HS}	4	1.96	32.8	8.3	1
E358G Fraction 8	1.5	1.52	38.6	13.9	1.67

Table 4.1: Partial purification of AGPase with WT LS and AGPase with mutant LS-E358G. Activity was measured in reverse direction by measuring the G1P production. Unit activity is defined as 1nmol G1P. Specific activities of CFE, ammonium sulfate salting out steps and flowthrough are not included in this assay.

4.7. Kinetic Characterization

Iodine staining results of glgC$^-$SS cells transformed with mutant LS-E358G indicated that, this mutation cause the AGPase to lose its catalytic activity in *E. coli* cell. Although iodine staining gives preliminary information about the changes in kinetic properties of mutants, it cannot precisely explain what exactly cause this loss of activity. This information can be obtained through kinetic characterization assays, which would reveal if the E358G mutation alters the regulatory properties of the enzyme or the catalytic properties or both simultaneously. This information would not only reveal the kinetic and regulatory properties of the enzyme but it would also provide information about what the mutation cause on structural level. Kinetic properties of AGPase with mutant LS-E358G and with wild type LS was made using reverse direction AGPase assay and forward direction AGPase assay.

4.7.1. Kinetic Characterization trough Reverse Direction Assay

Reverse direction AGPase assay was conducted as described in section 3.8.1. In order to avoid saturation, 1/10 (with 50mM HEPES solution) dilution was calculated to be appropriate for AGPase with wild type LS. On the other hand, AGPase with mutant LS-E358G was not diluted considering its low activity. During the assay, 5µL of solution containing AGPase was added to the reaction mixture in both cases and AGPase was allowed to catalyze reaction for 10 minutes.

Kinetic analyses were carried out on partially purified WT and LS-E358G AGPases by measuring as the total amount of G1P produced in 10 minutes. For each concentration of substrate (ADP-Glucose), activator (3PGA) or inhibitor (Pi), total amount of G1P produced in 10 minutes was measured and each case were repeated for at least three times. AGPase, containing WT LS or mutant, towards substrate, activator and inhibitor was obtained (**Figure 4.16**). Then following kinetic parameters were calculated: V_{max} (maximum reaction rate), K_M (Michaelis constant) values for ADP-Glucose, K_A (activation constant) values for 3PGA and K_i (inhibition constant) value for Pi (**Table 4.2**). Overall mutant showed reduced affinity for its substrate ADP-glucose and activator 3PGA. Mutant's K_M value for ADP-Glucose increased 4.21 folds (WT's K_M: 0.57, mutant's K_M: 2.4). For 3PGA, this fold change calculation was not possible as the K_a value was below assay detection range, however it can be said that it is more than 2.12 folds (considering for WT lower sensitivity end of assay is 0.25mM, Mutant K_a: 0.53) (**Table 4.2-A**). In terms of inhibition, mutant showed increased affinity towards its inhibitor Pi, its K_i value decreased -4.29 folds (WT's K_i: 1.16, mutant's K_i: 0.27) (**Table 4.2-B**).

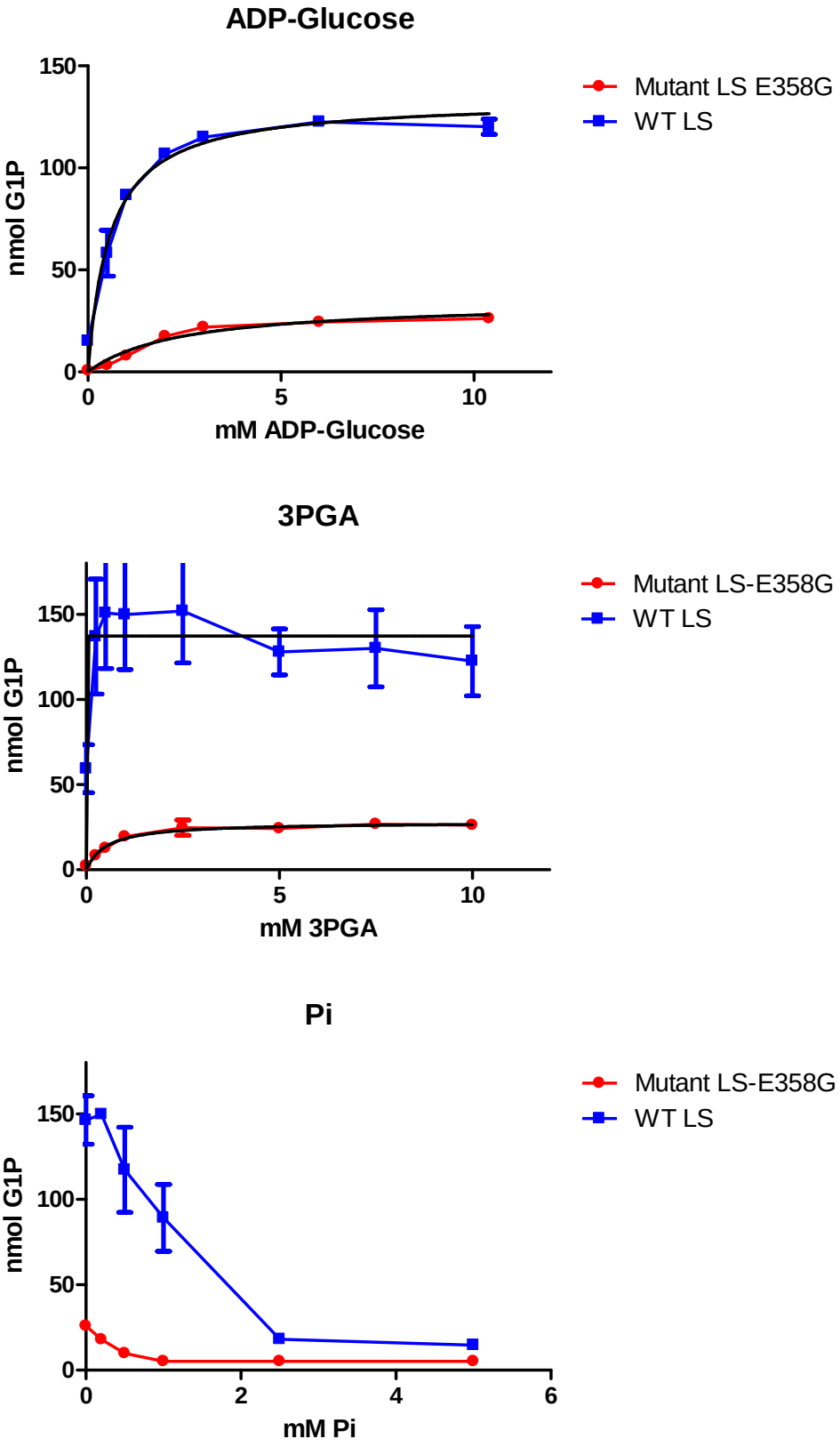

Figure 4.16: Response of AGPase with WT LS and AGPase with mutant LS-E358G towards ADP-Glucose, 3PGA and Pi. Blue line represents AGPase containing WT LS, red line represents AGPase containing mutant LS-E358G and black lines represents best fit curves.

A

AGPase	Substrate or Activator	V_{max} (nmol/min)	V_{min} (nmol/min)	K_A (mM)	Fold Change with Respect to Wild Type
WT LS	ADP-Glucose	13.35	0	0.57	1
	3PGA	13.71	5.93	*	1
Mutant LS-E358G	ADP-Glucose	3.457	0	2.40	4.21
	3PGA	2.64	0.23	0.53	**

B

AGPase	Inhibitor	V_{max} (nmol/min)	V_{min} (nmol/min)	K_i (mM)	Fold Change with Respect to Wild Type
WT LS	Pi	14.64	8.91	1.16	1
Mutant LS-E358G	Pi	2.59	0.51	0.27	-4.29

C

AGPase with Mutant LS-E358G	Variable	Percent Change of variable of AGPase with Mutant LS-E358G with Respect to AGPase with Wild Type LS
	Affinity for ADP-Glucose	-77.92 %
	Affinity for 3PGA	**
	Average V_{max}	-79.13 %
	Affinity for Pi	89 %

***Lower than assay sensitivity (0.25mM)**
**** Wild type value not available**

Table 4.2: Kinetic Properties of AGPase with WT LS and AGPase with mutant LS-E358G. All calculations are for per minute time interval. (A) V_{max}, V_{min} and K_M values of WT and mutant AGPases towards ADP-Glucose and 3PGA. (B) V_{max}, V_{min} and K_i values of WT and mutant AGPases towards Pi (C). Percent Change of given variables for AGPase with mutant LS-E358G with Respect to AGPase with Wild Type LS.

4.8. Autodock calculations for AGPase containing WT LS and AGPase containing mutant LS-E358G

Binding energies and K_A-K_i values of WT and mutant AGPase for 3PGA were computationally calculated at 25°C using autodock (**Table 4.4**) as described in section 3.10.3. Although Autodock results are not generally appropriate to be used as absolute values, they can be used for comparison purposes. Autodock results predicted AGPase with mutant LS-E358G to have a higher affinity towards both 3PGA and Pi compared to wild type. This data agrees with the experimental data for Pi which also indicated higher affinity towards Pi. However it did not hold for 3PGA which indicated the wild type to have higher affinity. This miscalculation for 3PGA can be explained by the fact that, Autodock assumes proteins to be rigid and therefore could not toke in to account any conformational changes that might be induced by the mutation. As 3PGA is a larger ligand compared to Pi, it is more sensitive to conformational changes since such changes might physically limit the accession of 3PGA to the binding site more so than they limit Pi. Moreover, autodock results claims, orientation of binding of 3PGA did changed as a result of the E358G mutation. While binding to wild type, phosphate group of 3PGA faces beta-sheets which E358 is found on. However when this Glu was mutated to Gly, binding orientation of 3PGA molecules was reversed and its hydroxyl end faced to the beta sheets. Pi on the other hand totally changed its binding position most likely due to change of charge distribution resulted from replacement of Glu with Gly (**Figure 4.17)**.

AGPase Large Subunit	3PGA binding Energy (kcal/mol)	K_A for 3PGA (µmol)	Pi binding Energy (kcal/mol)	K_i for Pi (µmol)
WT LS	-5.72	64.27	-4.01	1160
Mutant LS-E358G	-7.73	2.15	-6.70	12.34

Table 4.4: Autodock results for of AGPase with WT LS and AGPase with mutant LS-E358G

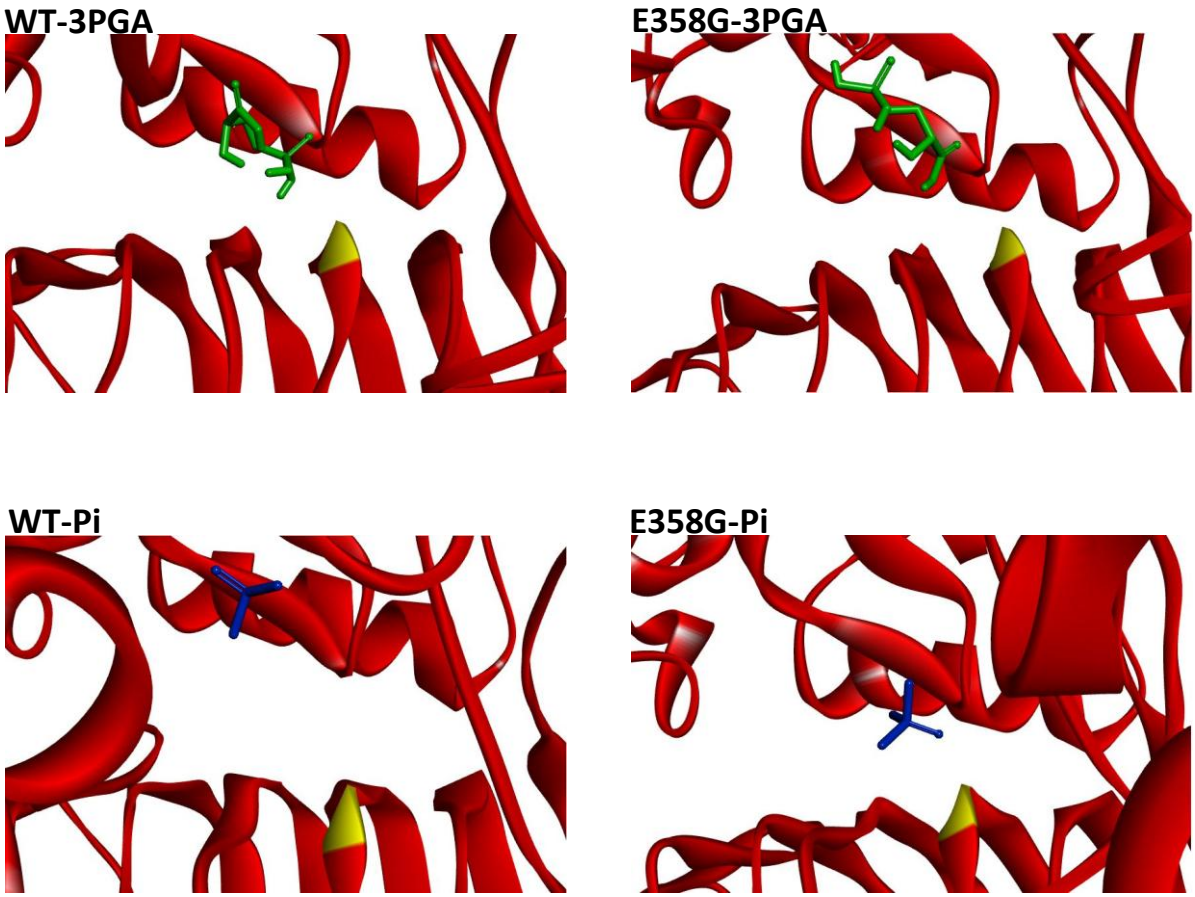

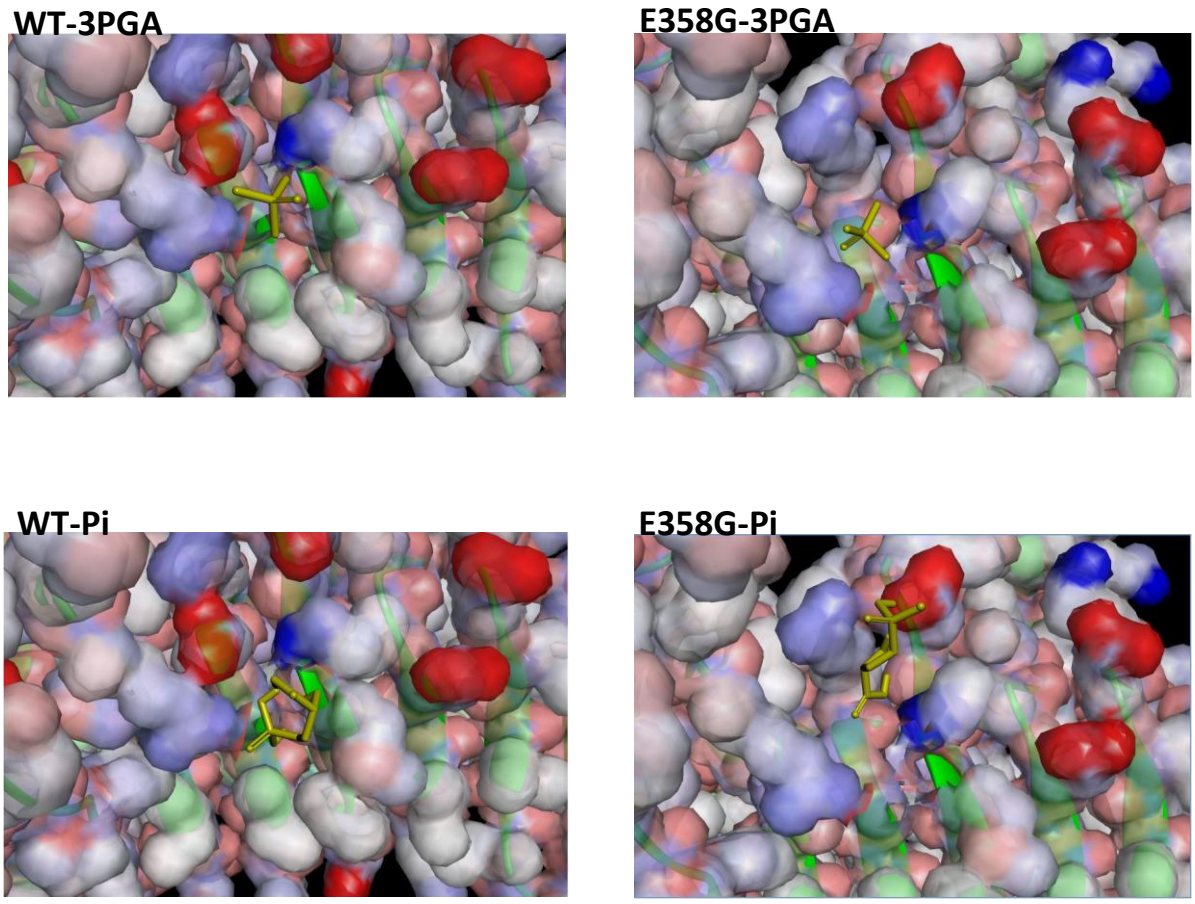

Figure 4.17: Binding orientation of 3PGA and Pi to WT AGPase and Mutant AGPase LS-E358G. Red color represents AGPase protein. Yellow color represents E358 in WT and G358 in mutant. Green color represents 3PGA. Blue color represents P

CHAPTER 5

DISCUSSION

AGPase is an enzyme that catalyzes the first committed and rate limiting step of starch biosynthesis in a variety of, mostly photosynthetic, organisms including plants. Considering the important role of AGPase plays in starch biosynthesis and the agricultural and industrial value of starch, it is not surprising it has been extensively studied. Despite this great research effort, limited amount of data is available about the structure of AGPases largely due to the fact that only two crystal structures of AGPases were obtained. These two structures belonged to the small subunit homotetramer of potato AGPase [54] and the AGPase of bacteria *A. tumefaciens* [58]. Although these two structures provided invaluable information about the structure of AGPase, due to the purification procedure, both structures were obtained in enzymes inhibited state. Furthermore, crystal structure of small subunit homotetramer of potato AGPase represented a form of AGPase, which is only found in residual amounts in plant cells and *A. tumefaciens* AGPase was not a good representative for plant AGPases since it is a bacterial AGPase. To date, no group was successful in obtaining crystal or NMR structure of plant AGPase in heterotetrameric form. As a result of this, most of the structural data about the plant AGPase was obtained through modifying specific amino acid residues or motifs found on AGPase and than monitoring the change in the properties of enzymes and relating this information to the structure.

In this study, prospectus amino acid position on potato tuber AGPase large subunit, which may influence certain properties and functions of potato tuber AGPase, were investigated. These residues was previously obtained in the study of Bengisu [6] and found to be; Ala 91, Phe 101, Phe 311 Glu 358. These amino acid residues were found to alter the properties of AGPase when Ala 91 was mutated to Thr, Phe 101 was mutated to Leu, Phe 311 was mutated to Leu and Glu 358 was mutated to Gly. All four mutations were applied on to wild type potato tuber AGPase large subunit trough the usage of site directed mutagenesis and the change in structural (for all four mutations) and kinetic (E358G) properties was investigated. Computational tools were frequently used together with experimental approaches to provide precise predictions and to support data. Among the

investigated positions, Glu 358, on potato tuber AGPase large subunit was found to play important roles on tetramer assembly, allosteric regulation and catalytic properties. Mutating Glu 358 to Gly caused the AGPase within cells to be mostly tetramers, reducing cellular amounts of monomer and dimer. Despite of this, deficient cells transformed with AGPase containing LS-E358G mutation was not stained with iodine. Activity assays revealed mutation caused AGPase to lose much of its catalytic activity and greatly altered its allosteric properties. Overall, compared to wild type, mutant enzyme had lowered affinity towards forward direction substrate ATP and reverse direction substrate ADP-glucose. It had lower affinity towards activator 3PGA but had higher affinity towards inhibitor Pi.

Investigation of locations of mutation on 3D structure of heterotetrameric potato tuber AGPase generated by homology modeling in the study of Tuncel et. al. [10] reveled mutations A91T, F101L and E358G correspond to structurally and functionally important regions and mutation F311L, although not seem to be directly on such a region, is in close proximity to LS-SS subunit interface (**Figure 4.2**). In order to check the importance of these residues conservation of residues of potato tuber AGPase large subunit was investigated using ConSurf. If investigated amino acids and the regions they are found on really have structural/functional properties, they are expected to be under negative selection. Among the investigated residues A91 was found to be moderately conserved residue found within a highly conserved region (**Figure 4.3)**. Residue F101 was found to be a highly conserved and functional residue found in a highly conserved region (**Figure 4.3)**. Despite previously F311 was not observed to be on a functional/structural region, it was also found to be a highly conserved residue, found on a moderately conserved region, (**Figure 4.3)**. Residue E358 was found to be a moderately conserved amino acid in a moderately conserved region (**Figure 4.3)**. This region is known to take part in binding of allosteric effectors 3PGA and Pi and substrate G1P and partially substrate ATP. As different organisms have different allosteric regulators for AGPase, moderate conservation of this region is in fact not surprising. Even though, E358 was moderately conserved residue, among AGPase homologs Glu at position 358 does not known naturally to evolve to Gly (E358G) as ConSurf could not identified any such homolog. In addition to this, E358 was found to be in between two extremely well conserved, functional and structural amino acids G357 and R359. G357 particularly, is such

well conserved that among AGPase homologs it was not observed to mutate into any other amino acid.

The reason why E358G mutation did not naturally occur among AGPase homologs and why if this mutation is inflicted artificially, properties of AGPase drastically change can be explained by two factors.

First possible factor; Glu is a negatively charged amino acid and at position 358, it is next to an arginine which is positively charged. Mutating negative Glu at position 358 to natural Gly severely alters the charge distribution and perhaps the conformation of the region, by making the region more positive. As one of the allosteric regulators of potato AGPase, Pi, binds to this region and it is a negatively charged molecule. Making this region more positive would change the allosteric properties of the enzyme by increasing its affinity towards Pi. Experimental and computational results also suggests this mutation increases the affinity of AGPase towards Pi (**Table 4.2-B** and **Table 4.4**).

Second possible factor; among all amino Gly is the smallest and the most flexible one. Mutating Glu at position 358 to Gly would provide considerable flexibility to the region. Under such conditions, this region can experience conformational changes that might alter the whole structure of the protein. In fact, experimental studies suggest; AGPase with mutant LS-E358G has a different assembly profile compared to wild type. E358G mutant has higher tetramer and lower monomer dimer fractions compared to wild type AGPase (**Figure 4.10** to **Figure 4.12**). In addition to this any type of conformational change on such a region that takes part in binding to allosteric regulators and substrates would alter the enzymes affinity towards them. Under this new conformation, considerably large and branched ligands that bind to this region, such as 3PGA, ADP-Glucose and ATP, would have a hard time fitting and reaching to their binding sites. Even if those molecules can somehow reach and fit to their binding sites, due to the conformational change, substrates might not be in the correct orientation to react properly and regulators might lose their effectiveness. Small and symmetrical ligands, such as Pi, on the other hand, may find it easier to reach and fit to their binding sites even if the conformation is altered. In addition to this, since such molecules are symmetrical, regardless of the way they bind, they would have a single orientation. Experimental results also support this view as E358G mutant has reduced affinity towards

3PGA, ADP-Glucose and ATP (**Table 4.2-A** and **Appendix C**) and increased affinity towards Pi (**Table 4.2-B).** Controversy to this, Autodock predicted increased affinity for E358G mutant towards 3PGA whereas experimental results showed the opposite (**Table 4.4**). This result might be originating from the fact that, while calculating binding energy, Autodock could not consider the conformational change inflicted upon mutation and therefore for a ligand such as 3PGA, its results might not be reliable (**Figure 4.17)**.

Since these two factors individually explain some of the observed properties of the mutant, overall observed properties were produced by a combinatory effect of these two factors. As a result of the mutation E358G, charge distribution of the region changed and it also gained flexibility. In return, this region that takes part in LS-SS interaction and substrate and allosteric effectors binding, experienced conformational changes. This conformational change altered the LS-SS interaction and therefore assembly profile of the protein increasing its tetramer and reducing dimer monomer fraction (**Figure 4.10** to **Figure 4.12**). Conformational change together with the alterations in charge distribution also modified the binding of ligands to the region. Compared to wild type; large, branched ligands such as 3PGA, ADP-Glucose and ATP lost affinity towards the mutant enzyme (**Table 4.2-A** and **Appendix C**) whereas small, symmetrical Pi was mostly unaffected of conformational change and the shifting of charge distribution towards positive increased affinity of negatively charged Pi towards the enzyme(**Table 4.2-B)**.

It is known that presence of Pi in the environment increases the stability of AGPases. As the AGPase with mutant LS-E358G has higher affinity towards Pi, increased heterotetramer fraction might also be resulting as an outcome of this. Since the heterotetramer form of the mutant is unusually stable, once monomers and dimers form a tetramer, it does not disassemble back to dimers and monomers as easily as the wild type. As a result of this, equilibrium shift towards the heterotetramer form and cellular fraction of tetramer increase and dimer and monomer decrease (**Figure 4.10)**. This would also explain why enzyme is not heat stable, as increased heterotetramer stability of enzyme is provided by the Pi, as the heat goes up more and more Pi leave the AGPase. As a result of this, AGPase loses its stability (**Figure 4.12**).

Kinetic characterization of enzyme revealed, compared to wild type AGPase, E358G mutant's affinity towards ADP-glucose reduced 77.92%. In addition to this, V_{max} of the enzyme also reduced in a quite similar amount of 79.13%. These results suggest; reduced activity of E358G mutant in reverse direction is directly proportional to its loss of affinity towards the substrate. As the mutant enzyme cannot bind to its substrate as effectively as wild type enzyme, maximum rate at which it can catalyze the reaction reduced, equal to the amount of affinity it lost towards substrate (**Table 4.2-C**). As the substrates of reverse and forwards reactions use the same binding sites, affinity of AGPases towards ATP also reduced (**Appendix C**). This also explains why glgC$^-$SS cells transformed with mutant LS-E358G are not iodine staining. At lower ATP concentrations this mutant has very low activity, as iodine staining experiments were done on glgC$^-$SS/LS cells that are on stationary phase, these cells intercellular ATP concentrations were also low ,around 0.5 mM [77]. At these ATP concentrations activity of mutant is low (**Appendix C**) and therefore it cannot provide enough ADP-glucose. As ADP-glucose levels are low only small amount of glycogen can be produced under best of circumstances and it cannot be detected by iodine staining (**Figure 4.8**). These results indicate, even if large subunit is mostly regulatory, it still has certain important roles in mediating catalyses, as mutating a residue on it may directly alter enzymes catalytic properties.

CHAPTER 5

CONCLUSION

Starch is the major storage polysaccharide of plants and certain other, mostly photosynthetic, organisms. In addition to its biological function, starch is also commercial important agricultural product, which is used as both food source human and animal consumption and a raw material for industrial processes and applications.

Starch is produced within plants through a series of enzyme catalyzed reactions where basically individual sugar molecules are connected to each other in a multi step reaction, forming amylose and amylopectin. Rate limiting step of this biosynthesis is the conversion of G1P and ATP to ADP-glucose and PPi by the activity of enzyme ADP-glucose pyrophosphorylase (AGPase). In vitro, AGPase can freely catalyze the reaction in both reverse and forwards directions. Plant AGPases are heterotetrameric enzymes of two identical small subunits and two identical large subunits. Among these two, large subunit specialized mostly in regulation and small subunit is mostly specialized in catalyses. Within plant cells, AGPase activity is regulated according to the ratio of activator 3PGA and inhibitor Pi, which reflects the metabolic state of the cell. High 3PGA/Pi ratios indicate a high energy state and therefore and active AGPase, whereas low ratios indicate a low energy state and an inactive enzyme.

Considering importance of starch and the role of AGPase in its synthesis, AGPase is a widely studied enzyme. Despite of this research effort, structure-function relationship of plant AGPases is largely unknown. Due to the absence of the crystal structure of plant AGPases, much of the structure-function relationship of AGPase is obtained through the modification of amino acids residues and motifs, observing the resulted changes in enzyme properties and relating these changes in properties to structure.

In this study, prospectus mutated position on potato tuber AGPase large subunit (A91T, F101L, F311L and E358G), which may alter properties of potato tuber AGPase, was investigated. These mutations were applied on wild type potato tuber AGPase large subunits

trough the usage of site directed mutagenesis PCR. Change in the properties of resulted mutant AGPases with respect to wild type AGPase was investigated through the usage of iodine staining's, SDS and native PAGE's, kinetic assays and several computational approaches. Among the mutants, AGPase with mutant LS-E358G was found to have considerably different properties compared to wild type. Mutant had high heterotetramer and low dimer monomer fractions, its affinity towards 3PGA, ADP-Glucose and ATP decreased whereas its affinity towards Pi increased.

These results suggested potato tuber AGPase large subunit residue E358 has critical roles and mutating it Gly severely alter the structural, regulatory and catalytic properties of the enzyme. Direct alterations of catalytic properties of AGPase through mutating large subunit indicated; although large subunit is mostly regulatory, it still has roles in mediating catalyses. As structure- function relationship of AGPase is largely unknown, these kinds of data bring us closer to understanding the enzyme.

In the future, LS mutation E358G can be combined with other mutation for the purpose of finding an AGPase mutant that has high heterotetramer fraction like E358G mutant and still retains its activity. In addition to this, residue E358 can be mutated to other amino acids, as this position has important roles, one such amino acid might generate a highly active AGPase mutant.

BIBLIOGRAPHY

1. Slattery, C.J., I.H. Kavakli, and T.W. Okita, *Engineering starch for increased quantity and quality.* Trends Plant Sci, 2000. **5**(7): p. 291-8.
2. Zeeman, S.C., J. Kossmann, and A.M. Smith, *Starch: its metabolism, evolution, and biotechnological modification in plants.* Annu Rev Plant Biol, 2010. **61**: p. 209-34.
3. Ballicora, M.A., A.A. Iglesias, and J. Preiss, *ADP-Glucose Pyrophosphorylase: A Regulatory Enzyme for Plant Starch Synthesis.* Photosynth Res, 2004. **79**(1): p. 1-24.
4. Patron, N.J. and P.J. Keeling, *COMMON EVOLUTIONARY ORIGIN OF STARCH BIOSYNTHETIC ENZYMES IN GREEN AND RED ALGAE1: EVOLUTION OF STARCH SYNTHESIS.* Journal of Phycology, 2005. **41**(6): p. 1131-1141.
5. Ball, S., et al., *The evolution of glycogen and starch metabolism in eukaryotes gives molecular clues to understand the establishment of plastid endosymbiosis.* J Exp Bot, 2011. **62**(6): p. 1775-801.
6. Seferoglu, A.B., *Identification of Important Residues for Modulation of Allosteric Properties of Potato Tuber ADP Glucose Pyrophosphorylase*, in *Graduate School of Sciences and Engineering*2011, Koc University. p. 71.
7. Nakamura, Y., et al., *Some Cyanobacteria synthesize semi-amylopectin type alpha-polyglucans instead of glycogen.* Plant Cell Physiol, 2005. **46**(3): p. 539-45.
8. Ashkenazy, H., et al., *ConSurf 2010: calculating evolutionary conservation in sequence and structure of proteins and nucleic acids.* Nucleic Acids Res, 2010. **38**(Web Server issue): p. W529-33.
9. Morris, G.M., et al., *AutoDock4 and AutoDockTools4: Automated docking with selective receptor flexibility.* J Comput Chem, 2009. **30**(16): p. 2785-91.
10. Tuncel, A., I. Kavakli, and O. Keskin, *Insights into subunit interactions in the heterotetrameric structure of potato ADP-glucose pyrophosphorylase.* Biophys J, 2008. **95**(8): p. 3628-3639.
11. Ball, S.G. and M.K. Morell, *From bacterial glycogen to starch: understanding the biogenesis of the plant starch granule.* Annu Rev Plant Biol, 2003. **54**: p. 207-33.
12. Boehlein, S.K., et al., *Studies of the kinetic mechanism of maize endosperm ADP-glucose pyrophosphorylase uncovered complex regulatory properties.* Plant Physiol, 2010. **152**(2): p. 1056-64.
13. Adl, S.M., et al., *The new higher level classification of eukaryotes with emphasis on the taxonomy of protists.* J Eukaryot Microbiol, 2005. **52**(5): p. 399-451.

14. Deschamps, P., et al., *Metabolic symbiosis and the birth of the plant kingdom.* Mol Biol Evol, 2008. **25**(3): p. 536-48.
15. Suzuki, E., et al., *Physicochemical variation of cyanobacterial starch, the insoluble alpha-Glucans in cyanobacteria.* Plant Cell Physiol, 2013. **54**(4): p. 465-73.
16. Smith, A.M., *The biosynthesis of starch granules.* Biomacromolecules, 2001. **2**(2): p. 335-41.
17. Tiessen, A., et al., *Subcellular analysis of starch metabolism in developing barley seeds using a non-aqueous fractionation method.* J Exp Bot, 2012. **63**(5): p. 2071-87.
18. Comparot-Moss, S. and K. Denyer, *The evolution of the starch biosynthetic pathway in cereals and other grasses.* J Exp Bot, 2009. **60**(9): p. 2481-92.
19. Kuhn, M.L., et al., *The ancestral activation promiscuity of ADP-glucose pyrophosphorylases from oxygenic photosynthetic organisms.* BMC Evol Biol, 2013. **13**: p. 51.
20. Rosti, S. and K. Denyer, *Two paralogous genes encoding small subunits of ADP-glucose pyrophosphorylase in maize, Bt2 and L2, replace the single alternatively spliced gene found in other cereal species.* J Mol Evol, 2007. **65**(3): p. 316-27.
21. Deschamps, P., et al., *The relocation of starch metabolism to chloroplasts: when, why and how.* Trends Plant Sci, 2008. **13**(11): p. 574-82.
22. Yoon, H.S., et al., *A molecular timeline for the origin of photosynthetic eukaryotes.* Mol Biol Evol, 2004. **21**(5): p. 809-18.
23. MARTIN, W. and K.V. KOWALLIK, *Annotated English translation of Mereschkowsky's 1905 paper 'Über Natur und Ursprung der Chromatophoren im Pflanzenreiche'.* European Journal of Phycology, 1999. **34**(03): p. 287-295.
24. McFadden, G.I. and G.G. van Dooren, *Evolution: red algal genome affirms a common origin of all plastids.* Curr Biol, 2004. **14**(13): p. R514-6.
25. Marin, K., et al., *The ggpS gene from Synechocystis sp. strain PCC 6803 encoding glucosyl-glycerol-phosphate synthase is involved in osmolyte synthesis.* J Bacteriol, 1998. **180**(18): p. 4843-9.
26. Dinges, J.R., et al., *Molecular structure of three mutations at the maize sugary1 locus and their allele-specific phenotypic effects.* Plant Physiol, 2001. **125**(3): p. 1406-18.
27. Keeling, P.J., *Chromalveolates and the evolution of plastids by secondary endosymbiosis.* J Eukaryot Microbiol, 2009. **56**(1): p. 1-8.
28. Morden, C.W. and A.R. Sherwood, *Continued evolutionary surprises among dinoflagellates.* Proc Natl Acad Sci U S A, 2002. **99**(18): p. 11558-60.
29. Koning, R.E. *Calvin Cycle*. 1994 5.16.2013]; Available from: http://plantphys.info/plant_physiology/calvincycle.shtml.

30. Ball, S., et al., *From glycogen to amylopectin: a model for the biogenesis of the plant starch granule.* Cell, 1996. **86**(3): p. 349-52.

31. Ballicora, M.A., A.A. Iglesias, and J. Preiss, *ADP-glucose pyrophosphorylase, a regulatory enzyme for bacterial glycogen synthesis.* Microbiol Mol Biol Rev, 2003. **67**(2): p. 213-25, table of contents.

32. Viola, R., P. Nyvall, and M. Pedersen, *The unique features of starch metabolism in red algae.* Proc Biol Sci, 2001. **268**(1474): p. 1417-22.

33. Okita, T.W., et al., *The Subunit Structure of Potato Tuber ADPglucose Pyrophosphorylase.* Plant Physiol, 1990. **93**(2): p. 785-90.

34. Corbi, J., et al., *Accelerated evolution and coevolution drove the evolutionary history of AGPase sub-units during angiosperm radiation.* Ann Bot, 2012. **109**(4): p. 693-708.

35. Preiss, J., et al., *Starch biosynthesis and its regulation.* Biochem Soc Trans, 1991. **19**(3): p. 539-47.

36. Smith-White, B.J. and J. Preiss, *Comparison of proteins of ADP-glucose pyrophosphorylase from diverse sources.* J Mol Evol, 1992. **34**(5): p. 449-64.

37. Cross, J.M., et al., *Both subunits of ADP-glucose pyrophosphorylase are regulatory.* Plant Physiol, 2004. **135**(1): p. 137-44.

38. Geigenberger, P., *Regulation of starch biosynthesis in response to a fluctuating environment.* Plant Physiol, 2011. **155**(4): p. 1566-77.

39. Ventriglia, T., et al., *Two Arabidopsis ADP-glucose pyrophosphorylase large subunits (APL1 and APL2) are catalytic.* Plant Physiol, 2008. **148**(1): p. 65-76.

40. Kuhn, M.L., C.A. Falaschetti, and M.A. Ballicora, *Ostreococcus tauri ADP-glucose pyrophosphorylase reveals alternative paths for the evolution of subunit roles.* J Biol Chem, 2009. **284**(49): p. 34092-102.

41. Lin, T.P., et al., *A Starch Deficient Mutant of Arabidopsis thaliana with Low ADPglucose Pyrophosphorylase Activity Lacks One of the Two Subunits of the Enzyme.* Plant Physiol, 1988. **88**(4): p. 1175-81.

42. Salamone, P.R., et al., *Isolation and characterization of a higher plant ADP-glucose pyrophosphorylase small subunit homotetramer.* FEBS Lett, 2000. **482**(1-2): p. 113-8.

43. Tetlow, I.J., M.K. Morell, and M.J. Emes, *Recent developments in understanding the regulation of starch metabolism in higher plants.* J Exp Bot, 2004. **55**(406): p. 2131-45.

44. Scheible, W.R., et al., *Nitrate Acts as a Signal to Induce Organic Acid Metabolism and Repress Starch Metabolism in Tobacco.* Plant Cell, 1997. **9**(5): p. 783-798.

45. Nielsen, T.H., et al., *The sugar-mediated regulation of genes encoding the small subunit of Rubisco and the regulatory subunit of ADP glucose pyrophosphorylase is modified by phosphate and nitrogen.* Plant, Cell & Environment, 1998. **21**(5): p. 443-454.

46. Buchanan, B.B., *Role of Light in the Regulation of Chloroplast Enzymes.* Annual Review of Plant Physiology, 1980. **31**(1): p. 341-374.

47. Wolosiuk, R.A., M.A. Ballicora, and K. Hagelin, *The reductive pentose phosphate cycle for photosynthetic CO2 assimilation: enzyme modulation.* FASEB J, 1993. **7**(8): p. 622-37.

48. Fu, Y., et al., *Mechanism of reductive activation of potato tuber ADP-glucose pyrophosphorylase.* J Biol Chem, 1998. **273**(39): p. 25045-52.

49. Ballicora, M.A., et al., *Activation of the potato tuber ADP-glucose pyrophosphorylase by thioredoxin.* J Biol Chem, 2000. **275**(2): p. 1315-20.

50. Geigenberger, P., A. Kolbe, and A. Tiessen, *Redox regulation of carbon storage and partitioning in response to light and sugars.* J Exp Bot, 2005. **56**(416): p. 1469-79.

51. Tiessen, A., et al., *Starch synthesis in potato tubers is regulated by post-translational redox modification of ADP-glucose pyrophosphorylase: a novel regulatory mechanism linking starch synthesis to the sucrose supply.* Plant Cell, 2002. **14**(9): p. 2191-213.

52. Schliebner, I., et al., *A Survey of Chloroplast Protein Kinases and Phosphatases in Arabidopsis thaliana.* Curr Genomics, 2008. **9**(3): p. 184-90.

53. Baginsky, S. and W. Gruissem, *The chloroplast kinase network: new insights from large-scale phosphoproteome profiling.* Mol Plant, 2009. **2**(6): p. 1141-53.

54. Jin, X., et al., *Crystal structure of potato tuber ADP-glucose pyrophosphorylase.* EMBO J, 2005. **24**(4): p. 694-704.

55. Rossman, M.G., et al., *2 Evolutionary and Structural Relationships among Dehydrogenases*, in *The Enzymes*, D.B. Paul, Editor. 1975, Academic Press. p. 61-102.

56. Morell, M., M. Bloom, and J. Preiss, *Affinity labeling of the allosteric activator site(s) of spinach leaf ADP-glucose pyrophosphorylase.* J Biol Chem, 1988. **263**(2): p. 633-7.

57. Haugen, T.H. and J. Preiss, *Biosynthesis of bacterial glycogen. The nature of the binding of substrates and effectors to ADP-glucose synthase.* J Biol Chem, 1979. **254**(1): p. 127-36.

58. Cupp-Vickery, J.R., et al., *Structural Analysis of ADP-Glucose Pyrophosphorylase from the Bacterium Agrobacterium tumefaciens†,‡.* Biochemistry, 2008. **47**(15): p. 4439-4451.

59. Greene, T.W., et al., *Mutagenesis of the potato ADPglucose pyrophosphorylase and characterization of an allosteric mutant defective in 3-phosphoglycerate activation.* Proc Natl Acad Sci U S A, 1996. **93**(4): p. 1509-13.

60. Baris, I., et al., *Investigation of the interaction between the large and small subunits of potato ADP-glucose pyrophosphorylase.* PLoS computational biology, 2009. **5**(10).

61. Boehlein, S., et al., *Probing allosteric binding sites of the maize endosperm ADP-glucose pyrophosphorylase.* Plant Physiol, 2010. **152**(1): p. 85-95.

62. Laughlin, M., S. Chantler, and T. Okita, *N- and C-terminal peptide sequences are essential for enzyme assembly, allosteric, and/or catalytic properties of ADP-glucose pyrophosphorylase.* Plant J, 1998. **14**(2): p. 159-168.

63. Kavakli, I., et al., *Analysis of allosteric effector binding sites of potato ADP-glucose pyrophosphorylase through reverse genetics.* J Biol Chem, 2001. **276**(44): p. 40834-40840.

64. Laughlin, M., J. Payne, and T. Okita, *Substrate binding mutants of the higher plant ADP-glucose pyrophosphorylase.* Phytochemistry, 1998. **47**(4): p. 621-629.

65. Hwang, S.-K., P. Salamone, and T. Okita, *Allosteric regulation of the higher plant ADP-glucose pyrophosphorylase is a product of synergy between the two subunits.* FEBS Lett, 2005. **579**(5): p. 983-990.

66. Cross, J., et al., *A polymorphic motif in the small subunit of ADP-glucose pyrophosphorylase modulates interactions between the small and large subunits.* Plant J, 2005. **41**(4): p. 501-511.

67. Dawar, C., S. Jain, and S. Kumar, *Insight into the 3D structure of ADP-glucose pyrophosphorylase from rice (Oryza sativa L.).* J Mol Model, 2013.

68. Corbi, J., et al., *Accelerated evolution and coevolution drove the evolutionary history of AGPase sub-units during angiosperm radiation.* Ann Bot, 2012. **109**(4): p. 693-708.

69. Bradford, M.M., *A rapid and sensitive method for the quantitation of microgram quantities of protein utilizing the principle of protein-dye binding.* Anal Biochem, 1976. **72**: p. 248-54.

70. Sowokinos, J.R., *Pyrophosphorylases in Solanum tuberosum: I. Changes in ADP-Glucose and UDP-Glucose Pyrophosphorylase Activities Associated with Starch Biosynthesis during Tuberization, Maturation, and Storage of Potatoes.* Plant Physiol, 1976. **57**(1): p. 63-8.

71. Boehlein, S.K., et al., *Purification and characterization of adenosine diphosphate glucose pyrophosphorylase from maize/potato mosaics.* Plant Physiol, 2005. **138**(3): p. 1552-62.

72. Shapiro, A.L., E. Vinuela, and J.V. Maizel, Jr., *Molecular weight estimation of polypeptide chains by electrophoresis in SDS-polyacrylamide gels.* Biochem Biophys Res Commun, 1967. **28**(5): p. 815-20.

73. Laemmli, U.K., *Cleavage of structural proteins during the assembly of the head of bacteriophage T4.* Nature, 1970. **227**(5259): p. 680-5.

74. Burnette, W.N., *"Western blotting": electrophoretic transfer of proteins from sodium dodecyl sulfate--polyacrylamide gels to unmodified nitrocellulose and radiographic detection with antibody and radioiodinated protein A.* Anal Biochem, 1981. **112**(2): p. 195-203.

75. Berezin, C., et al., *ConSeq: the identification of functionally and structurally important residues in protein sequences.* Bioinformatics, 2004. **20**(8): p. 1322-4.

76. Lasko, D. and D. Wang, *On-line monitoring of intracellular ATP concentration in Escherichia coli fermentations.* Biotechnol Bioeng, 1996. **52**(3): p. 364-372.

VITA

Kaan Koper was born in Ankara, Turkey, on 01.01.1990. He received his B.Sc degree in Chemical and Biological Engineering from Koç University, Istanbul in 2011. From September 2011 to August 2013 he worked as a teaching and research assistant at Koç University. He worked on “Mutation of Glu at Position 358 to Gly on *Solanum Tuberosum* (Potato Plant) Tuber AGPase Large Subunits Strikingly Alters the Structural, Regulatory and Catalytic Properties of the Heterotetrameric Enzyme” during his M.Sc. studies

APPENDIX A: LOCATIONS OF MUTATION ON AGPASE LARGE SUBUNIT SEQUENCE

NKIKPGVAYSVITTENDTQTVFVDMPRLERRRANPKDVA
AVILGGGEGTKLFPLTSRTATPAVPVGGCYRLIDIPMSNC
INSAINKIFVLTQYNSAPLNRHI**A**RTYFGNGVS**F**GDGFVE
VLAATQTPGEAGKKWFQGTADAVRKFIWVFEDAKNKNIE
NIVVLSGDHLYRMDYMELVQNHIDRNADITLSCAPAEDSR
ASDFGLVKIDSRGRVVQFAEKPKGFDLKAMQVDTTLVGL
SPQDAKKSPYIASMGVYVFKTDVLLKLLKWSYPTSNDFG
SEIIPAAIDDYNVQAYIFKDYWEDIGTIKSFYNASLALTQE
FPEFQ**F**YDPKTPFYTSPRFLPPTKIDNCKIKDAIISHGCFL
RDCSVEHSIVG**E**RSRLDCGVELKDTFMMGADYYQTESEI
ASLLAEGKVPIGIGENTKIRKCIIDKNAKIGKNVSIINKDG
VQEADRPEEGFYIRSGIIIILEKATIRDGTVI

A91T **F101L** **F311L** **E358G**

APPENDIX B: MAPS OF EXPRESSION VECTORS

LS expression vector pML7

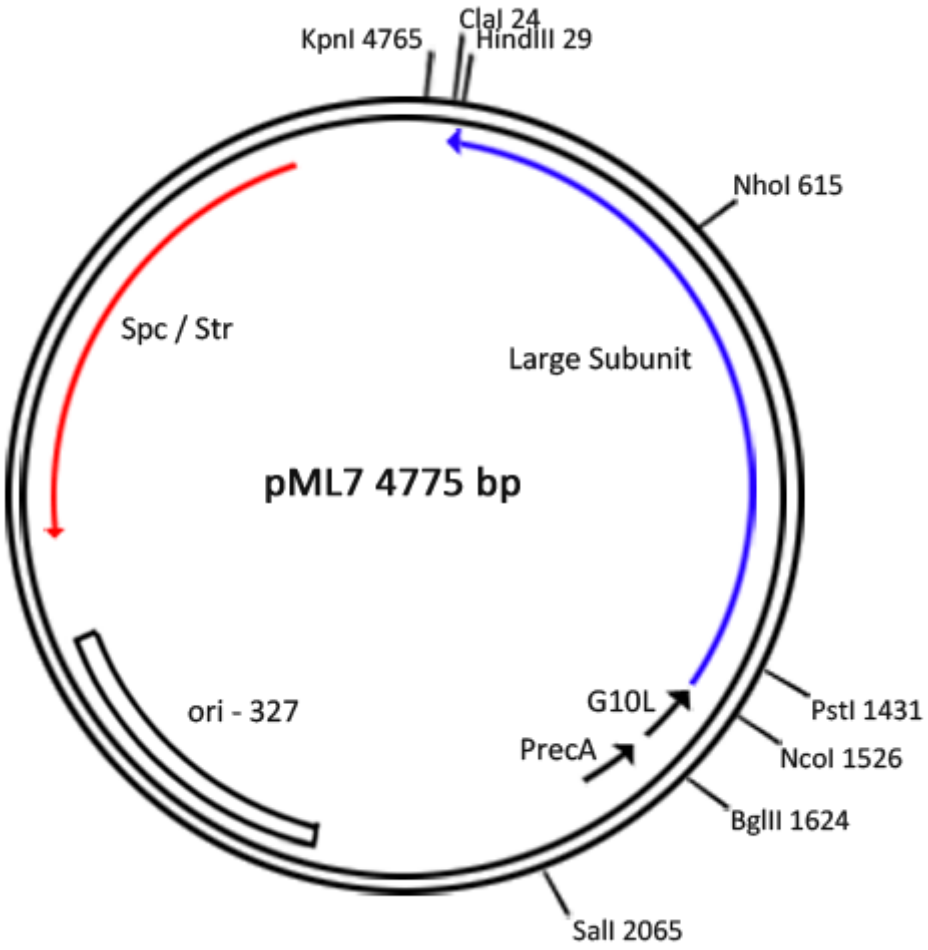

Small subunit expression vector pML10

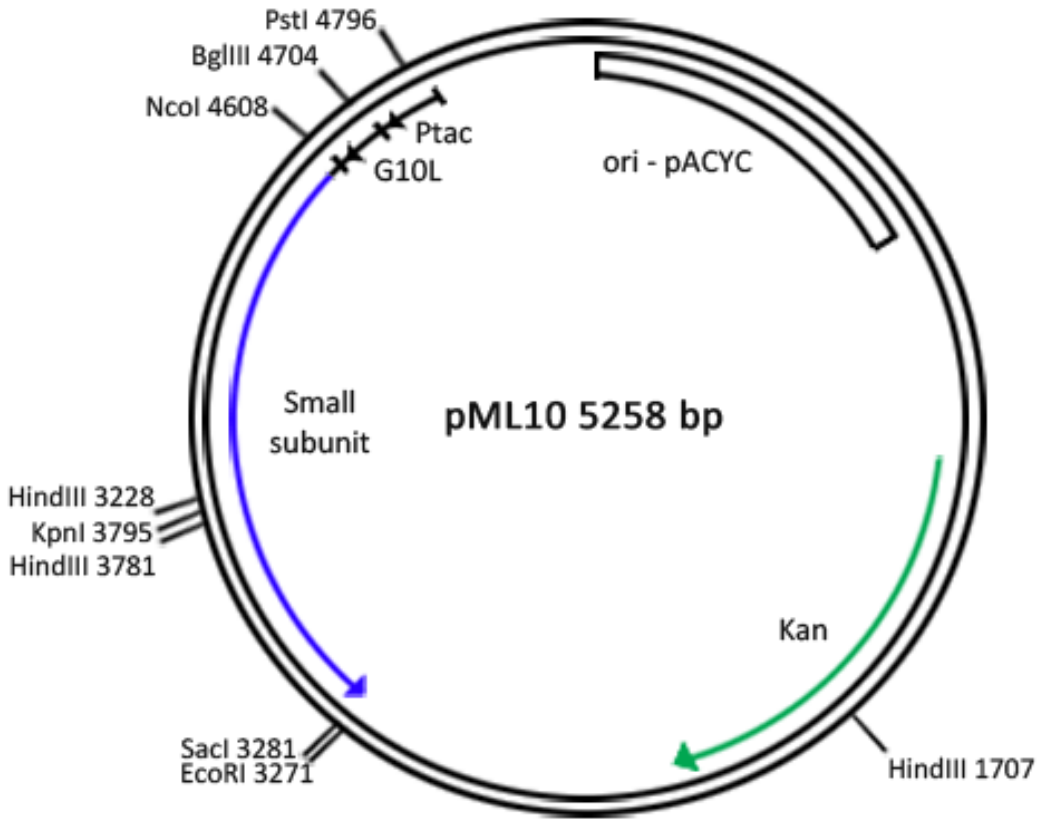

APPENDIX C: KINETIC CHARACTERIZATION TROUGH FORWARD DIRECTION ASSAY

Forward direction AGPase assay was conducted as described in section 3.8.2. During the assay, 5µL undiluted solution containing AGPase was added to the reaction mixture and AGPase was allowed to catalyze reaction for 10 minutes.

Enzymatic activity of AGPase containing mutant LS-E358G was measured as the total amount of pyrophosphate (PPi) produced in 10 minutes. For each concentration of substrate ATP, total amount of PPi produced in 10 minutes was measured. Obtained data were plotted and response of AGPase, containing mutant LS-E358G, towards ATP was obtained. Based on the graphs V_{max} (maximum reaction rate), K_M (Michaelis constant) values for ATP was calculated and compared to wild type.

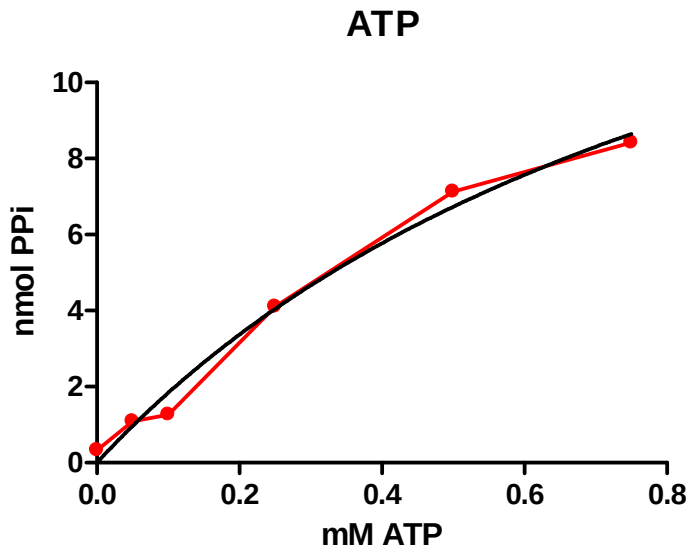

Response of AGPase with mutant LS-E358G towards ATP. Red line represents real response and black lines represents best fit curve.

A

AGPase Large Subunit	Variable	V_{max} (nmol/min)	V_{min} (nmol/min)	K_M (mM)
WT LS	ATP	11.67	0	0.07
Mutant LS-E358G	ATP	2.01	0	0.11

B

AGPase with Mutant LS-E358G	Variable	Percent Change of variable of AGPase with Mutant LS-E358G with Respect to AGPase with Wild Type LS
	Affinity for ATP	-36.36 %
	V_{max}	-82.35 %

Kinetic Properties of AGPase with WT LS or mutant LS-E358G. (A) V_{max}, V_{min} and K_M values of WT and mutant AGPases towards ATP. (B) Percent Change of given variables for AGPase with mutant LS-E358G with Respect to AGPase with Wild Type LS

APPENDIX D: AUTODOCK FILES

GPF File

```
npts 126 126 126                # num.grid points in xyz
gridfld RepairPDB_wt.maps.fld       # grid_data_file
spacing 0.15                    # spacing(A)
receptor_types A C HD N NA OA SA    # receptor atom types
ligand_types P C HD OA              # ligand atom types
receptor RepairPDB_wt.pdbqt         # macromolecule
gridcenter 49.125 19.79 59.39       # xyz-coordinates or auto
smooth 0.5                      # store minimum energy w/in rad(A)
map RepairPDB_wt.P.map              # atom-specific affinity map
map RepairPDB_wt.C.map              # atom-specific affinity map
map RepairPDB_wt.HD.map             # atom-specific affinity map
map RepairPDB_wt.OA.map             # atom-specific affinity map
elecmap RepairPDB_wt.e.map          # electrostatic potential map
dsolvmap RepairPDB_wt.d.map             # desolvation potential map
dielectric -0.1465              # <0, AD4 distance-dep.diel;>0, constant
```

DPF file (for wild type)

```
autodock_parameter_version 4.2       # used by autodock to validate parameter set
outlev 1                             # diagnostic output level
intelec                              # calculate internal electrostatics
seed pid time                        # seeds for random generator
ligand_types P C HD OA               # atoms types in ligand
fld RepairPDB_wt.maps.fld            # grid_data_file
map RepairPDB_wt.P.map               # atom-specific affinity map
map RepairPDB_wt.C.map               # atom-specific affinity map
map RepairPDB_wt.HD.map              # atom-specific affinity map
map RepairPDB_wt.OA.map              # atom-specific affinity map
elecmap RepairPDB_wt.e.map           # electrostatics map
desolvmap RepairPDB_wt.d.map         # desolvation map
move 3PGA.pdbqt                      # small molecule
about -0.0831 -0.1603 0.0549         # small molecule center
tran0 random                         # initial coordinates/A or random
axisangle0 random                    # initial orientation
dihe0 random                         # initial dihedrals (relative) or random
tstep 2.0                            # translation step/A
qstep 50.0                           # quaternion step/deg
dstep 50.0                           # torsion step/deg
torsdof 8                            # torsional degrees of freedom
rmstol 2.0                           # cluster_tolerance/A
extnrg 1000.0                        # external grid energy
e0max 0.0 10000                      # max initial energy; max number of retries
ga_pop_size 150                      # number of individuals in population
ga_num_evals 2500000                 # maximum number of energy evaluations
```

```
ga_num_generations 27000          # maximum number of generations
ga_elitism 1                      # number of top individuals to survive to next generation
ga_mutation_rate 0.02             # rate of gene mutation
ga_crossover_rate 0.8             # rate of crossover
ga_window_size 100                #
ga_cauchy_alpha 0.0               # Alpha parameter of Cauchy distribution
ga_cauchy_beta 1.0                # Beta parameter Cauchy distribution
set_ga                            # set the above parameters for GA or LGA
sw_max_its 300                    # iterations of Solis & Wets local search
sw_max_succ 4                     # consecutive successes before changing rho
sw_max_fail 4                     # consecutive failures before changing rho
sw_rho 1.0                        # size of local search space to sample
sw_lb_rho 0.01                    # lower bound on rho
ls_search_freq 0.06               # probability of performing local search on individual
set_psw1                          # set the above pseudo-Solis & Wets parameters
unbound_model bound               # state of unbound ligand
ga_run 10                         # do this many hybrid GA-LS runs
analysis                          # perform a ranked cluster analysis
```

APPENDIX E: CONSEQ RAW DATA

POSITION ACCORDING TO THIS STUDY	POS	SEQ	SCORE	COLOR	CONFIDENCE INTERVAL	CONFIDENCE INTERVAL COLORS	B/E	FUNCTION	MSA DATA	RESIDUE VARIETY
			(normalized)							
N/A	1	N	2.162	1	0.977, 2.926	1,1	e		21/218	Q,N,K,R,E
N/A	2	K	-0.105	5	-0.573, 0.214	7,4	e		23/218	T,R,K,V
N/A	3	I	2.326	1	0.977, 2.926	1,1	e		23/218	A,F,T,I,L,V
N/A	4	K	1.188	1	0.404, 1.497	3,1	e		25/218	A,Q,T,N,R,K
N/A	5	P	0.504	3*	-0.069, 0.977	5,1	e		25/218	H,Q,T,P,L
N/A	6	G	1.150	1	0.404, 1.497	3,1	e		28/218	H,N,R,G,V
N/A	7	V	0.247	4*	-0.182, 0.645	6,2	b		30/218	S,A,T,I,L,V
N/A	8	A	0.374	3	-0.069, 0.645	5,2	b		31/218	S,A,T,C,I,V
N/A	9	Y	2.526	1	0.977, 2.926	1,1	b		31/218	A,S,F,M,C,R,Y,V
N/A	10	S	0.391	3	-0.069, 0.645	5,2	b		38/218	A,S,C,G
N/A	11	V	0.480	3	-0.069, 0.645	5,2	b		38/218	S,C,I,L,V
N/A	12	I	0.959	1	0.214, 1.497	4,1	b		38/218	F,A,T,M,I,L,V
1	13	T	-0.510	7	-0.727,-0.365	8,7	b		38/218	M,T,I,L,V
2	14	T	0.854	1	0.214, 0.977	4,1	e		38/218	A,S,T,N,K,P,E,H,D,R
3	15	E	2.214	1	0.977, 2.926	1,1	e		38/218	F,S,N,K,Y,E,V,D,I,G
4	16	N	1.551	1	0.645, 1.497	2,1	e		38/218	A,F,T,N,P,V,H,D,I
5	17	D	2.903	1	1.497, 2.926	1,1	e		38/218	F,S,A,N,K,P,Y,C,D,I,G
6	18	T	2.215	1	0.977, 2.926	1,1	e		34/218	S,Q,T,N,P,R,K,E
7	19	Q	0.755	2	0.214, 0.977	4,1	e		34/218	A,Q,D,K,G,L,E
8	20	T	1.500	1	0.645, 1.497	2,1	e		35/218	F,S,A,T,N,P,E,V,H,M,I,L
9	21	V	2.711	1	1.497, 2.926	1,1	b		35/218	A,T,P,K,V,M,I,L
10	22	F	1.865	1	0.977, 2.926	1,1	e		35/218	A,S,F,T,N,P,K,E,V,H,M,I,L

11	23	V	2.801	1	1.497, 2.926	1,1	e		36/218	S,A,F,N,Y,V,H,Q,R,I,L
12	24	D	2.315	1	0.977, 2.926	1,1	e		45/218	A,S,T,K,P,E,V,H,Q,D,R
13	25	M	2.883	1	1.497, 2.926	1,1	e		52/218	F,S,A,T,N,K,P,E,V,Q,M,R,G,L
14	26	P	1.701	1	0.645, 2.926	2,1	e		57/218	A,S,T,N,K,P,H,Q,M,D,R
15	27	R	2.920	1	1.497, 2.926	1,1	e		57/218	F,S,T,N,P,E,Y,V,Q,M,D,R,I,L
16	28	L	2.835	1	1.497, 2.926	1,1	e		65/218	S,A,F,T,Y,E,V,M,D,R,I,L
17	29	E	2.782	1	1.497, 2.926	1,1	e		70/218	S,A,T,N,P,E,H,Q,M,C,D,R,I,G,L
18	30	R	2.650	1	1.497, 2.926	1,1	e		72/218	S,A,T,N,K,E,V,H,Q,M,I,R,G,L
19	31	R	2.640	1	1.497, 2.926	1,1	e		72/218	A,S,T,N,K,P,E,V,H,Q,D,R,L
20	32	R	2.771	1	1.497, 2.926	1,1	e		79/218	S,A,T,W,N,P,K,Y,E,H,Q,D,I,R,G,L
21	33	A	0.610	2	0.214, 0.977	4,1	e		89/218	F,S,A,T,K,P,V,H,M,D,I,R,G,L
22	34	N	1.029	1	0.404, 1.497	3,1	e		95/218	A,S,T,N,P,K,E,Q,D,I,R,G,L
23	35	P	-0.107	5	-0.279, 0.060	6,5	e		152/218	S,A,T,N,K,P,E,V,H,Q,M,D,R,L
24	36	K	0.880	1	0.404, 0.977	3,1	e		171/218	A,S,T,N,P,K,E,Q,M,D,R
25	37	D	0.614	2	0.214, 0.645	4,2	e		179/218	A,S,T,N,K,E,H,Q,D,R,I
26	38	V	-0.868	9	-0.937,-0.846	9,9	b	s	182/218	A,M,T,P,I,L,V
27	39	A	-0.092	5	-0.279, 0.060	6,5	b		182/218	S,F,A,T,V,H,M,I,L
28	40	A	-0.268	6	-0.442,-0.182	7,6	b		184/218	S,A,T,C,G,V
29	41	V	-0.363	7	-0.511,-0.279	7,6	b		186/218	M,I,L,V
30	42	I	-0.877	9	-0.937,-0.846	9,9	b	s	186/218	I,V
31	43	L	-0.911	9	-0.985,-0.879	9,9	b	s	187/218	M,L
32	44	G	-0.997	9	-1.054,-0.963	9,9	b	s	187/218	A,S,G
33	45	G	-1.029	9	-1.065,-1.006	9,9	b	s	187/218	S,G
34	46	G	-1.029	9	-1.065,-1.006	9,9	b	s	187/218	D,G
35	47	E	-0.438	7	-0.573,-0.365	7,7	e		188/218	S,A,T,N,K,P,E,V,Q,D,R,G
36	48	G	-0.964	9	-1.024,-0.937	9,9	e	f	188/218	S,F,R,G
37	49	T	-0.658	8	-0.770,-0.629	8,8	e	f	214/218	S,A,T,D,I,K,V
38	50	K	-0.871	9	-0.937,-0.846	9,9	e	f	215/218	H,Q,N,R,K

39	51	L	-1.063	9	-1.081,-1.054	9,9	b	s	214/218	L
40	52	F	0.061	5	-0.182, 0.214	6,4	b		214/218	S,A,F,N,K,E,Y,V,H,Q,L
41	53	P	-1.038	9	-1.074,-1.024	9,9	e	f	215/218	P,L
42	54	L	-1.063	9	-1.081,-1.054	9,9	b	s	215/218	L
43	55	T	-1.027	9	-1.065,-1.006	9,9	e	f	215/218	A,T,R,V
44	56	S	0.083	5	-0.182, 0.214	6,4	e		215/218	A,S,N,K,Y,E,H,Q,M,D,I,R,G,L
45	57	R	1.207	1	0.645, 1.497	2,1	e		215/218	F,S,T,N,K,Y,E,V,Q,M,L,A,P,H,D,R,I
46	58	T	-0.994	9	-1.040,-0.963	9,9	e	f	216/218	S,A,Q,T,R
47	59	A	-0.853	9	-0.937,-0.810	9,8	e	f	216/218	S,A,C
48	60	T	-1.005	9	-1.054,-0.985	9,9	e	f	216/218	M,T,K,E
49	61	P	-1.038	9	-1.074,-1.024	9,9	e	f	216/218	Q,P
50	62	A	-1.071	9	-1.081,-1.065	9,9	b	s	216/218	A
51	63	V	-1.040	9	-1.065,-1.024	9,9	b	s	216/218	I,V
52	64	P	-0.837	9	-0.937,-0.770	9,8	e	f	216/218	S,N,P,E
53	65	V	-0.401	7	-0.573,-0.279	7,6	b		216/218	F,T,M,I,L,V
54	66	G	-0.687	8	-0.810,-0.629	8,8	e	f	216/218	A,S,R,G
55	67	G	-0.868	9	-0.963,-0.810	9,8	b	s	216/218	S,A,G
56	68	C	-0.705	8	-0.810,-0.629	8,8	e	f	216/218	S,A,N,K,Q,M,C,R,G
57	69	Y	-0.869	9	-0.963,-0.810	9,8	b	s	216/218	F,H,T,Y
58	70	R	-1.031	9	-1.065,-1.024	9,9	e	f	216/218	Q,K,R
59	71	L	-0.838	9	-0.937,-0.770	9,8	b	s	216/218	M,I,L
60	72	I	-0.943	9	-1.006,-0.909	9,9	b	s	216/218	N,I,V
61	73	D	-1.069	9	-1.081,-1.065	9,9	b	s	216/218	D
62	74	I	-0.906	9	-0.963,-0.879	9,9	b	s	216/218	F,I,L,V
63	75	P	-0.985	9	-1.040,-0.963	9,9	b	s	216/218	S,A,P
64	76	M	-0.780	8	-0.879,-0.727	9,8	b		216/218	M,I,L,V
65	77	S	-1.059	9	-1.080,-1.054	9,9	b	s	216/218	A,S
66	78	N	-1.040	9	-1.065,-1.024	9,9	b	s	216/218	T,N,L

67	79	C	-0.835	9	-0.937,-0.770	9,8	b	s	216/218	S,C
68	80	I	-0.740	8	-0.846,-0.680	9,8	b		217/218	F,M,I,L,V
69	81	N	-0.944	9	-1.006,-0.909	9,9	e	f	217/218	H,N,R
70	82	S	-0.963	9	-1.006,-0.937	9,9	e	f	217/218	A,S,N
71	83	A	0.254	4	-0.069, 0.404	5,3	e		217/218	S,A,N,K,Y,E,Q,C,D,R,G
72	84	I	-0.323	6	-0.511,-0.279	7,6	b		217/218	F,M,C,I,Y,L,V
73	85	N	0.129	4	-0.069, 0.214	5,4	e		217/218	F,S,T,N,P,K,Y,E,V,H,Q,D,I,R,L
74	86	K	-0.425	7	-0.573,-0.365	7,7	e		217/218	S,H,Q,N,R,K,E
75	87	I	-0.645	8	-0.770,-0.573	8,7	b		217/218	A,M,I,L,V
76	88	F	-0.366	7	-0.511,-0.279	7,6	b		217/218	H,S,A,F,M,L,Y
77	89	V	-0.574	7	-0.680,-0.511	8,7	b		217/218	C,I,L,V
78	90	L	-0.776	8	-0.879,-0.727	9,8	b		217/218	M,I,R,L,V
79	91	T	-1.043	9	-1.065,-1.024	9,9	b	s	217/218	S,T
80	92	Q	-1.069	9	-1.081,-1.065	9,9	e	f	217/218	Q
81	93	Y	-0.819	8	-0.909,-0.770	9,8	b		217/218	F,Y
82	94	N	-0.990	9	-1.040,-0.963	9,9	e	f	217/218	H,M,N,L
83	95	S	-1.032	9	-1.065,-1.024	9,9	e	f	217/218	S,T
84	96	A	-0.636	8	-0.727,-0.573	8,7	e	f	217/218	S,F,A,W,T,Y,E,V,H,Q,M
85	97	P	-1.031	9	-1.065,-1.024	9,9	e	f	217/218	F,S,M,P
86	98	L	-1.063	9	-1.081,-1.054	9,9	b	s	217/218	L
87	99	N	-0.975	9	-1.024,-0.963	9,9	e	f	217/218	H,N
88	100	R	-0.441	7	-0.573,-0.365	7,7	e		217/218	A,S,T,N,K,H,Q,M,I,R,G,L
89	101	H	-1.070	9	-1.081,-1.065	9,9	e	f	217/218	H
90	102	I	-0.498	7	-0.629,-0.442	8,7	b		217/218	I,L,V
91	103	A	0.042	5	-0.182, 0.214	6,4	e		217/218	F,S,A,T,N,K,Y,V,H,Q,R,G,L
92	104	R	-0.305	6	-0.442,-0.182	7,6	e		216/218	S,N,K,E,H,Q,M,D,R,G
93	105	T	-0.574	7	-0.680,-0.511	8,7	b		217/218	A,S,T,I,G
94	106	Y	-0.871	9	-0.963,-0.810	9,8	b	s	217/218	F,Y

95	107	F	-0.065	5	-0.279, 0.060	6,5	b		215/218	A,S,F,W,T,N,P,V,Q,M,C,R,I,G,L
96	108	G	-0.543	7	-0.680,-0.511	8,7	e		216/218	A,S,T,N,P,E,Q,C,D,G
97	109	N	-0.004	5	-0.279, 0.214	6,4	e		98/218	S,T,N,K,E,V,H,M,D,I,G,L
98	110	G	-0.719	8	-0.879,-0.629	9,8	e	f	96/218	A,C,G,V
99	111	V	0.680	2	0.214, 0.977	4,1	e		114/218	A,S,T,N,E,V,C,I,G,L
100	112	S	1.131	1	0.645, 1.497	2,1	e		216/218	F,A,S,T,N,P,Y,V,H,Q,M,D,R,I,G,L
101	113	F	-0.625	8	-0.770,-0.573	8,7	e	f	217/218	S,A,F,T,N,P,K,Y,C,I,R,L
102	114	G	-0.242	6	-0.442,-0.182	7,6	e		217/218	A,S,T,N,K,E,H,Q,D,R,G
103	115	D	0.863	1	0.404, 0.977	3,1	e		217/218	A,S,T,N,K,E,H,Q,D,R,G
104	116	G	-0.843	9	-0.937,-0.810	9,8	b	s	217/218	A,S,G,E
105	117	F	-0.507	7	-0.680,-0.442	8,7	b		217/218	A,S,F,W,T,Y,H,M,C
106	118	V	-0.943	9	-1.006,-0.909	9,9	b	s	218/218	A,T,C,I,V
107	119	E	-0.808	8	-0.879,-0.770	9,8	e	f	218/218	S,Q,D,R,E
108	120	V	-0.807	8	-0.879,-0.770	9,8	b		218/218	A,I,L,V
109	121	L	-0.798	8	-0.909,-0.727	9,8	b		218/218	F,W,M,I,L,V
110	122	A	-1.009	9	-1.054,-0.985	9,9	b	s	218/218	S,A,T,P
111	123	A	-1.039	9	-1.065,-1.024	9,9	b	s	218/218	A,C,G
112	124	T	-0.824	8	-0.909,-0.770	9,8	e	f	218/218	H,S,A,Q,T,N,E
113	125	Q	-0.975	9	-1.024,-0.937	9,9	e	f	218/218	H,Q,I,K
114	126	T	-0.936	9	-0.985,-0.909	9,9	e	f	218/218	S,M,T,N,K,R,G
115	127	P	0.671	2	0.214, 0.977	4,1	e		218/218	F,S,T,N,K,Y,E,V,Q,M,L,A,P,H,D,I,G
116	128	G	-0.623	8	-0.846,-0.511	9,7	e	f	70/218	D,G,E
117	129	E	0.097	5	-0.279, 0.214	6,4	e		73/218	F,S,N,E,V,Q,D,L
118	130	A	1.182	1	0.645, 1.497	2,1	e		218/218	S,A,T,N,K,P,E,V,H,Q,M,D,I,R,G,L
119	131	G	-0.264	6	-0.442,-0.182	7,6	e		218/218	S,A,T,N,K,E,H,Q,D,I,R,G
120	132	K	0.524	3	0.214, 0.645	4,2	e		214/218	S,A,T,N,P,K,E,V,Q,M,D,I,R,L
121	133	K	0.905	1	0.404, 0.977	3,1	e		218/218	A,S,T,N,K,Y,E,V,H,Q,M,D,R,G
122	134	W	-1.044	9	-1.080,-1.024	9,9	e	f	218/218	W

123	135	F	-0.746	8	-0.846,-0.680	9,8	b		218/218	F,Y
124	136	Q	-0.816	8	-0.909,-0.770	9,8	e	f	218/218	Q,R,G,E
125	137	G	-1.062	9	-1.081,-1.054	9,9	b	s	217/218	G
126	138	T	-1.028	9	-1.065,-1.006	9,9	b	s	218/218	S,A,T,P
127	139	A	-1.071	9	-1.081,-1.065	9,9	b	s	218/218	A
128	140	D	-1.051	9	-1.074,-1.040	9,9	e	f	218/218	H,D
129	141	A	-1.040	9	-1.065,-1.024	9,9	b	s	218/218	S,A
130	142	V	-1.024	9	-1.054,-1.006	9,9	b	s	218/218	F,I,V
131	143	R	-1.051	9	-1.074,-1.040	9,9	e	f	218/218	T,R
132	144	K	-0.457	7	-0.573,-0.365	7,7	e		218/218	H,Q,R,K,E
133	145	F	-0.747	8	-0.846,-0.680	9,8	b		218/218	S,F,Q,T,N,C,G,Y,V
134	146	I	0.396	3	0.060, 0.645	5,2	b		218/218	S,A,F,W,T,E,V,H,Q,M,D,R,I,G,L
135	147	W	0.725	2	0.404, 0.977	3,1	e		218/218	F,S,T,N,K,Y,E,V,Q,L,A,W,P,H,D,I,R,G
136	148	V	-0.337	6	-0.511,-0.279	7,6	b		218/218	F,A,T,N,K,E,Y,V,H,Q,M,C,D,I,L
137	149	F	0.150	4	-0.069, 0.214	5,4	b		218/218	A,F,T,M,I,L,V
138	150	E	0.877	1	0.404, 0.977	3,1	e		218/218	A,S,T,N,K,E,V,H,Q,D,I,R,G,L
139	151	D	0.180	4	-0.069, 0.214	5,4	e		218/218	A,S,T,N,K,P,E,V,H,Q,D,R,G
140	152	A	0.603	2	0.214, 0.645	4,2	e		217/218	F,S,T,N,K,E,Y,V,Q,M,C,L,A,W,P,H,I,G
141	153	K	0.189	4	-0.182, 0.404	6,3	e		77/218	S,M,N,D,R,K,E,V
142	154	N	0.377	3	0.060, 0.645	5,2	e		77/218	S,A,H,Q,T,N,R,G,L
143	155	K	0.163	4	-0.182, 0.404	6,3	e		78/218	S,A,T,N,I,R,K,E
144	156	N	0.880	1	0.404, 0.977	3,1	e		218/218	F,A,S,W,N,P,K,E,V,H,Q,M,D,C,R,G
145	157	I	0.124	4	-0.069, 0.214	5,4	b		218/218	F,S,A,W,T,P,E,Y,V,H,D,C,I,L
146	158	E	0.009	5	-0.182, 0.060	6,5	e		218/218	S,T,N,K,E,Q,M,D,R,L
147	159	N	0.123	4	-0.069, 0.214	5,4	e		218/218	F,T,N,E,Y,H,Q,M,D,I,L
148	160	I	0.014	5	-0.182, 0.060	6,5	b		218/218	A,F,T,Y,V,M,I,L
149	161	V	-0.214	6	-0.442,-0.069	7,5	b		218/218	A,M,I,L,V
150	162	V	-0.831	8	-0.909,-0.810	9,8	b		218/218	I,V

151	163	L	-1.005	9	-1.054,-0.985	9,9	b	s	218/218	A,I,L
152	164	S	-0.847	9	-0.909,-0.810	9,8	b	s	218/218	A,S,C,G
153	165	G	-1.063	9	-1.081,-1.054	9,9	b	s	218/218	G
154	166	D	-1.050	9	-1.074,-1.040	9,9	e	f	218/218	Q,D
155	167	H	-0.922	9	-0.985,-0.879	9,9	b	s	218/218	A,H,Q
156	168	L	-1.006	9	-1.054,-0.985	9,9	b	s	218/218	M,L,V
157	169	Y	-0.998	9	-1.054,-0.963	9,9	b	s	218/218	F,C,Y
158	170	R	-0.905	9	-0.963,-0.879	9,9	b	s	218/218	S,Q,N,K,R,L
159	171	M	-1.038	9	-1.065,-1.024	9,9	b	s	218/218	M,I
160	172	D	-0.787	8	-0.879,-0.727	9,8	e	f	218/218	N,D
161	173	Y	-0.568	7	-0.727,-0.511	8,7	b		218/218	F,I,L,Y
162	174	M	0.042	5	-0.182, 0.214	6,4	e		218/218	A,S,T,N,K,E,Q,M,D,R,G,L
163	175	E	1.581	1	0.977, 1.497	1,1	e		218/218	A,S,T,N,P,K,E,V,H,Q,D,R,L
164	176	L	-0.208	6	-0.365,-0.069	7,5	b		218/218	F,M,I,Y,L,V
165	177	V	0.235	4	-0.069, 0.404	5,3	b		218/218	A,F,T,W,Y,V,M,I,L
166	178	Q	0.988	1	0.645, 0.977	2,1	e		218/218	S,F,A,T,N,K,E,H,Q,M,D,R,G,L
167	179	N	0.729	2	0.404, 0.977	3,1	e		218/218	F,A,S,T,N,K,E,Y,V,H,Q,D,R
168	180	H	-1.018	9	-1.054,-1.006	9,9	e	f	218/218	A,H,Q,M
169	181	I	0.299	4	0.060, 0.404	5,3	e		218/218	A,S,W,K,E,V,H,Q,M,D,C,I,R,L
170	182	D	1.093	1	0.645, 1.497	2,1	e		218/218	S,A,T,N,K,E,H,Q,D,I,R,G
171	183	R	0.050	5	-0.182, 0.214	6,4	e		218/218	A,F,S,T,N,P,K,V,H,M,C,D,R,G
172	184	N	1.184	1	0.645, 1.497	2,1	e		218/218	A,Q,C,D,N,R,K,G,E
173	185	A	-0.842	9	-0.909,-0.810	9,8	b	s	218/218	S,A,T,N,R,G,V
174	186	D	-0.484	7	-0.629,-0.442	8,7	e		218/218	A,Q,N,D,K,G,E
175	187	I	-0.522	7	-0.629,-0.442	8,7	b		218/218	A,F,M,I,L,V
176	188	T	-0.789	8	-0.879,-0.727	9,8	b		218/218	S,T,C,V
177	189	L	-0.294	6	-0.442,-0.182	7,6	b		218/218	I,L,V
178	190	S	-0.799	8	-0.879,-0.770	9,8	b		218/218	A,S,T,C,G

179	191	C	-0.581	7	-0.680,-0.511	8,7	b		218/218	A,S,T,C,I,G,V
180	192	A	0.051	5	-0.182, 0.214	6,4	b		218/218	A,T,N,K,Y,V,H,Q,M,R,I,L
181	193	P	-0.700	8	-0.810,-0.629	8,8	e	f	218/218	S,A,T,P,L,V
182	194	A	-0.271	6	-0.442,-0.182	7,6	e		218/218	F,S,A,T,Y,V,M,C,I,L
183	195	E	0.396	3	0.060, 0.404	5,3	e		218/218	S,A,T,N,P,E,V,D,C,R,G,L
184	196	D	0.527	3	0.214, 0.645	4,2	e		218/218	S,T,N,K,Y,E,V,Q,L,A,W,P,H,D,R,I,G
185	197	S	0.721	2	0.404, 0.977	3,1	e		218/218	A,S,T,P,K,Y,E,V,H,Q,D,R,G,L
186	198	R	-0.123	6	-0.279,-0.069	6,5	e		218/218	A,T,N,K,E,V,H,Q,M,D,R,L
187	199	A	-0.921	9	-0.985,-0.879	9,9	b	s	218/218	A,T,I,P,V
188	200	S	-0.129	6	-0.279,-0.069	6,5	e		218/218	F,A,S,T,N,P,K,Y,E,V,H,Q,R,G
189	201	D	0.426	3	0.060, 0.645	5,2	e		218/218	A,S,N,K,E,H,Q,D,C,R,G,L
190	202	F	-0.317	6	-0.511,-0.182	7,6	b		218/218	F,M,C,N,R,L,Y
191	203	G	-1.003	9	-1.054,-0.985	9,9	b	s	218/218	D,G,E
192	204	L	-0.840	9	-0.909,-0.810	9,8	b	s	218/218	I,L,V
193	205	V	-0.551	7	-0.680,-0.511	8,7	b		218/218	T,M,I,L,V
194	206	K	-0.421	7	-0.573,-0.365	7,7	e		218/218	S,N,K,V,H,Q,D,R,G,L
195	207	I	-0.145	6	-0.365,-0.069	7,5	b		218/218	S,F,A,T,V,Q,M,C,R,I,L
196	208	D	-0.383	7	-0.511,-0.279	7,6	e		218/218	S,A,N,K,E,B,H,D,G
197	209	S	2.926	1	1.497, 2.926	1,1	e		218/218	A,S,T,N,P,K,E,V,H,Q,D,R,G,L
198	210	R	1.766	1	0.977, 1.497	1,1	e		218/218	A,F,S,T,N,K,E,V,H,Q,M,D,R,G
199	211	G	0.058	5	-0.182, 0.214	6,4	e		218/218	F,S,A,N,K,Y,H,Q,R,G,L
200	212	R	0.845	1	0.404, 0.977	3,1	e		218/218	F,S,T,N,K,E,Y,V,Q,M,C,L,A,W,H,R,I
201	213	V	-0.571	7	-0.680,-0.511	8,7	b		218/218	A,I,V
202	214	V	0.927	1	0.404, 0.977	3,1	b		218/218	S,F,T,N,K,E,Y,V,Q,M,C,L,A,H,D,R,I,G
203	215	Q	0.505	3	0.214, 0.645	4,2	e		218/218	A,S,F,T,N,K,E,Y,H,Q,D,R,G,L
204	216	F	-1.062	9	-1.081,-1.054	9,9	b	s	218/218	F
205	217	A	0.558	3	0.214, 0.645	4,2	e		218/218	F,S,A,T,N,K,E,Y,V,H,Q,M,C,I,R,L
206	218	E	-1.068	9	-1.081,-1.065	9,9	e	f	218/218	E

207	219	K	-1.046	9	-1.074,-1.040	9,9	e	f	218/218	N,K
208	220	P	-1.064	9	-1.081,-1.054	9,9	e	f	218/218	P
209	221	K	0.564	3	0.214, 0.645	4,2	e		218/218	A,S,T,N,P,K,E,V,Q,M,D,R,G
210	222	G	0.000	5	-0.182, 0.060	6,5	e		218/218	A,T,N,K,P,Y,E,Q,D,I,R,G,L
211	223	F	1.511	1	0.977, 1.497	1,1	e		218/218	A,S,F,T,N,K,P,E,V,H,Q,M,D,I,G,L
212	224	D	0.993	1	0.645, 0.977	2,1	e		217/218	A,S,T,N,K,E,V,H,Q,M,D,R,I,G,L
213	225	L	-0.666	8	-0.770,-0.573	8,7	b		218/218	F,Q,T,M,I,R,L,V
214	226	K	1.538	1	0.977, 1.497	1,1	e		218/218	A,S,T,N,P,K,E,V,H,Q,M,D,R,G,L
215	227	A	0.950	1	0.404, 0.977	3,1	e		218/218	S,A,T,N,P,K,Y,E,H,Q,M,D,R,G,L
216	228	M	-0.477	7	-0.629,-0.365	8,7	b		218/218	F,W,K,Y,V,M,C,I,L
217	229	Q	1.461	1	0.977, 1.497	1,1	e		216/218	S,A,T,W,N,K,Y,E,V,H,Q,M,R,G
218	230	V	-0.420	7	-0.573,-0.365	7,7	e		216/218	F,S,A,T,K,V,M,D,C,I,L
219	231	D	-0.152	6	-0.365,-0.069	7,5	e		212/218	A,S,N,P,K,E,H,Q,D,G
220	232	T	-0.474	7	-0.629,-0.365	8,7	e		210/218	A,S,T,K,P,E,V,Q,M,D,R,G,L
221	233	T	0.447	3	0.214, 0.645	4,2	e		210/218	S,A,T,N,P,K,E,V,Q,D,I,G
222	234	L	1.499	1	0.977, 1.497	1,1	e		182/218	F,A,S,W,T,K,Y,V,Q,M,D,R,I,L
223	235	V	0.445	3	0.060, 0.645	5,2	e		182/218	F,T,K,P,E,Y,V,H,M,I,R,G,L
224	236	G	0.057	5	-0.182, 0.214	6,4	e		183/218	S,A,N,P,K,E,H,Q,M,D,I,R,G,L
225	237	L	0.277	4	-0.069, 0.404	5,3	e		182/218	S,A,F,T,N,K,P,E,Y,V,Q,M,D,R,G,L
226	238	S	0.399	3	0.060, 0.645	5,2	e		205/218	F,A,S,T,N,K,P,Y,E,V,H,Q,M,D,R,G,L
227	239	P	2.659	1	1.497, 2.926	1,1	e		199/218	S,A,T,N,K,P,E,V,H,Q,D,I,R,G,L
228	240	Q	1.000	1	0.645, 0.977	2,1	e		203/218	S,T,N,K,Y,E,V,Q,M,L,A,P,H,D,I,R
229	241	D	0.853	1	0.404, 0.977	3,1	e		218/218	S,A,F,T,N,P,K,E,V,H,Q,D,R,I,G,L
230	242	A	-0.032	5	-0.279, 0.060	6,5	e		218/218	F,S,A,T,N,K,P,E,V,H,Q,C,D,R,G
231	243	K	2.926	1	1.497, 2.926	1,1	e		218/218	S,A,T,N,P,K,E,V,H,Q,M,D,R,I,G,L
232	244	K	1.565	1	0.977, 1.497	1,1	e		218/218	A,S,T,N,K,E,V,H,Q,D,I,R,G,L
233	245	S	0.642	2	0.214, 0.645	4,2	e		218/218	A,F,S,T,N,P,K,E,Y,Q,M,D,C,R,G,L
234	246	P	0.310	4	0.060, 0.404	5,3	e		218/218	S,T,N,K,P,E,Y,V,H,Q,C,D,R,I,L

235	247	Y	-0.124	6	-0.365,-0.069	7,5	b		218/218	H,F,W,C,L,Y
236	248	I	-0.655	8	-0.770,-0.573	8,7	b		218/218	F,S,E,V,H,Q,M,I,L
237	249	A	-1.039	9	-1.065,-1.024	9,9	b	s	218/218	A,G
238	250	S	-1.032	9	-1.065,-1.024	9,9	b	s	218/218	S,N,P
239	251	M	-1.055	9	-1.074,-1.040	9,9	b	s	218/218	M,I
240	252	G	-1.063	9	-1.081,-1.054	9,9	b	s	218/218	G
241	253	V	-0.914	9	-0.985,-0.879	9,9	b	s	218/218	M,I,L,V
242	254	Y	-1.030	9	-1.065,-1.006	9,9	b	s	218/218	S,Y
243	255	V	-0.487	7	-0.629,-0.442	8,7	b		218/218	F,A,M,C,I,L,V
244	256	F	-0.668	8	-0.770,-0.573	8,7	b		218/218	A,F,M,I,L,V
245	257	K	-0.161	6	-0.365,-0.069	7,5	e		218/218	S,T,D,N,R,K
246	258	T	-0.140	6	-0.365,-0.069	7,5	e		218/218	A,T,K,H,M,R,I,L
247	259	D	1.481	1	0.977, 1.497	1,1	e		218/218	A,S,T,N,P,K,E,H,Q,D,R,G
248	260	V	0.205	4	-0.069, 0.404	5,3	b		218/218	S,A,T,P,K,V,M,I,L
249	261	L	-0.642	8	-0.770,-0.573	8,7	b		218/218	M,I,L
250	262	L	1.358	1	0.645, 1.497	2,1	e		218/218	F,S,A,T,N,K,Y,E,V,H,M,D,C,R,I,G,L
251	263	K	1.446	1	0.977, 1.497	1,1	e		218/218	A,S,T,N,K,E,H,Q,D,R,G
252	264	L	0.031	5	-0.182, 0.214	6,4	b		218/218	S,A,F,W,V,Q,M,C,I,L
253	265	L	-0.809	8	-0.909,-0.770	9,8	b		218/218	F,M,I,L,V
254	266	K	0.667	2	0.214, 0.977	4,1	e		102/218	S,T,N,K,E,H,Q,M,D,R,G,L
255	267	W	2.925	1	1.497, 2.926	1,1	e		154/218	A,S,T,W,N,K,E,H,Q,C,D,I,R,G
256	268	S	2.878	1	1.497, 2.926	1,1	e		193/218	A,S,T,N,K,E,V,H,Q,D,C,R,I,G,L
257	269	Y	0.699	2	0.404, 0.977	3,1	e		218/218	S,F,T,N,K,E,Y,V,Q,M,C,A,H,D,R,G
258	270	P	0.656	2	0.214, 0.645	4,2	e		216/218	A,S,T,N,K,P,E,V,H,Q,D,R,I,G,L
259	271	T	1.464	1	0.977, 1.497	1,1	e		218/218	S,A,T,N,P,K,E,H,Q,D,I,R,G,L
260	272	S	0.763	2	0.404, 0.977	3,1	e		218/218	F,A,S,T,K,E,Y,H,Q,M,C,D,R,G,L
261	273	N	-0.255	6	-0.442,-0.182	7,6	e		218/218	A,S,T,N,P,K,E,V,H,Q,M,D,I,G,L
262	274	D	-1.069	9	-1.081,-1.065	9,9	e	f	218/218	D

263	275	F	-1.062	9	-1.081,-1.054	9,9	e	f	218/218	F
264	276	G	-1.063	9	-1.081,-1.054	9,9	b	s	218/218	G
265	277	S	-0.646	8	-0.770,-0.573	8,7	e	f	218/218	S,N,R,K,G,Y,L
266	278	E	-0.786	8	-0.879,-0.727	9,8	e	f	218/218	H,Q,D,G,E
267	279	I	-0.456	7	-0.573,-0.365	7,7	b		218/218	I,L,V
268	280	I	-0.912	9	-0.985,-0.879	9,9	b	s	218/218	F,I,L
269	281	P	-1.064	9	-1.081,-1.054	9,9	e	f	218/218	P
270	282	A	1.429	1	0.977, 1.497	1,1	e		218/218	F,S,T,N,K,E,Y,Q,M,L,A,W,H,D,I,R,G
271	283	A	-0.212	6	-0.365,-0.182	7,6	b		218/218	S,A,T,N,K,V,M,C,I,L
272	284	I	-0.332	6	-0.511,-0.279	7,6	b		218/218	S,A,T,N,K,Y,V,M,I,L
273	285	D	2.839	1	1.497, 2.926	1,1	e		218/218	S,A,T,N,P,K,E,V,H,Q,M,D,R,G,L
274	286	D	0.994	1	0.645, 0.977	2,1	e		218/218	A,S,T,N,K,E,V,H,Q,D,R,G
275	287	Y	1.221	1	0.645, 1.497	2,1	e		218/218	A,F,S,N,K,Y,V,H,Q,M,D,C,I,R,G,L
276	288	N	0.602	2	0.214, 0.645	4,2	e		218/218	S,F,T,N,K,Y,Q,C,L,A,P,H,D,R,I,G
277	289	V	-0.435	7	-0.573,-0.365	7,7	b		218/218	T,M,I,L,V
278	290	Q	0.447	3	0.214, 0.645	4,2	e		218/218	S,F,N,K,Y,E,V,Q,M,C,L,A,H,R,I,G
279	291	A	-0.674	8	-0.770,-0.629	8,8	b		218/218	S,A,T,I,G,L,V
280	292	Y	-0.259	6	-0.442,-0.182	7,6	b		218/218	H,F,C,Y
281	293	I	0.132	4	-0.069, 0.214	5,4	b		218/218	A,F,T,N,P,Y,E,V,Q,M,D,I,L
282	294	F	-0.460	7	-0.629,-0.365	8,7	b		218/218	H,F,Y
283	295	K	0.371	3	0.060, 0.404	5,3	e		218/218	S,T,N,P,K,E,Y,H,Q,D,R,I,G
284	296	D	-0.397	7	-0.573,-0.279	7,6	e		218/218	A,S,D,G,E
285	297	Y	-0.958	9	-1.024,-0.909	9,9	e	f	218/218	A,F,Y
286	298	W	-1.044	9	-1.080,-1.024	9,9	b	s	218/218	W
287	299	E	-0.834	9	-0.909,-0.770	9,8	e	f	218/218	S,A,T,K,E,V,Q,R
288	300	D	-1.069	9	-1.081,-1.065	9,9	e	f	218/218	D
289	301	I	-1.010	9	-1.054,-0.985	9,9	b	s	218/218	I,L,V
290	302	G	-1.033	9	-1.074,-1.006	9,9	b	s	218/218	N,G

291	303	T	-0.968	9	-1.024,-0.937	9,9	e	f	218/218	H,S,T,N
292	304	I	-0.928	9	-0.985,-0.909	9,9	b	s	218/218	M,I,L,V
293	305	K	0.213	4	-0.069, 0.404	5,3	e		218/218	A,S,P,K,Y,E,H,Q,D,R,G
294	306	S	-0.732	8	-0.810,-0.680	8,8	b		218/218	A,S,T,D,N,R
295	307	F	-0.942	9	-1.006,-0.909	9,9	b	s	218/218	F,Y,L
296	308	Y	-0.367	7	-0.511,-0.279	7,6	b		218/218	H,F,W,C,Y
297	309	N	0.096	5	-0.182, 0.214	6,4	e		218/218	H,A,Q,D,N,K,R,E
298	310	A	-0.823	8	-0.909,-0.770	9,8	b		218/218	S,A,M,T,C,E,V
299	311	S	-0.918	9	-0.985,-0.879	9,9	b	s	218/218	H,S,T,N
300	312	L	-0.487	7	-0.629,-0.442	8,7	b		218/218	M,I,L
301	313	A	0.028	5	-0.182, 0.060	6,5	e		218/218	S,A,T,N,K,E,Q,M,D,R,G
302	314	L	-0.921	9	-0.985,-0.879	9,9	b	s	218/218	F,C,I,L,V
303	315	T	-0.459	7	-0.573,-0.365	7,7	e		218/218	A,M,T,N,C,I,G,V
304	316	Q	1.155	1	0.645, 1.497	2,1	e		218/218	S,A,T,N,K,E,V,H,Q,D,C,R,G,L
305	317	E	0.233	4	-0.069, 0.404	5,3	e		218/218	A,S,T,N,K,P,Y,E,V,H,Q,D,I,R,L
306	318	F	0.374	3	0.060, 0.404	5,3	e		217/218	S,F,T,N,K,Y,E,V,Q,M,L,P,H,D,R,I,G
307	319	P	-0.661	8	-0.770,-0.573	8,7	e	f	218/218	S,A,H,N,P,G
308	320	E	1.390	1	0.977, 1.497	1,1	e		218/218	S,A,T,N,P,K,E,V,H,Q,M,D,I,R,L
309	321	F	-1.002	9	-1.054,-0.985	9,9	b	s	218/218	F,I,Y
310	322	Q	-0.234	6	-0.365,-0.182	7,6	e		218/218	S,N,K,Y,E,H,Q,D,R
311	323	F	-0.564	7	-0.680,-0.511	8,7	b		218/218	F,M,C,I,L
312	324	Y	-0.273	6	-0.442,-0.182	7,6	e		218/218	S,A,F,T,N,Y,V,H,D,R,I
313	325	D	-0.377	7	-0.511,-0.279	7,6	e		217/218	A,S,T,N,Y,E,V,Q,D,R,G,L
314	326	P	0.351	4	0.060, 0.404	5,3	e		210/218	S,A,T,N,K,P,Y,E,V,H,Q,M,D,R,G,L
315	327	K	2.583	1	1.497, 2.926	1,1	e		218/218	F,S,T,N,K,E,V,Q,M,L,A,P,H,D,I,R,G
316	328	T	0.297	4	0.060, 0.404	5,3	e		218/218	F,S,A,T,N,K,E,Y,H,Q,M,D,R,G
317	329	P	-0.553	7	-0.680,-0.511	8,7	e		218/218	S,A,T,N,K,P,V,H,R,I,G
318	330	F	-0.803	8	-0.879,-0.770	9,8	b		218/218	F,T,M,I,L,V

319	331	Y	-0.236	6	-0.442,-0.182	7,6	e		218/218	F,N,I,L,Y
320	332	T	-0.938	9	-0.985,-0.909	9,9	e	f	218/218	S,T,N
321	333	S	-0.493	7	-0.629,-0.442	8,7	e		218/218	A,F,S,N,Y,H,Q,M,C,R,L
322	334	P	0.521	3	0.214, 0.645	4,2	e		218/218	S,A,T,N,P,Y,V,H,Q,M,D,I,R,G,L
323	335	R	-0.909	9	-0.985,-0.879	9,9	e	f	218/218	S,Y,H,Q,D,R,G,L
324	336	F	0.213	4	-0.069, 0.404	5,3	e		218/218	A,S,F,N,P,Y,V,H,M,D,C,I,L
325	337	L	-0.977	9	-1.040,-0.937	9,9	e	f	218/218	F,S,L,V
326	338	P	-0.959	9	-1.024,-0.937	9,9	e	f	218/218	S,A,P
327	339	P	-0.559	7	-0.680,-0.511	8,7	e		218/218	A,T,C,P,G
328	340	T	-0.502	7	-0.629,-0.442	8,7	e		218/218	A,S,T,C,N,V
329	341	K	-0.584	7	-0.727,-0.511	8,7	e		218/218	S,A,T,K,H,Q,M,D,R,I,L
330	342	I	0.429	3	0.060, 0.645	5,2	e		218/218	S,A,F,T,Y,V,Q,M,C,I,L
331	343	D	0.423	3	0.060, 0.645	5,2	e		218/218	S,F,T,N,K,Y,E,V,Q,M,L,A,H,D,I,R,G
332	344	N	0.566	3	0.214, 0.645	4,2	e		218/218	A,F,S,T,N,K,Y,E,V,Q,D,R,G
333	345	C	0.071	5	-0.182, 0.214	6,4	b		218/218	A,S,T,C,P,G,V
334	346	K	0.711	2	0.404, 0.977	3,1	e		217/218	A,F,S,T,N,K,Y,E,V,H,Q,M,D,I,R,L
335	347	I	0.015	5	-0.182, 0.060	6,5	b		218/218	F,A,M,I,L,V
336	348	K	0.745	2	0.404, 0.977	3,1	e		218/218	A,S,T,N,K,Y,E,V,H,Q,M,D,R,I,L
337	349	D	0.580	3	0.214, 0.645	4,2	e		218/218	S,A,T,N,K,Y,E,H,Q,M,C,D,R,G
338	350	A	-0.539	7	-0.680,-0.511	8,7	b		218/218	S,A,T,C,V
339	351	I	-0.298	6	-0.442,-0.182	7,6	b		218/218	F,Q,T,M,I,L,V
340	352	I	-0.289	6	-0.442,-0.182	7,6	b		218/218	F,A,M,T,C,I,L,V
341	353	S	-0.411	7	-0.573,-0.365	7,7	b		218/218	A,S,T,C,N,G
342	354	H	-0.718	8	-0.810,-0.680	8,8	e	f	218/218	S,H,Q,D,E
343	355	G	-1.033	9	-1.074,-1.024	9,9	b	s	218/218	F,G
344	356	C	-0.430	7	-0.573,-0.365	7,7	b		218/218	A,S,T,C,I,G,V
345	357	F	-0.180	6	-0.365,-0.069	7,5	b		217/218	A,S,F,T,K,E,Y,V,Q,M,C,R,I,L
346	358	L	-0.507	7	-0.629,-0.442	8,7	b		217/218	F,I,L,V

347	359	R	0.758	2	0.404, 0.977	3,1	e		217/218	A,S,T,N,K,E,V,H,Q,M,D,I,R,G,L
348	360	D	0.903	1	0.404, 0.977	3,1	e		218/218	A,S,T,N,K,Y,E,H,Q,D,R,G
349	361	C	-0.151	6	-0.365,-0.069	7,5	b		218/218	A,S,T,D,C,K,G,E,V
350	362	S	0.819	2	0.404, 0.977	3,1	e		218/218	A,F,S,T,N,K,E,Y,V,H,Q,C,R,I,L
351	363	V	-0.579	7	-0.680,-0.511	8,7	b		218/218	F,C,I,L,V
352	364	E	1.277	1	0.645, 1.497	2,1	e		218/218	F,S,T,N,K,Y,E,V,Q,L,A,H,D,R,I,G
353	365	H	0.180	4	-0.069, 0.214	5,4	e		218/218	S,N,K,Y,E,H,Q,D,R,G
354	366	S	-0.755	8	-0.846,-0.727	9,8	b		218/218	A,S,T,C,V
355	367	I	-0.488	7	-0.629,-0.442	8,7	b		218/218	S,T,M,I,L,V
356	368	V	-0.300	6	-0.442,-0.182	7,6	b		218/218	I,L,V
357	369	G	-1.063	9	-1.081,-1.054	9,9	b	s	218/218	G
358	370	E	0.032	5	-0.182, 0.060	6,5	b		218/218	F,N,P,E,V,Q,D,I,L
359	371	R	-0.970	9	-1.024,-0.937	9,9	e	f	218/218	S,N,C,P,R,L
360	372	S	-0.709	8	-0.810,-0.680	8,8	b		218/218	A,S,Q,M,T,C
361	373	R	-0.135	6	-0.365,-0.069	7,5	e		218/218	F,A,S,T,W,N,K,Y,V,Q,C,R,I,L
362	374	L	-0.463	7	-0.573,-0.365	7,7	b		218/218	I,L,V
363	375	D	0.345	4	0.060, 0.404	5,3	e		218/218	A,S,N,K,E,H,Q,D,R,G
364	376	C	1.294	1	0.645, 1.497	2,1	e		218/218	F,A,S,T,N,K,P,E,Y,V,H,Q,M,C,D,R,I,G
365	377	G	0.345	4	0.060, 0.404	5,3	e		218/218	S,A,N,K,E,H,Q,D,R,G
366	378	V	0.044	5	-0.182, 0.214	6,4	b		218/218	S,A,T,C,I,V
367	379	E	0.742	2	0.404, 0.977	3,1	e		218/218	F,A,S,T,N,K,E,V,H,Q,C,D,I,R,L
368	380	L	-0.261	6	-0.442,-0.182	7,6	b		218/218	F,M,I,L,V
369	381	K	0.715	2	0.404, 0.977	3,1	e		218/218	S,T,N,K,Y,E,V,H,Q,M,D,I,R
370	382	D	-0.286	6	-0.442,-0.182	7,6	e		218/218	A,S,N,E,H,Q,D,R,G
371	383	T	-0.004	5	-0.182, 0.060	6,5	b		218/218	S,A,T,C,V
372	384	F	-0.200	6	-0.365,-0.069	7,5	b		218/218	F,M,I,Y,L,V
373	385	M	0.102	5	-0.182, 0.214	6,4	b		218/218	S,W,M,C,I,L,V
374	386	M	-0.863	9	-0.937,-0.810	9,8	b	s	218/218	M,I,L

375	387	G	-1.063	9	-1.081,-1.054	9,9	b	s	218/218	G
376	388	A	-0.471	7	-0.629,-0.442	8,7	b		218/218	S,A,N,C,G,L
377	389	D	-0.975	9	-1.024,-0.937	9,9	b	s	218/218	S,T,N,D,E
378	390	Y	1.626	1	0.977, 1.497	1,1	e		218/218	S,F,T,N,K,E,Y,V,Q,M,C,L,W,H,D,I,R
379	391	Y	-0.625	8	-0.770,-0.573	8,7	e	f	218/218	F,I,E,Y
380	392	Q	-0.224	6	-0.442,-0.182	7,6	e		218/218	S,A,T,P,E,V,H,Q,D,R,G,L
381	393	T	-0.055	5	-0.279, 0.060	6,5	e		218/218	S,T,N,Y,E,V,Q,M,L,A,W,P,H,D,R,G
382	394	E	1.917	1	0.977, 2.926	1,1	e		218/218	S,F,T,K,Y,E,V,Q,M,L,A,P,H,D,R,I,G
383	395	S	1.471	1	0.977, 1.497	1,1	e		216/218	F,S,T,N,K,Y,E,V,Q,C,L,A,P,H,D,I,R,G
384	396	E	0.572	3	0.214, 0.645	4,2	e		216/218	S,T,N,K,E,V,Q,M,L,A,P,H,D,I,R,G
385	397	I	0.342	4	0.060, 0.404	5,3	e		210/218	S,A,T,N,K,E,V,H,M,D,C,I,R,L
386	398	A	1.372	1	0.977, 1.497	1,1	e		211/218	S,F,T,N,K,E,V,Q,M,L,A,H,D,R,I,G
387	399	S	2.903	1	1.497, 2.926	1,1	e		210/218	F,S,T,N,K,Y,E,V,Q,C,L,A,P,H,D,R,I,G
388	400	L	1.363	1	0.645, 1.497	2,1	e		210/218	S,F,T,N,K,Y,E,V,Q,M,C,L,A,H,D,I,R,G
389	401	L	2.920	1	1.497, 2.926	1,1	e		210/218	F,S,T,N,K,E,Y,V,Q,M,C,L,A,P,H,D,R,I,G
390	402	A	2.585	1	1.497, 2.926	1,1	e		211/218	F,S,T,N,K,E,V,Q,L,A,P,H,D,R,I,G
391	403	E	1.959	1	0.977, 2.926	1,1	e		207/218	S,T,N,K,E,V,Q,C,L,A,P,H,D,R,I,G
392	404	G	0.144	4	-0.069, 0.214	5,4	e		207/218	S,A,T,N,K,E,V,H,Q,D,R,G,L
393	405	K	1.594	1	0.977, 1.497	1,1	e		217/218	S,T,N,K,Y,E,V,Q,C,L,P,H,D,R,I,G
394	406	V	-0.017	5	-0.279, 0.060	6,5	b		218/218	S,A,T,N,P,E,V,D,I,L
395	407	P	0.410	3	0.060, 0.645	5,2	e		218/218	S,T,N,K,Y,E,V,Q,M,C,L,A,P,H,D,I,R,G
396	408	I	0.769	2	0.404, 0.977	3,1	b		218/218	F,A,T,K,P,V,Q,M,I,L
397	409	G	-0.972	9	-1.024,-0.937	9,9	b	s	218/218	S,Q,N,G
398	410	I	-0.661	8	-0.770,-0.629	8,8	b		218/218	I,L,V
399	411	G	-1.004	9	-1.054,-0.985	9,9	b	s	218/218	A,G
400	412	E	1.485	1	0.977, 1.497	1,1	e		218/218	A,S,T,N,P,K,Y,E,H,Q,D,R
401	413	N	0.041	5	-0.182, 0.214	6,4	e		218/218	F,N,K,Y,E,H,Q,D,R,G
402	414	T	-0.318	6	-0.511,-0.279	7,6	b		218/218	S,A,T,C,V

403	415	K	1.026	1	0.645, 0.977	2,1	e	218/218	F,S,T,K,Y,E,V,H,C,R,I,L
404	416	I	-0.726	8	-0.810,-0.680	8,8	b	218/218	M,I,Y,L,V
405	417	R	0.921	1	0.404, 0.977	3,1	e	218/218	A,S,T,N,K,E,V,H,Q,M,D,R
406	418	K	0.231	4	-0.069, 0.404	5,3	e	218/218	A,S,T,N,K,E,H,Q,D,R,G,L
407	419	C	-0.775	8	-0.879,-0.727	9,8	b	218/218	A,T,C,V
408	420	I	-1.010	9	-1.054,-0.985	9,9	b s	218/218	I,L,V
409	421	I	-0.340	6	-0.511,-0.279	7,6	b	218/218	I,L,V
410	422	D	-1.051	9	-1.074,-1.040	9,9	e f	218/218	D,E
411	423	K	-0.859	9	-0.937,-0.810	9,8	e f	218/218	Q,M,D,R,K,E,L
412	424	N	-0.931	9	-0.985,-0.909	9,9	e f	218/218	S,D,N,K,G,Y
413	425	A	-0.317	6	-0.442,-0.279	7,6	b	218/218	S,A,T,C,P,V
414	426	K	-0.151	6	-0.365,-0.069	7,5	e	218/218	A,S,N,K,Y,H,Q,M,C,R
415	427	I	-0.946	9	-1.006,-0.909	9,9	b s	218/218	I,G,L,V
416	428	G	-1.033	9	-1.074,-1.024	9,9	e f	218/218	W,G
417	429	K	1.236	1	0.645, 1.497	2,1	e	218/218	A,S,N,P,K,E,H,Q,M,C,D,R
418	430	N	-0.267	6	-0.442,-0.182	7,6	e	218/218	H,D,N,R,K,G,E
419	431	V	-0.760	8	-0.846,-0.727	9,8	b	217/218	S,A,T,C,R,V
420	432	S	1.191	1	0.645, 1.497	2,1	e	217/218	S,T,N,K,Y,E,V,H,Q,M,C,I,R,L
421	433	I	-0.888	9	-0.963,-0.846	9,9	b s	218/218	H,I,L,V
422	434	I	0.845	1	0.404, 0.977	3,1	e	217/218	F,S,A,T,N,K,E,V,M,D,R,I,G,L
423	435	N	-0.699	8	-0.810,-0.629	8,8	e f	217/218	F,A,N,P,K,Y,V,Q,M,C,I,G
424	436	K	0.720	2	0.404, 0.977	3,1	e	217/218	F,S,A,T,N,K,E,V,H,Q,C,D,R,I,G,L
425	437	D	1.054	1	0.645, 0.977	2,1	e	217/218	S,A,T,N,P,K,E,H,Q,D,R,G,L
426	438	G	0.765	2	0.404, 0.977	3,1	e	215/218	S,T,N,P,K,E,V,H,Q,D,I,R,G,L
427	439	V	-0.046	5	-0.279, 0.060	6,5	e	215/218	A,S,N,K,P,E,Y,V,M,I,R,G,L
428	440	Q	1.175	1	0.645, 1.497	2,1	e	217/218	A,S,F,T,P,K,E,V,H,Q,M,D,I,R,G,L
429	441	E	-0.315	6	-0.511,-0.182	7,6	e	217/218	S,T,N,Y,E,V,H,Q,D,R,L
430	442	A	0.192	4	-0.069, 0.214	5,4	e	217/218	F,S,A,T,N,K,P,Y,V,Q,M,C,R,I,G,L

431	443	D	0.187	4	-0.069, 0.214	5,4	e	217/218	F,A,S,W,T,N,K,E,V,Q,D,G
432	444	R	0.340	4	0.060, 0.404	5,3	e	217/218	S,F,T,N,K,Y,E,Q,M,C,A,H,D,R,I,G
433	445	P	0.701	2	0.404, 0.977	3,1	e	217/218	A,S,T,N,P,E,D,R,G
434	446	E	1.765	1	0.977, 1.497	1,1	e	217/218	F,A,S,T,N,P,K,Y,E,V,H,Q,M,D,R,G,L
435	447	E	1.000	1	0.404, 0.977	3,1	e	147/218	S,N,K,E,V,H,Q,D,R,G,L
436	448	G	-0.497	7	-0.680,-0.365	8,7	e	153/218	S,A,N,Y,H,D,R,G,L
437	449	F	0.148	4	-0.069, 0.214	5,4	b	217/218	F,W,C,I,G,L,Y,V
438	450	Y	0.646	2	0.214, 0.977	4,1	b	217/218	A,S,F,T,W,N,Y,V,H,Q,M,C,R,I,L
439	451	I	-0.653	8	-0.770,-0.573	8,7	b	217/218	A,S,M,T,I,L,V
440	452	R	-0.475	7	-0.629,-0.365	8,7	e	216/218	S,A,N,K,V,H,Q,M,C,R
441	453	S	-0.540	7	-0.680,-0.511	8,7	e	216/218	A,S,T,N,E,H,C,D,G
442	454	G	-0.816	8	-0.909,-0.770	9,8	b	215/218	S,H,N,K,R,G,E
443	455	I	-0.797	8	-0.879,-0.770	9,8	b	215/218	H,I,L,V
444	456	I	-0.497	7	-0.629,-0.442	8,7	b	215/218	S,T,D,P,I,Y,L,V
445	457	I	-0.559	7	-0.680,-0.511	8,7	b	215/218	A,T,C,I,V
446	458	I	-0.005	5	-0.182, 0.060	6,5	b	215/218	T,I,L,V
447	459	L	0.484	3	0.214, 0.645	4,2	b	215/218	F,A,S,T,N,K,P,E,V,Q,M,C,D,R,I,L
448	460	E	-0.783	8	-0.879,-0.727	9,8	e	f 215/218	N,R,K,E
449	461	K	-0.280	6	-0.442,-0.182	7,6	e	215/218	S,F,N,K,Y,E,H,D,R,G
450	462	A	-0.302	6	-0.442,-0.182	7,6	b	215/218	F,S,A,T,V,Q,M,C,G
451	463	T	0.486	3	0.214, 0.645	4,2	e	215/218	F,S,T,N,K,Y,E,V,Q,M,C,L,A,W,H,D,I,R
452	464	I	-0.648	8	-0.770,-0.573	8,7	b	214/218	F,I,L,V
453	465	R	0.425	3	0.060, 0.645	5,2	e	214/218	S,A,T,N,P,K,Y,E,V,Q,M,R,L
454	466	D	0.122	4	-0.069, 0.214	5,4	e	214/218	A,S,T,N,K,P,H,D,G
455	467	G	-0.231	6	-0.442,-0.069	7,5	e	214/218	S,H,N,D,R,G,E
456	468	T	-0.528	7	-0.629,-0.442	8,7	e	207/218	A,S,F,W,T,Y,V,M,I,L
457	469	V	0.407	3	0.060, 0.645	5,2	e	207/218	S,A,W,T,K,E,V,H,Q,M,R,I,L
458	470	I	-0.920	9	-0.985,-0.879	9,9	e	f 204/218	D,I,L,V

APPENDIX F: DNA AND PROTEIN MARKERS

DNA Molecular Weight Marker

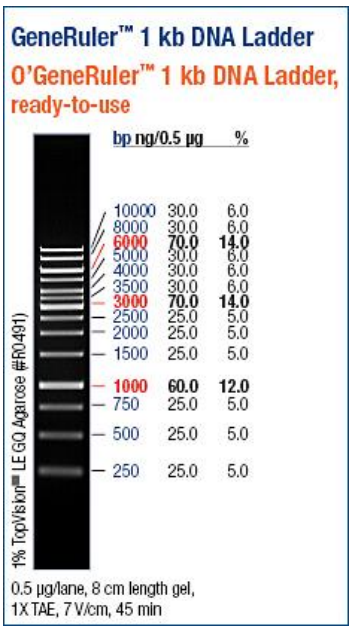

Protein Molecular Weight Marker

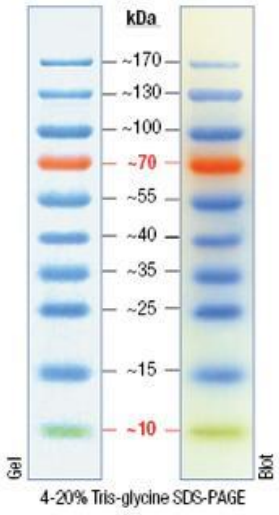

PageRuler Prestained Protein Ladders

APPENDIX G: LAB EQUIPMENTS

Autoclaves	**:** CL-40S/SDP (60L) ALP autoclave
Centrifuges	**:** 4K15, Sigma Laboratory
	:1-15, Sigma Laboratory
	: Microfuge 14-15, Sigma Laboratory
Computer Systems	**:** INtellistation Z Pro, MT:9228, S/N 99B0492,
	Product ID: Z289BTT, IBM
Deep freezes and refrigerators	**:** New Brunswick Scientific Ultra Low Temperature Freezer
	: 2021 D deep freezer, Arcelik.
	: 1061 M refrigerator, Arcelik.
	:2556 A++D refrigerator, Arcelik
Electrophoresis equipments	**:** E-C Mini Cell Primo EC320, E-C Apparatus.
	: Mini-PROTEAN 3 Cell and Single-Row AnyGel Stand, Catalog# 165-3321,Bio-Rad.
Gel documentation system	**:** UVIpro GAS7000, UVItec Limited.
Shaker	**:** Innova 4300 incubator shaker
Magnetic stirrer	**:** Heidolph MR 3001
Pipettes	**:** Pipetteman P10, P 100, P1000, Eppendorf
	: Finnpipette F1 1-10µl, F1 10-100µl, F1 100-1000µl, TermoScientific
pH meter	**:** Inolab pH level 1, order# 1A10-1113,
Power supply	**:** PowerPac Basic (300V,400mA,75W) Biorad
Pure water systems	**:** DV25 PureLab Option ELGA

Spectrophotometer	**:** W-1700 PharmaSpec, Shimadzu Corporation.
	: V-1200 Spectrometer, VWR
Vortexing machine	**:** Reax Top, Heidolph2.2.